Crystal Engineering of Ionic Cocrystals

by

Naga Kiran Duggirala

Department of Chemical and Environmental Sciences, University of Limerick

Major Professor: **Dr. Michael J. Zaworotko**
Dr. Denise Croker
Dr. Magali B. Hickey
Dr. Emmet O'Reilly

A Thesis Submitted to the University of Limerick for the Degree of Doctor of Philosophy
December 2015

Key words: Crystal Engineering, Pharmaceutical Cocrystals, Molecular Cocrystals, Ionic Cocrystals, Chloride Salts, Lithium Salts

Table of contents

Schemes

Figures

Tables

Declaration

I declare that the work in this thesis has not been submitted for a degree to this or any other University.

This thesis was defended on the 4th of November, 2015.

-Naga Kiran Duggirala
23/11/2015

Acknowledgments

I would like to thank my professor Michael J. Zaworotko for his support and guidance over the years for my professional growth and development. I am truly indebted for his encouragement and advice, without whom, this dissertation would not have been possible.

I am thankful to my committee members: Dr. Denise Croker and Dr. Magali Hickey for their support and valuable feedback for my research and Dr. Emmet O'Reilly for kindly agreeing to serve as the chair person.

I would like to acknowledge all the past members at University of South Florida (USF) and present member at University of Limerick (UL) for their support and help. My special thanks to Dr. Łukasz Wojtas for his help with crystallography and Dr. Miranda L. Perry for her support and providing scientific inputs during my research. I also would like to thank Dr. John L. Perry, Dr. Padmini Kavuru and Dr. Matteo Lusi for thought provoking discussions and advice.

I would like to thank to collaborators Dr. R. Douglas Shytle, Dr. Adam J. Smith, Dr. Kapildev Arora and Dr. Geoffrey P. F. Wood for their valuable contributions to achieve the common goal.

Finally, I would like to express my deepest thanks to my family members and friends for their love and support throughout this journey.

Abstract

Pharmaceutical cocrystals are long known but relatively understudied class of compounds. In the past decade there is heightened interest in pharmaceutical cocrystals to the point now they are in the advance stage of drug product development. In general, cocrystals can be classified into two categories: ***molecular cocrystals*** (MCCs) that comprise only neutral components in the crystal lattice (coformers); ***ionic cocrystals*** (ICCs), which consist at least a salt i.e. ionic compound. ICCs are recently emerging class of crystal forms for the new fundamental science in the context of crystal engineering and have been barely studied in the context of pharmaceutical science.

Chapter 1 highlights a brief history of molecular cocrystals (MCCs) but focuses primarily upon advances in discovery, design and development of pharmaceutical cocrystals that have occurred since an earlier review published in 2004. Further two case studies that demonstrate how pharmaceutical cocrystals can improve the physicochemical properties and clinical performance of API's are presented.

Chapter 2 mainly focusses on history, the advantages, the diversity and case studies of ionic cocrystals to improve the physicochemical properties of API's.

Chapter 3 addresses the propensity to form chloride···carboxylic acid *versus* chloride···phenol hydrogen bonds (supramolecular heterosynthons) through a combination of Cambridge Structural Database (CSD) data mining and the structural characterization of 12 novel ICCs, including 4 hydrates containing carboxylic acids, phenol groups, and chloride anions.

Chapter 4 highlights a crystal engineering approach for the preparation and characterization of ionic cocrystals (ICCs) of lithium chloride (LIC) and lithium bromide (LIB) with glucose (GLU); further demonstrated the physical stability and

pharmacokinetic studies of lithium chloride-glucose (LICGLU) ICC compared to that of lithium chloride.

Chapter 5 concludes by emphasizing the need to explore ionic cocrystals in terms of design and their relevance to pharmaceutical science.

Portions of this chapter have been previously published: Naga, K. Duggirala, Miranda, L. Perry, Ö. Almarsson and Michael, J. Zaworotko, *ChemCommun.,* 2016, Advanced article, DOI: 10.1039/C5CC08216A – Reproduced by permission of the Royal Society of Chemistry.

http://pubs.rsc.org/en/content/articlepdf/2016/cc/c5cc08216a

Chapter 1: Pharmaceutical cocrystals: Along the path to the improved medicines

1.1 Introduction

Early drug discovery and development is comprised of three stages that could be termed "molecules, materials and medicines", respectively[1] (Scheme 1.1).

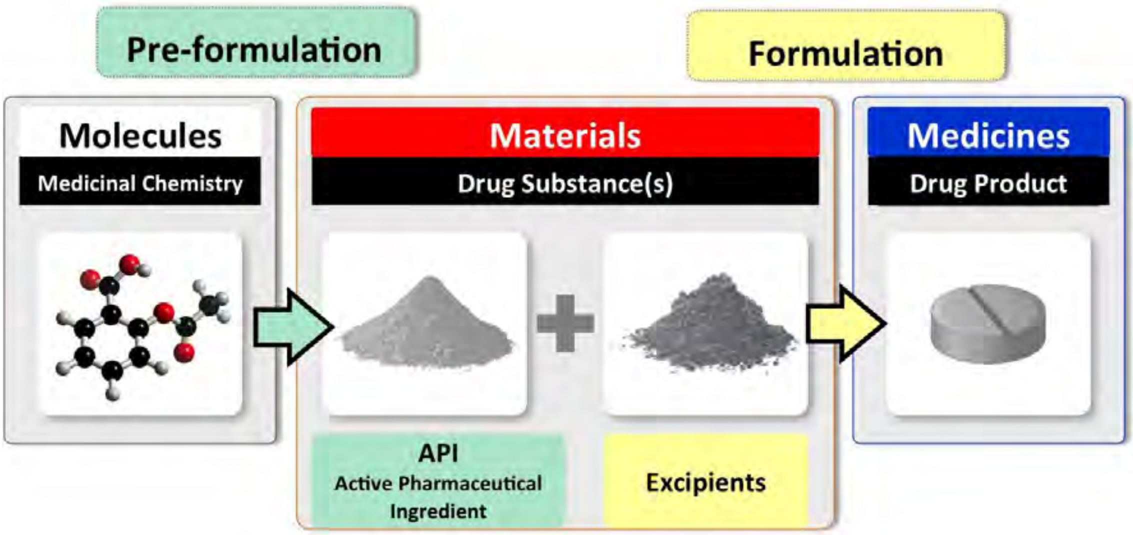

Scheme 1.1 The three stages of early drug discovery and development: Identify a molecule that is biologically active; create a material (drug substance or active pharmaceutical ingredient, API) suitable for use in a drug product; formulate the resulting API with excipients to afford a drug product (medicine).

The "molecules" stage includes medicinal chemistry for the discovery of new chemical entities along with biological and pharmacological screening for activity. The "materials" or pre-formulation stage addresses the discovery of a drug substance, normally a solid, suitable for use as a material in a drug product. The "medicines" or formulation stage combines this material (also known as the drug substance or active pharmaceutical ingredient) with inactive ingredients, excipients, to afford a drug product. The materials stage came to the fore in the 1990's after regulatory bodies issued guidance that in effect mandated characterisation of the solid forms of a drug substance.[2] Intellectual property issues, first highlighted by litigations involving ranitidine hydrochloride, Zantac®,[3] which at the time was the world's best-selling drug product, further emphasized the importance of pre-formulation research. This was compounded by performance problems caused by a previously undiscovered polymorph of ritonavir, in a capsule formulation marketed under the trade name Norvir®, which resulted in market withdrawal and subsequent reformulation of the capsule product.[4, 5]

The motivation to create new solid forms of drug molecules is therefore a consequence of how important drug substances are to the performance of orally administered drug products, the heart of which is almost always a crystalline solid.[6] It should be noted that amorphous solids have also been selected for use in drug products, but the need to meet specifications in terms of thermodynamic stability, purity and processability means that crystalline drug substance are generally preferred.[7, 8] That the physicochemical properties of a crystal form are inherently dependent upon the composition and the crystal packing of the molecules/ions means that exerting control over composition and crystal packing could in turn lead to control over properties. It is in this context that crystal engineering[9, 10] research on pharmaceutical cocrystals started in earnest with the main goals of improving the stability and/or the solubility of drug substances.[11-16] Crystal forms of drug molecules, as would be expected, are a microcosm of molecular solids in general. For example, they can be either single-component or multi-component. Single-component crystals provide limited opportunity to modulate the physicochemical properties of a compound since they are limited to polymorphs, which tend to exhibit only subtle changes in properties.[17] For example; the solubility difference between two polymorphs is typically less than two-fold. Multi-component crystals, however, are a different story. They can be stoichiometric or non-stoichiometric and encompass hydrates, solvates, salts, solid solutions (mixed crystals), inclusion compounds and cocrystals (Scheme 1.2).

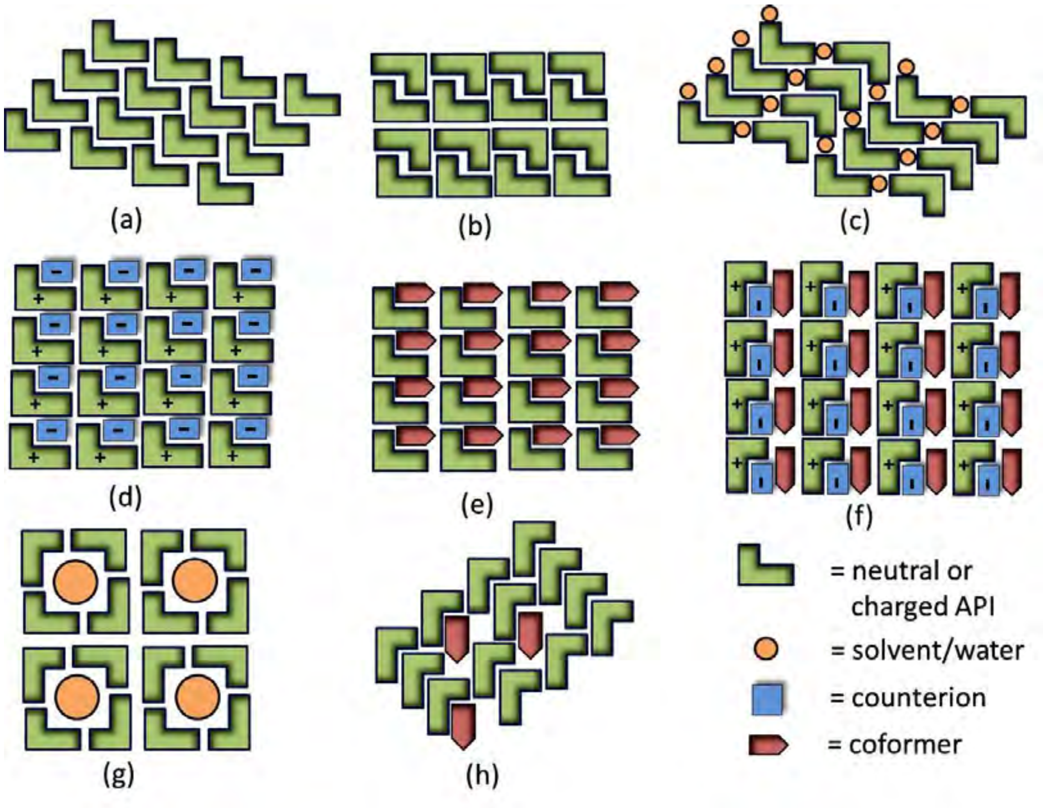

Scheme 1.2. Possible crystalline forms for an API: (a) & (b) polymorphs; (c) solvate/hydrate; (d) salt; (e) molecular cocrystal; (f) ionic cocrystal; (g) non-stoichiometric inclusion compounds including channel hydrates, solvates; (h) solid solutions (mixed crystals).

However, the development of multi-component crystalline drug substances presents additional challenges vs. single component variants. For example, stability can be an issue for solvates, hydrates or inclusion compounds.[18, 19] However, Often solvates can be marketed as final drug products provided they are physically stable. Some of the currently marketed drug products where the solvate is a drug substance include ethanol solvates such as Darunavir ethanolate.[20] Zhang *et al.*[21] reported solvate of ivacaftor with 2-methyl butyric acid that is physically stable and has shown better in vivo bioavailability in animal pharmacokinetic studies. For some of the API's solvates are inevitable exemplified by sulfathiazole where > 100 solvates were reported in the literature.[22] The solvates existed for most of the API's was summarized by Harry Brittain in his annual reviews.[23] Hydrates, which have been termed a "nemesis to crystal engineering",[24] are of particular relevance, thanks to the ubiquity of water vapour, variable stoichiometry and their tendency to exhibit low thermal stability.[25-27] Nevertheless, hydrates have been used in marketed drug products.[28] A solvate might also suffer from poor stability to elevated temperature or humidity, making it an unlikely candidate for a drug product.[29, 30] Salts, however, are a well-established approach to generate novel solid forms that can dramatically change physicochemical properties.[31, 32] The primary drawback of salts is that they are limited to API's that contain ionisable moieties. Crystalline solid solutions (mixed crystals) could enable a continuum of physical properties because of their variable stoichiometry but they are not generally amenable to design and preparation of homogeneous phases is nontrivial.[33, 34] In principle, cocrystals do not suffer from the limitations of the other classes of multi-component crystalline solid mentioned above. Further, that they can be designed using crystal engineering approaches means that suitable coformers can be rationally selected from libraries of hundreds of potential cocrystal formers.

Although cocrystals are long known, there was little consensus concerning the scope of the term cocrystal until a recent perspective authored by 46 scientists in the field.[35] According to the perspective '*Cocrystals are solids that are crystalline single phase materials composed of two or more different molecular and/or ionic compounds generally in a stoichiometric ratio which are neither solvates nor simple salts*.' If at least one of the coformers is an API and the other is pharmaceutically acceptable, then it is recognized as a pharmaceutical cocrystal.[11] Our research group classified cocrystals into molecular cocrystals (MCCs) that contain only neutral components (coformers) and ionic cocrystals (ICCs), which are comprised of at least one ionic coformer that is a salt.

Herein in this chapter we mainly focussed upon MCCs history, advances of pharmaceutical cocrystals (both MCCs and ICCs) at various stages of drug development.

1.2 History and Nomenclature of Molecular Cocrystals, (MCCs)

The MCC of quinone and hydroquinone, quinhydrone, was reported in 1844 by Wöhler.[36] The composition was not confirmed by single crystal X-ray analysis until the 1960's when it was revealed to be a 1:1 MCC sustained by a C=O···H-O supramolecular heterosynthon[37, 38] (Figure 1.1). An MCC with pharmaceutical utility was patented by Von Heyden et al. who claimed compositions of barbiturates with 4-oxy-5-nitropyridine, 2-ethoxy-5-acetaminopyridine, N-methyl-α-pyridine and α-aminopyridine.[39]

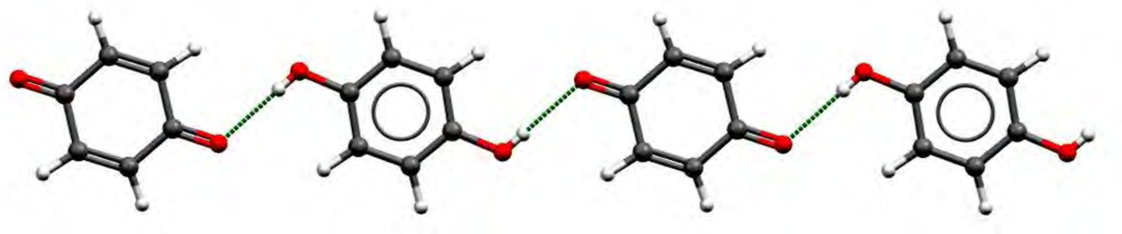

Figure 1.1. Illustration of the 1D chain that is sustained by O-H···O hydrogen bonded interactions in hydroquinone-quinone, quinhydrone.

Nomenclature of MCCs was inconsistent in the early literature: '*molecular organic compounds'* was used by Buehler and Heap to describe MCCs of 1,2-dinitrotoluene, 2,4-dinitrobenzene and 2,4-dinitrophenol with amino derivatives of naphthalene, benzidine and aniline,[40] '*organic molecular compounds'* was used by Anderson in 1937.[41] Use of MCCs (termed a '*complex'* by the authors[42]) to improve the performance of a drug substance is exemplified by digoxin and hydroquinones. Digoxin is indicated for the treatment of mild to moderate heart failure but its dissolution rate and bioavailability are low. Higuchi and Ikeda found that the solubility of digoxin increases in the presence of hydroquinone. Bochner et al.[43] later conducted clinical trials in humans that compared MCCs with commercially available tablets of digoxin. These studies revealed that peak serum digoxin concentrations for the MCC were achieved faster than commercial digoxin tablets. Even as early as 1974, the potential use of MCCs to improve the clinical performance of low solubility drugs was envisioned by the authors who stated that '*the principle of complexing a drug with substances such as hydroquinone to enhance the dissolution might be applied to other medication whose absorption is erratic following poor in vivo dissolution.*'

Ambiguity concerning whether a compound should be classified as a salt or a cocrystal is a topical subject[44, 45] but was also discussed as far back as the 1930's. Two MCCs from 1934, were initially considered to be salts formed between urea and oxalic acid (in 1:1 & 1:2 stoichiometry).[46] Subsequent analysis by Harkema et al. revealed that they are addition compounds, i.e. MCCs (CSD refcodes: UROXAL[47] and UROXAM[48]).

Another term used to describe MCCs is '*hydrogen bond complex*'. Hoogsteen prepared such MCCs to provide evidence to support the existence of purine-pyrimidine base pairs in DNA. The MCC between 9-methyladenine and 1-methylthymine[49] exhibited that is now known as a Hoogsteen base pair. The crystal structure is sustained by two point hydrogen bonds (N-H···O and N-H···N) as shown in Figure 1.2. It was later determined by Margaret Etter that the Hoogsteen base pair is persistent even in the presence of a third competing coformer by solid-state grinding.[50]

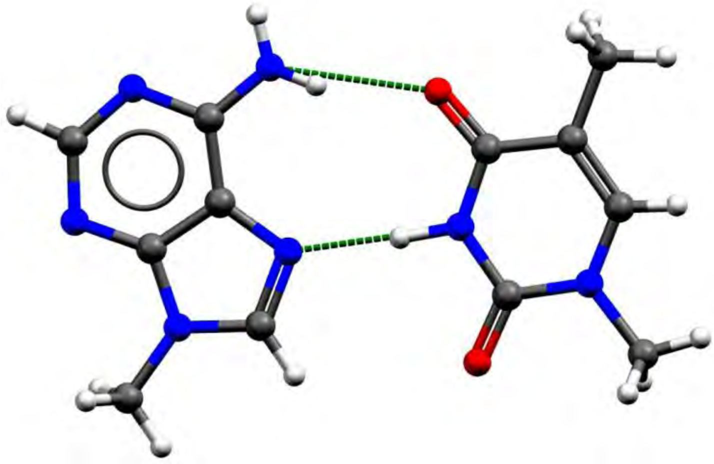

Figure 1.2. A Hoogsteen base pair as observed in the MCC of 9-methyl adenine and 1-methyl thymine is sustained by N-H···O and N-H···N hydrogen bonds.

The term cocrystal was not popularized until the 1990's, due in large part to Etter, who extensively studied hydrogen bonds as design elements for the preparation of multi-component crystals. Her research contributions to the field of cocrystal design include concepts that are still used today for determining the propensity for hydrogen bond interactions.[51-53] However, despite increasing use of the term cocrystal in the crystal engineering field, researchers have continued to use different terms. For example, Pekker et al.[54] reported '*heteromolecular crystals'* of fullerene and cubane in 2005.

In summary, MCCs have been termed *molecular organic compounds, organic molecular compounds, addition compounds, mixed crystals, complexes, hydrogen bonded complexes and heteromolecular crystals*.

1.3 Design of Pharmaceutical Cocrystals

The design and synthesis of new cocrystals may appear to be established given that thousands of cocrystals have been synthesized. However, the complexity of most drug molecules means that there remains a need to understand and manipulate intermolecular interactions in a competitive hydrogen bond environment, i.e. crystal engineering. In this section, we address how crystal engineering has been applied to cocrystal design.

1.3.1 Crystal Engineering - Supramolecular Chemistry in the Solid State

The term crystal engineering can be traced back to 1955 and Pepinsky.[9, 10] His ideas were subsequently implemented by Schmidt's group, where the goal was to use crystal engineering to control organic solid-state photochemical reactions.[55] Crystal engineering further evolved in the 1980's largely thanks to Desiraju.[56] Today, crystal engineering has evolved to encompass a broad range of chemical species ranging from drug molecules (especially in the context of cocrystals) to transition metal clusters or cations (especially in the context of coordination networks[57]). A unifying theme that cuts across chemical types is that crystal structures are treated as if they are sustained by a series of repeating supramolecular interactions. The first step in a crystal engineering experiment is therefore to understand the interactions that sustain and direct crystal packing. Etter developed a set of empirical rules to determine the propensity for hydrogen bonding given various donor/acceptor combinations. Etter's rules included the following: the best proton donor will hydrogen bond to the best proton acceptor; six membered ring intramolecular hydrogen bonds are favourable.[58] Etter's rules are applicable to cocrystals and are particularly useful when there are multiple functional groups capable of hydrogen bonding. Etter also pioneered the use of graph set theory to describe hydrogen bonded motifs in crystals.[59] However, this type of analysis has been superseded by supramolecular synthons, which are functional group specific.[60, 61]

1.3.2 Cocrystals and Supramolecular Synthons

There are two main types of supramolecular synthons, supramolecular homosynthons and supramolecular heterosynthons (Figure 1.3).[62] Supramolecular heterosynthons are of particular interest to cocrystal design since, if the functional groups of a supramolecular heterosynthon are in different molecules (coformers), and then they can be the primary driving force for cocrystal formation. Carboxylic acid-amide,[63-75] carboxylic acid-aromatic nitrogen,[76-87] alcohol-aromatic nitrogen,[88-95] and alcohol-amine[96-99] supramolecular synthons have been well studied in this context. During 2003-2004 four pharmaceutical cocrystal papers were published by three groups emphasizing the key role that crystal engineering plays in cocrystal design. Indeed, the first two words in each of these papers were "crystal engineering".[62, 66, 100, 101] Indeed, it was these four articles spurred the development and publication of cocrystals containing drug molecules.

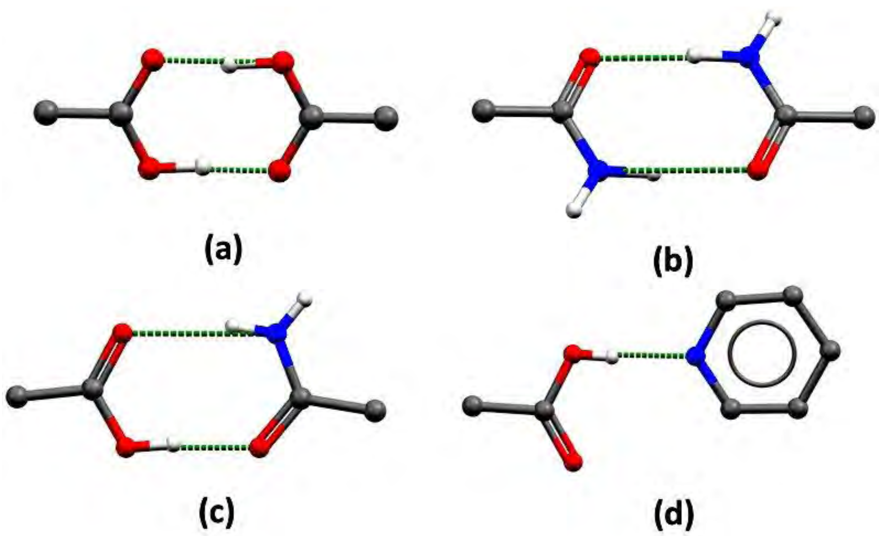

Figure 1.3. Supramolecular homosynthons (a) carboxylic acid homosynthon exist as dimer (b) amide homosynthon exist as dimer; supramolecular heterosynthons (c) carboxylic acid-amide heterosynthon (d) carboxylic acid-pyridine heterosynthon.

Molecules that are of interest for their biological activity, especially APIs, typically contain multiple hydrogen bond donor and acceptor groups. This creates a challenge to crystal engineering since understanding the hierarchy of these functional groups in the presence of other functional groups on coformers is the key to controlling not just the stoichiometry of cocrystals, but also their existence. Further, addressing this matter is unlikely to be as simple as it may sound. For example, carboxylic acids would be considered to be better hydrogen bond donors than phenols based upon pK_a. However, this is not necessarily the case as we[102] and Aakeröy[103] have reported. Further, although the CSD contains > 700,000 entries and continues to grow rapidly, this does not mean that the CSD provides statistically valid hit lists to address even relatively simple permutations of donors and acceptors. Therefore, systematic supramolecular synthon hierarchy studies remain an important aspect of crystal engineering and cocrystal design. Molecular surface electrostatic potentials and density functional theory calculations (DFT) are also useful tools to support synthetic studies. Another approach to predict cocrystal formation, initially reported by Galek et al.[104] utilized the CSD to generate a statistical analysis of hydrogen bond propensity between drug molecule and coformer.

1.3.3 Hierarchy of Supramolecular Synthons

Supramolecular synthon hierarchy based on hydrogen bonds:

Several research groups have delineated donor/acceptor hierarchies involving one or more of the following: carboxylic acids, carboxylates, amides, aromatic nitrogens, alcohols, phenols, cyano and cyanooxime moieties. One of our studies addressed the hierarchy of supramolecular synthons between carboxylic acids, aromatic nitrogens and phenols.[105] Interestingly, both carboxylic acid-aromatic nitrogen and phenol-aromatic nitrogen supramolecular heterosynthons were encountered. This observation suggests that carboxylic acid and phenol groups are competitive with respect to forming supramolecular heterosynthons with aromatic nitrogen atoms. Aakeröy and co-workers also examined hydrogen bond hierarchy between carboxylic acids, phenols and basic nitrogen atoms.[103] Two nitrogen atoms with different basicity were exploited to assess interactions with the two donors. Electrostatic surface potential calculations indicated that phenolic -OH moieties would be preferred to carboxylic acid moieties. Indeed carboxylic acids consistently formed supramolecular heterosynthons with the second best basic nitrogen.

In our recent hierarchy study we used ICCs to examine the propensity for chloride anions to interact with carboxylic acids vs. phenols.[102] Analysis of crystal structures and DFT/lattice energy calculations suggest that phenol to chloride anion interactions persist vs. carboxylic acid to chloride anion interactions. Other studies that have focused on delineation of supramolecular synthon hierarchy addressed alcohols vs. aromatic nitrogen atoms in the presence of a cyano moiety[102], hydrogen bonds between carboxylates and weakly acidic hydroxyl moieties in cocrystals of zwitterions[107] and phenols to the most basic acceptor in the presence of cyanooxime.[108]

The above hierarchy studies are consistent with Etter's "best hydrogen bond donor to best acceptor" guideline[58] and provide fundamental information of hierarchy of those interactions studied.

Supramolecular synthon hierarchy of halogen bonds *vs* hydrogen bonds:

Halogen bond is a reliable tool in crystal engineering and in some ways analogous to hydrogen bond in terms of strength and directionality.[109] Several research groups have addressed the strength and hierarchy studies of halogen bonds. In some instances halogen bonds prevail over hydrogen bonds and vice versa. For example a dipyridyl derivative and N,N,N',N'- tetraethylenediamine prefers to cocrystallize with halogen bond donors in a competitive environment of hydrogen bond donors.[110] In one of the case study Aakeröy research group investigated hydrogen bond *vs* halogen bond by selecting model compounds of 3,3'-azobipyridine and 4,4'-azobipyridine with bifunctional donor molecules containing both halogen and hydrogen bond donors. The single crystal analysis of six cocrystals revealed that 5/6 cocrystals are sustained by hydrogen bonds as primary interactions whereas halogen bonds are secondary interactions.[111] In other study where the model compounds are pyridine and amino pyridine with iodo and bromo substituted benzoic acids. The resultant cocrystals are a combination of hydrogen bonds and halogen bonds where amino pyridinium-carboxylate synthons are primary interactions and I···N, Br···N, and I···O halogen bonds are responsible to form 1D and 2D networks.[112]

These studies have collectively provided insight into donor/acceptor hierarchy and it is likely that they can be generally applied to cocrystal design. However, many drug molecules fall outside the realm of current studies and the information archived in the Cambridge Structural Database, CSD,[113, 114] requiring new hierarchy studies to be conducted.

1.4 Advances in Pharmaceutical Cocrystal Development Since 2004

There has been a surge of interest in pharmaceutical cocrystals within the past decade for their potential use as alternative drug substances with improved physicochemical properties. However, it is still true that taking a drug substance and developing it into a drug product is not a trivial task. In general, the development of a pharmaceutical cocrystal as the active ingredient in a drug product can be separated into eight stages (Scheme 1.3).

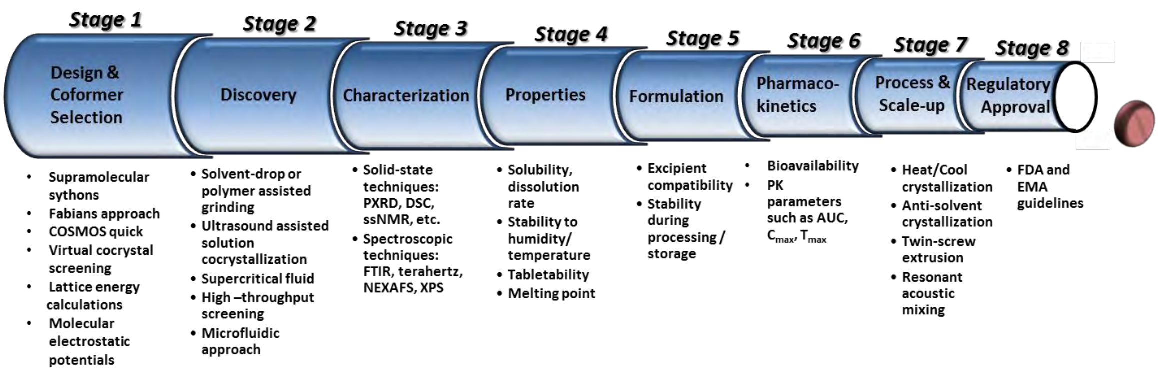

Scheme 1.3. Illustration of various states and advances at each stage along the drug development pathway of pharmaceutical cocrystals

1.4.1: Design + Coformer selection

Selection of a library of complementary coformers for a particular drug molecule is a critical aspect of cocrystal design and screening. A suitable coformer in the context of pharmaceutical cocrystals must be safe enough for use in a drug product. The Priority-based Assessment of Food Additives (PAFA) database contains chemical and toxicological information for ca. 2,000 substances, including those with the Generally Recognized As Safe (GRAS) designation,[115] which can be directly added to food. Including an additional 1,000 substances that are considered safe food additives, there are ca. 3,000 compounds that constitute the Everything Added to Food in the United States (EAFUS) database. The selection of a small subset of coformers (typically 40-50) that are likely to form cocrystals for a given API based upon supramolecular compatibility is the first step in discovery of a pharmaceutical cocrystal. Other approaches that can be used for library development include the following: Fabian's method[116] (based upon shape and polarity of coformer with respect to API); lattice energy calculations,[117] virtual cocrystal screening (based upon molecular electrostatic potential surfaces (MEPS));[118] the conductor-like screening model for real solvents (COSMO-RS).[119] Each approach has its merits and could be used independently or coupled with others.

1.4.2: Discovery

Once an appropriate library of coformer(s) has been selected, the next stage is discovery. Traditional methods used to discover cocrystals include slow solvent evaporation, slurry mediated transformation and mechanical grinding (both neat and solvent-drop or liquid assisted).[120, 121] More recently, polymer assisted grinding has been reported as an alternative to liquid assisted grinding to improve the rate of formation of cocrystals.[122] Other methods that are known to facilitate the formation of cocrystals include ultrasound assisted solution cocrystallization,[123] high-throughput screening,[124, 125] microfluidic approach[126] and supercritical fluid technologies.[127] Thermal and microscopic methods have been also utilized for identification of new cocrystals. Berry et al.[128] demonstrated the use of hot stage microscopy to identify cocrystal phases of nicotinamide with seven API's. In short, comprehensive screening including multiple techniques should be conducted to enable the discovery of new cocrystals. It is perhaps appropriate to paraphrase McCrone's statement concerning polymorphism[129] and assert that the number of cocrystals that will ultimately be discovered will only be proportional to the amount of time and money spent in researching them.

1.4.3: Characterization

The primary techniques used to characterize novel cocrystals are those used generally for crystal forms including powder X-ray diffraction (PXRD), single crystal X-ray diffraction (SCXRD), differential scanning calorimetry (DSC), thermogravimetric analysis (TGA), infrared and raman spectroscopies and solid- state nuclear magnetic resonance (ssNMR). SCXRD confirms composition but single crystals are not necessarily always available from the discovery stage. In such situations, structure solution from microcrystalline powder samples or advanced spectroscopic techniques has been demonstrated to be effective for cocrystals. For example, Lapidus et al.[130] determined crystal structures of 10 cocrystals from high resolution synchrotron X-ray powder diffraction. Spectroscopic methods have also been applied to identify the cocrystal phase during the discovery. Desiraju identified MCCs sustained by amide dimers from diagnostic N-H···O bands in IR spectra.[131] Raman spectroscopy has been used to identify cocrystal formation during high-throughput slurry screening as well as to distinguish cocrystal and physical mixture in formulated tablets.[132, 133] Vogt et al[134] demonstrated that ssNMR can be effective for the characterization of cocrystals by diagnosing hydrogen bonding and local conformational changes by ^{1}H-^{1}H, ^{1}H-^{13}C and ^{19}F-^{13}C coupling. Maruyoshi et al.[135] identified COOH···N_{arom} and CH_{arom}···O=C interactions in indomethacin-nicotinamide by using 2D ^{1}H double quantum and ^{14}N-^{1}H and ^{1}H-^{13}C heteronuclear magic angle spinning**.** Terahertz time-domain-spectroscopy has also been used to distinguish between chiral and racemic MCCs of malic acid and tartaric acid with theophylline.[136] Near edge X-ray absorption fine structure (NEXAFS) and X-ray photoelectron spectroscopy (XPS) were applied to differentiate between a salt and a cocrystal.[137]

1.4.4: Properties

A major driving force for the development of new solid forms of drug molecules is to improve the physicochemical properties that are of critical relevance to their performance as drug substances. These include aqueous solubility/dissolution rate and physical stability. Currently, there are >100 studies of cocrystals that demonstrate improved solubility and/or dissolution rates and this subject has been reviewed.

Improved physical stability, chemical stability and manufacturability *via* cocrystallization have also been addressed. Anhydrous caffeine and theophylline readily convert to their respective hydrated forms. Jones' research group prepared cocrystals of caffeine and theophylline with oxalic acid and they were found to exhibit superior physical stability vs. the anhydrous crystal forms when exposed to accelerated stability conditions (40 °C/75% RH).[138, 139] Vitamin D_3 cocrystals have been studied in the context of chemical stability.[140] Vitamin D_3 is widely used in the food and nutraceutical industries but is chemically unstable because it is susceptible to topochemical reaction. MCCs of vitamin D_3 with cholesterol and cholestanol were prepared (sustained by O-H···O-H supramolecular synthons) and subjected to accelerated stability testing for 6 months. The assay value of vitamin D_3 decreased to 4.4% under these conditions whereas the MCCs afforded 97.6% and 96.6% assay values, respectively. MCCs containing paracetamol and oxalic acid, theophylline, naphthalene and phenazine were pressed into tablets and subjected to mechanical stress. The MCCs were found to exhibit greater tensile strength than paracetamol.[141] The formulation of drug substances generally requires that the melting point should be high enough to avoid plastic deformation. In a recent patent application by UCB Pharma a novel ICC of (2S)-2-2[(4S)-4-(2,2-difluorovinyl)-2-oxopyrrolidinyl] butanamide with $MgCl_2$ and H_2O (2:1:4 stoichiometry) was claimed with a melting point ca. 50 °C higher than that of the pure API.[142]

1.4.5: Formulation

Before a cocrystal can be introduced into a drug product it is necessary to formulate the cocrystal. That cocrystals are typically sustained by hydrogen bonds means that their stability in the presence of excipients which also contain hydrogen bonding groups becomes an issue. Remenar et al.[143] and Alhalaweh et al.[144] highlighted the use of excipients to alter the rate of dissolution and capture the maximum potential of celecoxib-nicotinamide and indomethacin-saccharin MCCs, respectively. Huang and Rodriguez-Hornedo [145] manipulated the micellar solubilisation and stability of cocrystal components in solution. Abourahma et al.[146] studied the robustness of theophylline *p*-hydroxybenzoic acid in the presence of additives during solvent-drop grinding experiments. Their results indicated that the cocrystal is robust in the presence of additives that contain carboxylic acid, amide and phenol functional groups but not in the presence of acetamide. Arora et al.[147] recently demonstrated that carbamazepine nicotinamide MCC can be formed in a formulated tablet, a phase change attributed to release of lattice water from an excipient (dibasic calcium phosphate dihydrate).

A pharmaceutical cocrystal sustained by halogen bonds was recently reported by Baldrighi et al.[148] The commonly used preservative 3-iodo-2-propynyl-N-butylcarbamate exhibits unfavourable manufacturing properties, including a low melting point and a tendency of particles to stick and clump together. Four cocrystals were prepared and SCXRD experiments revealed that three of the cocrystals are sustained by halogen bonds involving pyridyl moieties. The fourth cocrystal is an ICC of $CaCl_2$. Melting points were observed to increase in a manner that correlates with the coformer. The clumping tendency of 3-iodo-2-propynyl-N-butylcarbamate was improved, especially in the case of the ICC.

Given that formulation of cocrystals is a necessary stage in drug development, it is likely that studies addressing formulation issues will increase in frequency.

1.4.6: Pharmacokinetics

In a recent comprehensive review by Shan et al.[149] the effect of cocrystallization upon API pharmacokinetics (PK) was examined. We provide a brief summary of the key findings of this study. 64 cocrystals representing 21 API's afforded 76 PK studies. 80% of the APIs are class II (low solubility, high permeability) according to the Biopharmaceutics Classification System (BCS).[150] This is unsurprising given that improving solubility has been a primary motivation for the study of pharmaceutical cocrystals. Analysis of the PK results suggests that solubility enhancements generally result in increases in area under the curve (AUC). The impact of cocrystals upon AUC can be significant, ranging from ca. 10.2-fold decrease to ca. 28.4-fold increase. C_{max} changes ranging from a 4-fold decrease to a 44-fold increase have been observed. Most cocrystals, however, were found to exhibit less significant changes in AUC and C_{max}.

Variations in PK after dosing different drug substances can affect the safety, efficacy and clinical performance of a drug product. Further, if there is a particular application for an API, such as fast onset of pain relief, then the ability to manipulate specific PK parameters becomes critical. For instance, to develop an API for acute pain relief, the time required to reach the effective concentration must be short. Weyna et al.[151] illustrated how meloxicam, an NSAID indicated for rheumatoid arthritis and postoperative pain, can be impacted by cocrystallization. Meloxicam is a BCS class II API with poor aqueous solubility and a 4-5 hour T_{max}. MCCs of meloxicam were synthesized and PK studies in rats were conducted. The results revealed an earlier onset of action, suggesting that a T_{max} of < 30 min is possible for some of the studied MCCs.

1.4.7: Process and Scale-up

The traditional solution methods (solvent evaporation/slurry) used for cocrystal discovery present challenges for large-scale manufacturing since we are dealing with at least a ternary phase diagram. Indeed, cocrystallization from solution could even be viewed as counterintuitive since this is the preferred approach to purify single component molecular compounds, in general, and APIs, in particular. However, if a cocrystal is thermodynamically favoured vs. single component crystals and the ternary phase diagram is well delineated, then solution crystallisation is suitable to process cocrystals. By understanding the TPD, Sheikh et al.[152] prepared carbamazepine-nicotinamide with >90% yield in a 1 L vessel. TPD can be constructed by solvent evaporation or solution mediated transformation methods for 3 components that include solvent, API and coformer. By determining the saturated liquid phases with solid phases and by analysing the final solids by PXRD, the possible solid phase regions (API/coformer/cocrystal/mixtures) can be identified. However it is important to note that the solvent system can affect the solid phase regions in TPD. Therefore understanding of TPD in different solvent systems is critical to identify the novel cocrystals. In a recent case study for p-toluenesulfonamide/tryphenyl phosphine oxide, authors discovered 1:1 cocrystal by constructing TPD in acetonitrile (MeCN) and dichloromethane (CH_2Cl_2) solvent systems highlights the importance of TPD for discovery of novel cocrystals.[153]

It is also possible that cocrystallization can solve problems associated with purification of APIs. A kinase inhibitor API in development at Sanofi has a tendency to form unstable solvates. Approaches such as chromatography, adsorption of impurities and multiple crystallizations afforded the API but with only ca. 90% purity. A purity of 99.1% was achieved using a process that involved cocrystallization of the API with benzoic acid. The process was successfully transferred to plant scale, affording a 10 kg batch size.[154] Myerson's research group has also used cocrystallization for purification of an API. By complexing an impurity in amoxicillin/amino acid solutions they improved the purity of amoxicillin trihydrate.[155] Cocrystallization has also been used to separate stereoisomers. Khan et al.[156] demonstrated selective separation of quinidine from its stereoisomer by forming MCCs with methylparaben. The authors attribute the separation to methylparaben serving as a *molecular hook* which sustains O-H···N supramolecular heterosynthons with only one isomer of quinidine as shown in Figure 1.4.

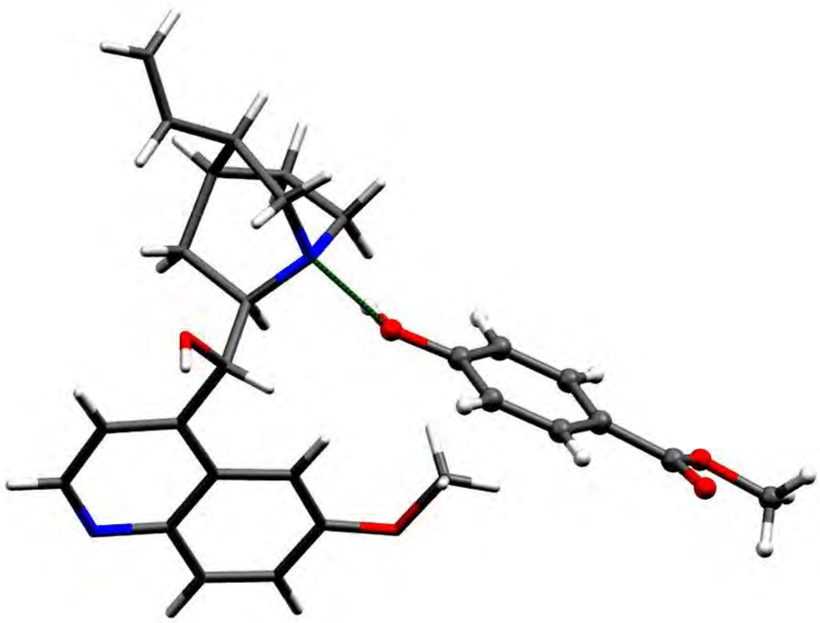

Figure 1.4. Illustration of O-H···N intermolecular hydrogen bond as seen in quinide-methylparaben molecular cocrystal.

In a study by Hickey et al.[157] the authors reported cocrystal scale-up in 30 g scale by cooling from alcoholic solution. The challenge for solution crystallization is the incongruent solubilities of molecular components. Thus, the less soluble compound in the solution tends to supersaturate and crystallize first. Rodriguez-Hornedo and her research group addressed this issue through reaction crystallization by focusing upon the kinetics of cocrystallization and analysis of stability domains of cocrystals in solution.[158, 159, 160] A commonly used and eco-friendly methods to prepare cocrystals at lab-scale is solid-state grinding (mechanochemistry). The main challenges with this method are high mechanical stress and the difficulty in achieving a homogeneous mix for larger scale processes. Alternatives to grinding include twin-screw extrusion (explored for AMG517-sorbic acid[161]) and resonant acoustic mixing (carbamazepine-nicotinamide[162]). Resonant acoustic mixing can be particularly beneficial for the preparation of volumes greater than 200 L and requires the addition of only small amounts of solvent during mixing. Synthesis of such quantities does, however, often require slurrying to obtain the desired cocrystal in high purity. Other methods used for cocrystal synthesis include super critical fluid technology, spray drying[163] and a continuous oscillatory baffled crystallizer.[164] Such cocrystallization methods facilitated by process analytical technology tools (PAT) are growing and could enable development of large-scale manufacturing of cocrystals.

1.4.8: Regulatory Approval

The ultimate step in developing a new drug is achieving regulatory approval. However, it should be noted that intellectual property protection will have supported an investment decision at some point during development. Within the past decade there have been numerous composition of matter patents granted for cocrystals on the premise that their cocrystals satisfy the three primary criteria for issuing a patent: 1) novelty (cocrystal is a new composition of matter), 2) non-obviousness/inventiveness (the physicochemical and 3) pharmacokinetic properties are difficult to predict with any degree of certainty) and utility (the drug substance has pharmacological activity and/or improved performance vs. the corresponding single component drug substance). The pharmaceutical cocrystal patent landscape has been reviewed by Almarsson, Peterson and Zaworotko.[165]

In 2011 the FDA released draft guidance for industry on the subject of pharmaceutical cocrystals. Within that guidance, a cocrystal was considered to be a dissociable "API-excipient" molecular complex, a drug product intermediate, and not a new API. This distinction is important because an intermediate in a drug development process is treated very differently than a different API. To gain product approval, the FDA also required the applicant to address two matters:

- The API and excipient must completely dissociate prior to reaching the pharmacologically active site.

- The API and excipient are in neutral states and do not interact by ionic bonds.

  Use of the ΔpK_a rule was suggested as a way to satisfy the second criterion.

In response to the FDA guidance, a perspective article was published in 2012.[35] To summarize, the authors opined that cocrystals should not be treated any differently than salts as the difference between a cocrystal and salt depends only upon the position of a proton that can be temperature dependent.[166] Pharmaceutical companies responded directly to the FDA with consensus that cocrystals should be treated as salts. That there are marketed drug substances that are considered by many to be cocrystals lends support to this argument. Caffeine citrate,[167] sodium valproate-valproic acid in Depakote®[168] and escitalopram oxalate with oxalic acid[169] are three such examples. The ICC of escitalopram oxalate oxalic acid is shown in Figure 1.5.

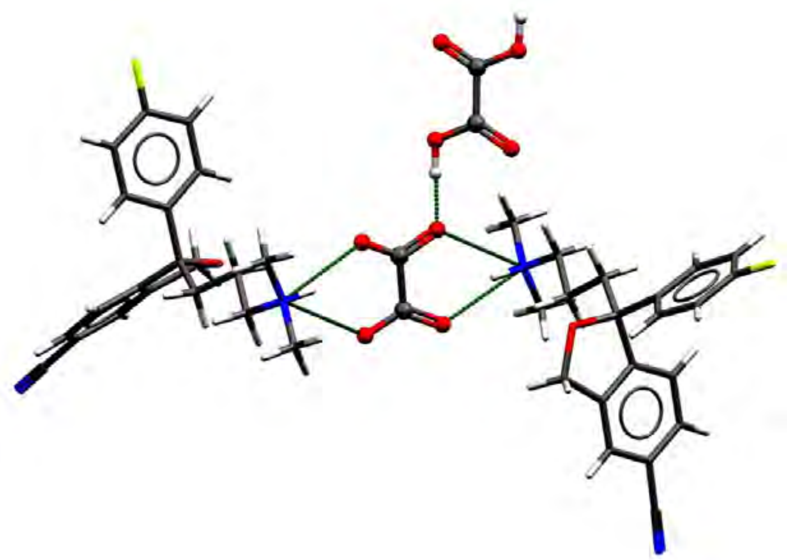

Figure 1.5. Observation of dioxalate anion and oxalic acid in the same crystal structure sustained by O-H···O interactions in the marketed drug; Escitalopram oxalate-oxalic acid ICC. Water molecule is removed for clarity.

The path to commercialization of a cocrystal in the United States remains unclear with respect to regulatory pathways to approval. Interestingly, the European Medicines Agency (EMA), which reviews and approves products in Europe, published a reflection paper summarizing their position on pharmaceutical cocrystals.[170] Currently, the EMA considers cocrystals to be homogeneous crystalline structures made up of two or more components in a definite stoichiometric ratio where the arrangement in the crystal lattice is not based on ion pairing. Other salient features within the EMA reflection paper on cocrystals include:

- Cocrystals are considered eligible for generic drug product applications in the same way as salts, solvates and amorphous solids would be.
- Cocrystals are not considered as New Active Substances (NAS) unless they demonstrate different safety and efficacy profiles.
- Cocrystals and salts share many conceptual similarities and therefore also similar principles for documentation should be applied.

Despite the very different positions taken by the FDA and EMA with respect to pharmaceutical cocrystals, and that there are position documents from both agencies provides guidance to industry and attests to the growing interest in the use of pharmaceutical cocrystals in drug products.

1.5 Pharmaceutical Cocrystal Case Studies

Two case studies of pharmaceutical cocrystals (MCCs) that address the improvement in bioavailability have been discussed.

1.5.1 Metaxalone

Metaxalone is the API in Skelaxin®, which is indicated for the relief of discomfort associated with musculoskeletal pain.[171] Nuformix has identified MCCs of metaxalone with superior properties that they are currently taking an MCC through clinical trials. Metaxalone is a BCS class II drug[172] and its oral bioavailability is greatly influenced by food. Attempts have previously been made to develop alternative crystalline or amorphous forms of metaxalone;[173, 174] however, MCCs of metaxalone show great promise with improved bioavailability in beagle dogs.[175] The oxazolidone moiety in metaxalone was exploited to form MCCs with adipic acid, fumaric acid, succinic acid, maleic acid and salicylic acid. A single dose PK study in beagle dogs was conducted to compare the fumaric and succinic acid MCCs with metaxalone. The greatest plasma concentration (C_{max}) was achieved after dosing the metaxalone fumaric acid MCC (3635 ng/ml). However the time to achieve maximum plasma concentration was the fastest for pure metaxalone. The area under the curve (AUC) for the metaxalone fumaric acid MCC and succinic acid MCCs were 5202 ng.h/ml and 4135 ng.h/ml, respectively, both greater than that of metaxalone.

1.5.2 Danazol

The behaviour of a cocrystal during formulation is largely unknown in the public domain. However, a recent publication by Childs et al.[176] provide insight into a danazol cocrystal formulation. The cocrystallization and formulation of danazol, a synthetic steroid approved for endometriosis[177] was addressed. With its low aqueous solubility (0.0067 mg/mL)[178] limiting its bioavailability, danazol is considered a BCS class II compound. Danazol is also non-ionisable, making cocrystallization a logical approach for improving solubility and PK performance. A MCC with vanillin was prepared that was sustained by O-H···O and O-H···N interactions (Figure 1.6).

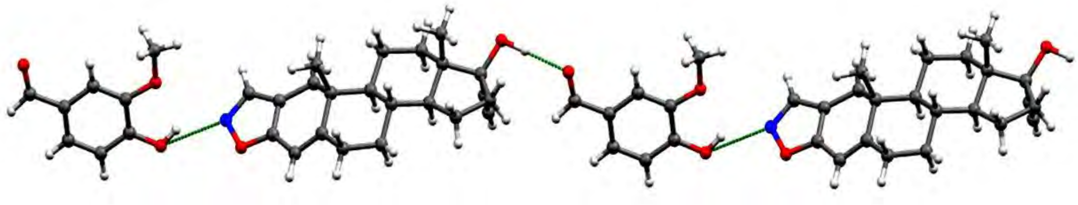

Figure 1.6. 1D hydrogen bonded chains observed in a danazol-vanillin MCC.

The MCC was subsequently evaluated with a variety of solubilizing agents and precipitation inhibitors to determine their effect upon performance. Intrinsic dissolution studies were conducted under non-sink conditions at 37 °C in fasted simulated intestinal fluid (FaSSIF) using compressed discs of pure MCC and danazol. During the first 15 minutes, the dissolution rate of the MCC was orders of magnitude greater than danazol although eventually the vanillin concentration was much greater than that of danazol. This phenomenon can be explained by assuming that danazol crystallises. Thus, in order to reduce or inhibit this effect, solubility studies were conducted using free flowing powder under sink and non-sink conditions. The sink condition powder dissolution study incorporated lactose to aid in the wetting and dispersion of the powder but the solubility advantage of MCC appeared to be hampered due to transformation to danazol at the surface. The non-sink conditions included two different excipients, a solubilizer (D-α-tocopheryl polyethylene glycol succinate, TPGS) and crystallization inhibitor (Klucel LF Pharma hydroxypropylcellulose, HPC). The use of TPGS and HPC enabled an increase in supersaturation 5.5-fold that of danazol free form. Taking into consideration the 10-fold increase in solubility from the MCC and the increase enabled by excipients, the solubility of the formulated MCC is close to the anticipated requirement for a human to absorb the entire 20 mg/kg dose (based upon maximum absorbable dose calculation using a 250 mL volume, 270 minute intestinal transit time and absorption value of 0.05/min). The performance of the MCC vs. danazol was also addressed in Sprague-Dawley rats. A single oral dose (20 mg/kg danazol) of an aqueous suspension containing MCC or danazol plus lactose and PVP was administered and plasma concentrations were monitored. An additional arm of the study determined the effect of formulation (1% TPGS and 2% HPC) on the performance of the MCC and danazol. It was determined that danazol and the MCC performed best when formulated with TPGS and HPC vs. a suspension with lactose and PVP (10% bioavailability vs. 8% for danazol; 100% bioavailability vs. 13% for the MCC). Considering the *in vitro* and *in vivo* data collectively, a positive correlation between the increase in dissolution and increase in absorption of danazol was observed.

1.6 Conclusions

After a decade of progress we return to reflect upon the question posed by Almarsson and Zaworotko in their review on pharmaceutical cocrystals: 'Do pharmaceutical co-crystals represent a new path to improved medicines?' It seems clear that significant progress has been made in all of steps of drug development (Scheme 4). In particular, pharmaceutical cocrystals can modulate important PK parameters such as T_{max}, C_{max} and AUC for APIs with poor solubility and they therefore offer an innovative approach to improve bioavailability. Pharmaceutical cocrystals can also be considered novel, non-obvious and of utility and as such they can be protected by composition of matter patents. Regulatory bodies have also recognized the potential of cocrystals by publishing guidelines for industry. In short, after 10 years of discovery and development of pharmaceutical cocrystals, many reported improvements in preclinical performance, regulatory attention and intellectual property protection, the answer is a qualified 'yes'

Certain challenges remain. Large-scale synthesis and stability in the presence of excipients are, as with any type of crystal form, unpredictable and must be addressed. Further, diversity is a double-edged sword, since the discovery of hundreds of cocrystals would require time for discovery and property evaluation. Time is a precious and often limiting commodity in pharmaceutical development. It is presumed that, if and when drug products that are enabled by cocrystals are finally introduced, they will gain more widespread acceptance and an even stronger foothold in pharmaceutical drug development.

1.7 References

(1) M3-Molecules Materials Medicines: An international conference on the role of materials science and engineering in drug development; http://www.rsc.org/events/detail/15863/M3%20%20Molecules,%20Materials%20and%20MedicinesAn%20International%20Conference%20on%20the%20Role%20of%20Materials%20Science%20and%20Engineering%20in%20Drug%20Development (accessed on August 10th, 2015).

(2) Guidelines for submitting supporting documentation in drug applications for the manufacture of drug substances; http://www.fda.gov/downloads/Drugs/GuidanceComplianceRegulatoryInformation/Guidances/UCM149494.pdf, 1987, (accessed on September 10th, 2015).

(3) Crookes, D. L. Amino alkyl furan derviative. 4,521,431, **1985**.

(4) Chemburkar, S. R.; Bauer, J.; Deming, K.; Spiwek, H.; Patel, K.; Morris, J.; Henry, R.; Spanton, S.; Dziki, W.; Porter, W.; Quick, J.; Bauer, P.; Donaubauer, J.; Narayanan, B. A.; Soldani, M.; Riley, D.; McFarland, K., Dealing with the impact of ritonavir polymorphs on the late stages of bulk drug process development. *Org. Process Res. Dev.,* **2000**, *4*(5), 413-417.

(5) Bauer, J.; Spanton, S.; Henry, R.; Quick, J.; Dziki, W.; Porter, W.; Morris, J., Ritonavir: An extraordinary example of conformational polymorphism. *Pharm. Res.,* **2001**, *18*(6), 859-866.

(6) Gardner, C. R.; Walsh, C. T.; Almarsson, Ö., Drugs as materials: valuing physical form in drug discovery. *Nat. Rev. Drug Discov.,* **2004**, *3*(11), 926-934.

(7) Pikal, M. J.; Lukes, A. L.; Lang, J. E.; Gaines, K., Quantitative crystallinity determinations for P-lactam antibiotics by solution calorimetry: Correlations with stability. *J. Pharm. Sci.,* **1978**, *67*(6), 767.

(8) Yoshioka.;, M.; Hancock.;, B. C.; Zografi., G., Crystallization of indomethacin from the amorphous state below and above Its glass transisition temperature. *J. Pharm. Sci.,* **1994**, *83*(12), 1700.

(9) Pepinsky, R.; Y. Okaya; Y. Siato, *Phys. Rev.,* **1955**, *98*, 1857.

(10) Pepinsky, R., *Phys. Rev.,* **1955**, *100*, 971.

(11) Almarsson, Ö.; Zaworotko, M. J., Crystal engineering of the composition of pharmaceutical phases. Do pharmaceutical co-crystals represent a new path to improved medicines? *Chem. Commun.,* **2004**, (17), 1889-1896.

(12) Aakeroy, C. B.; Salmon, D. J., Building co-crystals with molecular sense and supramolecular sensibility. *CrystEngComm.,* **2005**, *7*(72), 439-448.

(13) Vishweshwar, P.; McMahon, J. A.; Bis, J. A.; Zaworotko, M. J., Pharmaceutical co-crystals. *J. Pharm. Sci.,* **2006**, *95*(3), 499-516.

(14) Shan, N.; Zaworotko, M. J., The role of cocrystals in pharmaceutical science. *Drug Discovery Today.,* **2008**, *13*(9–10), 440-446.

(15) Jones, W.; Motherwell, W. D. S.; Trask, A. V., Pharmaceutical Cocrystals: An Emerging Approach to Physical Property Enhancement. *MRS Bull.,* **2006**, *31*(11), 875-879.

(16) Schultheiss, N.; Newman, A., Pharmaceutical cocrystals and their physicochemical properties. *Cryst. Growth Des.,* **2009**, *9*(6), 2950-2967.

(17) Pudipeddi, M.; Serajuddin, A., Trends in solubility of polymorphs. *J. Pharm. Sci.,* **2005**, *94*(5), 929-939.

(18) Cox, J. S. G.; Woodard, G. D.; McCrone, W. C., Solid-state chemistry of cromolyn sodium (disodium cromoglycate). *J. Pharm. Sci.,* **1971**, *60*(10), 1458-1465.

(19) Mimura, H.; Kitamura, S.; Kitagawa, T.; Kohda, S., Characterization of the non-stoichiometric and isomorphic hydration and solvation in FK041 clathrate. *Colloids Surf., B,* **2002**, *26*(4), 397-406.

(20) Van Gyseghem, E., Stokbroekx, S., de Armas, H. N., Dickens, J., Vanstockem, M., Baert, L., Rosier, J., Schueller, L. and Van den Mooter, G. 'Solid state characterization of the anti-HIV drug TMC114: Interconversion of amorphous TMC114, TMC114 ethanolate and hydrate', *Eur. J. Pharm. Sci.,* **2009**, 38(5), 489-497.

(21) Zhang, Y., Evans, J., Rowe, W., Dinehart, K., Quinn, B. and Connelly, P. Dosable solvates of ivacaftor with high boiling point liquids, *CrystEngComm,* **2012**, 14(7), 2422-2427.

(22) Bingham, A. L., Hughes, D. S., Hursthouse, M. B., Lancaster, R. W., Tavener, S. and Threlfall, T. L. Over one hundred solvates of sulfathiazole: solvates and adducts of sulfathiazole. *Chem. Commun.,***2001***,* 7, 603-604.

(23) Brittain, H. G. Polymorphism and solvatomorphism, *J. Phar,. Sci.,* **2010**, 101(2), 464-484.

(24) Clarke, H. D.; Arora, K. K.; Bass, H.; Kavuru, P.; Ong, T. T.; Pujari, T.; Wojtas, L.; Zaworotko, M. J., Structure−stability relationships in cocrystal hydrates: Does the promiscuity of water make crystalline hydrates the nemesis of crystal engineering? *Cryst. Growth Des.,* **2010**, *10*(5), 2152-2167.

(25) Tong, H. H.; Chow, A. S.; Chan, H.; Chow, A. H.; Wan, Y. K.; Williams, I. D.; Shek, F. L.; Chan, C. K., Process-induced phase transformation of berberine chloride hydrates. *J. Pharm. Sci.,* **2010**, *99*(4), 1942-1954.

(26) Vogt, F. G.; Dell'Orco, P. C.; Diederich, A. M.; Su, Q.; Wood, J. L.; Zuber, G. E.; Katrincic, L. M.; Mueller, R. L.; Busby, D. J.; DeBrosse, C. W., A study of variable hydration states in topotecan hydrochloride. *J. Pharm. Biomed. Anal.,* **2006**, *40*(5), 1080-1088.

(27) Khankari, R. K.; Grant, D. J., Pharmaceutical hydrates. *Thermochim. Acta.,* **1995**, *248*, 61-79.

(28) Hickey, M. B.; Peterson, M. L.; Manas, E. S.; Alvarez, J.; Haeffner, F.; Almarsson, Ö., Hydrates and solid-state reactivity: A survey of β-lactam antibiotics. *J. Pharm. Sci.,* **2007**, *96*(5), 1090-1099.

(29) Braun, D. E.; Kahlenberg, V.; Gelbrich, T.; Ludescher, J.; Griesser, U. J., Solid state characterisation of four solvates of R-cinacalcet hydrochloride. *CrystEngComm.,* **2008**, *10*(11), 1617-1625.

(30) Zencirci, N.; Griesser, U. J.; Gelbrich, T.; Kahlenberg, V.; Jetti, R. K. R.; Apperley, D. C.; Harris, R. K., New solvates of an old drug compound (Phenobarbital): Structure and stability. *J. Phys. Chem. B.,* **2014**, *118*(12), 3267-3280.

(31) Berge, S. M.; Bighley, L. D.; Monkhouse, D. C., Pharmaceutical salts. *J. Pharm. Sci.,* **1977**, *66*(1), 1-19.

(32) Stahl, P. H.; Wermuth, C. G., *Handbook of pharmaceutical salts: properties, selection, and use*. ed.; Wiley-Vch Weinheim, Germany: **2002**; Vol. 2.

(33) Lusi, M.; Vitorica-Yrezabal, I. J.; Zaworotko, M. J., Expanding the scope of molecular mixed crystals enabled by three component solid solutions. *Cryst. Growth Des.,* **2015**, *15*(8), 4098–4103.

(34) Kitaigorodsky, A. I., *Mixed crystals*. ed.; Springer Science & Business Media: 2**012**; Vol. 33.

(35) Aitipamula, S.; Banerjee, R.; Bansal, A. K.; Biradha, K.; Cheney, M. L.; Choudhury, A. R.; Desiraju, G. R.; Dikundwar, A. G.; Dubey, R.; Duggirala, N.; Ghogale, P. P.; Ghosh, S.; Goswami, P. K.; Goud, N. R.; Jetti, R. R. K. R.; Karpinski, P.; Kaushik, P.; Kumar, D.; Kumar, V.; Moulton, B.; Mukherjee, A.; Mukherjee, G.; Myerson, A. S.; Puri, V.; Ramanan, A.; Rajamannar, T.; Reddy, C. M.; Rodriguez-Hornedo, N.; Rogers, R. D.; Row, T. N. G.; Sanphui, P.; Shan, N.; Shete, G.; Singh, A.; Sun, C. C.; Swift, J. A.; Thaimattam, R.; Thakur, T. S.; Kumar Thaper, R.; Thomas, S. P.; Tothadi, S.; Vangala, V. R.; Variankaval, N.; Vishweshwar, P.; Weyna, D. R.; Zaworotko, M. J., Polymorphs, salts, and cocrystals: What's in a name? *Cryst. Growth Des.,* **2012**, *12*(5), 2147-2152.

(36) Wohler, F., *Annalen,* **1844**, *51*.

(37) Sakurai, T., The crystal structure of the triclinic modification of quinhydrone. *Acta Crystallogr.,* **1965**, *19*(3), 320-330.

(38) Sakurai, T., On the refinement of the crystal structures of phenoquinone and monoclinic quinhydrone. *Acta Crystallogr. Sect. B-Struct. Sci.,* **1968**, *24*(3), 403-412.

(39) F. von Heyden et al. 769,586, **1934**.

(40) Buehler, C.; Heap, A. G., A study of molecular organic molecular organic compounds. I. The molecular organic ompounds organic compounds of meta-

dinitrobenzene, 2-4-dinitoulene and 2-4-dinitrophenol.. *J. Am. Chem. Soc.,* **1926**, *48*(12), 3168-3172.

(41) Anderson, J. S., *Nature.,* **1937**, *140*, 583-584.

(42) Higuchi, T.; Ikeda, M., Rapidly dissolving forms of digoxin: Hydroquinone complex. *J. Pharm. Sci.,* **1974**, *63*(5), 809-811.

(43) Bochner, F.; Huffman, D. H.; Shen, D. D.; Azarnoff, D. L., Bioavailability of digoxin-hydroquinone complex: A new oral digoxin formulation. *J. Pharm. Sci.,* **1977**, *66*(5), 644-647.

(44) Childs, S. L.; Stahly, G. P.; Park, A., The salt-cocrystal continuum: the influence of crystal structure on ionization state. *Mol. Pharm.,* **2007,** *4*(3), 323-338.

(45) Aakeröy, C. B.; Fasulo, M. E.; Desper, J., Cocrystal or salt: Does it really matter? *Mol. Pharm.,* **2007**, *4*(3), 317-322.

(46) Dalman, L. H., Ternary systems of urea and acids. I. Urea, nitric acid and water. II. Urea, sulfuric acid and water. III. Urea, oxalic acid and water. *J. Am. Chem. Soc.,* **1934**, *56*(3), 549-553.

(47) Harkema, S.; Bats, J. W.; Weyenberg, A. M.; Feil, D., The crystal structure of urea oxalic acid (2:1). *Acta Crystallogr. Sect. B-Struct. Sci.,* **1972**, *28*(5), 1646-1648.

(48) Harkema, S.; Ter Brake, J. H. M., Structure and thermal expansion of urea-oxalic acid (1:1). *Acta Crystallogr. Sect. B-Struct. Sci.,* **1979**, *35*(4), 1011-1013.

(49) Hoogsteen, K., The structure of crystals containing a hydrogen-bonded complex of 1-methylthymine and 9-methyladenine. *Acta Crystallogr.,* **1959**, *12*(10), 822-823.

(50) Etter, M. C.; Reutzel, S. M.; Choo, C. G., Self-organization of adenine and thymine in the solid state. *J. Am. Chem. Soc.,* **1993**, *115*(10), 4411-4412.

(51) Etter, M. C.; Frankenbach, G. M., Hydrogen-bond directed cocrystallization as a tool for designing acentric organic solids. *Chem. Mater.,* **1989**, *1*(1), 10-12.

(52) Etter, M. C., Hydrogen bonds as design elements in organic chemistry. *J. Phys. Chem.,* **1991**, *95*(12), 4601-4610.

(53) Etter, M. C., Encoding and decoding hydrogen-bond patterns of organic compounds. *Acc. Chem. Res.,* **1990**, *23*(4), 120-126.

(54) Pekker, S.; Kovats, E.; Oszlanyi, G.; Benyei, G.; Klupp, G.; Bortel, G.; Jalsovszky, I.; Jakab, E.; Borondics, F.; Kamaras, K.; Bokor, M.; Kriza, G.; Tompa, K.; Faigel, G., Rotor-stator molecular crystals of fullerenes with cubane. *Nat. Mater.,* **2005**, *4*(10), 764-767.

(55) Schmidt, G., Photodimerization in the solid state. *Pure Appl. Chem.,* **1971**, *27*(4), 647-678.

(56) Desiraju, G. R., Crystal Engineering: The Design of Organic Solids. ed.; Elsevier: **1989**.

(57) Kitagawa, S.; Kitaura, R.; Noro, S. i., Functional porous coordination polymers. *Angew. Chem. Int. Ed.,* **2004**, *43*(18), 2334-2375.

(58) Etter, M. C., Hydrogen-bonds as design elements in organic-chemistry. *J. Phys. Chem.,* **1991**, *95*(12), 4601-4610.

(59) Etter, M. C.; MacDonald, J. C.; Bernstein, J., Graph-set analysis of hydrogen-bond patterns in organic crystals. *Acta Crystallogr. Sect. B-Struct. Sci.,* **1990**, *46*(2), 256-262.

(60) Nangia, A.; Desiraju, G. R., Supramolecular synthons and pattern recognition. *Design of Organic Solids.,* **1998**, *198*, 57-95.

(61) Desiraju, G. R., Supramolecular synthons in crystal engineering–a new organic synthesis. *Angew. Chem. Int. Ed.,* **1995**, *34*(21), 2311-2327.

(62) Walsh, R. D. B.; Bradner, M. W.; Fleischman, S.; Morales, L. A.; Moulton, B.; Rodriguez-Hornedo, N.; Zaworotko, M. J., Crystal engineering of the composition of pharmaceutical phases. *Chem. Commun.,* **2003**, (2), 186-187.

(63) Huang, C.-M.; Leiserowitz, L.; Schmidt, G. M. J., Molecular packing modes. Part XI. Crystal structures of the 2:1 complexes of benzamide with succinic acid and furamide with oxalic acid. *J. Chem. Soc., Perkin Trans. 2.,* **1973**, (5), 503-508.

(64) Leiserowitz, L.; Nader, F., The molecular packing modes and the hydrogen-bonding properties of amide:dicarboxylic acid complexes. *Acta Crystallogr. Sect. B-Struct. Sci.,* **1977**, *33*(9), 2719-2733.

(65) Aakeröy, C. B.; Beatty, A. M.; Helfrich, B. A., "Total Synthesis" supramolecular style: Design and hydrogen-bond-directed assembly of ternary supermolecules. *Angew. Chem. Int. Ed.,* **2001**, *40*(17), 3240-3242.

(66) Aakeröy, C. B.; Beatty, A. M.; Helfrich, B. A., A High-yielding supramolecular reaction. *J. Am. Chem. Soc.,* **2002**, *124*(48), 14425-14432.

(67) Aakeröy, C. B.; Beatty, A. M.; Helfrich, B. A.; Nieuwenhuyzen, M., Do polymorphic compounds make good cocrystallizing agents? A structural case study that demonstrates the importance of synthon flexibility. *Cryst. Growth Des.,* **2003**, *3*(2), 159-165.

(68) Fleischman, S. G.; Kuduva, S. S.; McMahon, J. A.; Moulton, B.; Bailey Walsh, R. D.; Rodríguez-Hornedo, N.; Zaworotko, M. J., Crystal Engineering of the composition of pharmaceutical phases: Multiple-component crystalline solids involving carbamazepine. *Cryst. Growth Des.,* **2003**, *3*(6), 909-919.

(69) Aakeroy, C. B.; Desper, J.; Helfrich, B. A., Heteromeric intermolecular interactions as synthetic tools for the formation of binary co-crystals. *CrystEngComm.,* **2004**, *6*(5), 19-24.

(70) Reddy, L. S.; Nangia, A.; Lynch, V. M., Phenyl-perfluorophenyl synthon mediated cocrystallization of carboxylic acids and amides. *Cryst. Growth Des.,* **2004**, *4*(1), 89-94.

(71) J. A. McMahon; J. A. Bis; P. Vishweshwar; T. R. Shattock; McLaughlin, O. L.; Zaworotko, M. J., Crystal engineering of the composition of pharmaceutical phases. 3. Primary amide supramolecular heterosynthons and their role in the design of pharmaceutical co-crystals. *Z. Kristallogr.,* **2005**, *220*(4), 340.

(72) Vishweshwar., P.; McMahon., J. A.; Peterson., M. L.; Hickey., M. B.; Shattock., T. R.; Zaworotko., M. J., Crystal engineering of pharmaceutical co-crystals from polymorphic active pharmaceutical ingredients. *Chem. Commun.,* **2005**, *36*(36), 4601-4603.

(73) Fernandes, P.; Bardin, J.; Johnston, A.; Florence, A. J.; Leech, C. K.; David, W. I. F.; Shankland, K., Carbamazepine trifluoroacetic acid solvate. *Acta Crystallogr. Sect. E:,* **2007**, *63*(11), o4269.

(74) Bhogala, B. R.; Basavoju, S.; Nangia, A., Tape and layer structures in cocrystals of some di- and tricarboxylic acids with 4,4[prime or minute]-bipyridines and isonicotinamide. From binary to ternary cocrystals. *CrystEngComm.,* **2005**, *7*(90), 551-562.

(75) Edwards, M. R.; Jones, W.; Motherwell, W. D. S., Cocrystal formation of 4-methyl and 4-chlorobenzamide with carboxylic acids: Chloro/methyl interchange and crystal structure. *CrystEngComm.,* **2006**, *8*(7), 545-551.

(76) Bensemann, I.; Gdaniec, M.; Lakomecka, K.; Milewska, M. J.; Polonski, T., Creation of hydrogen bonded 1D networks by co-crystallization of N,N '-bis(2-pyridyl)aryldiamines with dicarboxylic acids. *Org. Biomol. Chem.,* **2003**, *1*(8), 1425-1434.

(77) Bhogala, B. R.; Nangia, A., Ternary and quaternary co-crystals of 1,3-cis,5-cis-cyclohexanetricarboxylic acid and 4,4 '-bipyridines. *New J. Chem.,* **2008**, *32*(5), 800-807.

(78) Bis, J. A.; Zaworotko, M. J., The 2-aminopyridinium-carboxylate supramolecular heterosynthon: A robust motif for generation of multiple-component crystals. *Cryst. Growth Des.,* **2005**, *5*(3), 1169-1179.

(79) Du, M.; Zhang, Z. H.; Zhao, X. J., Cocrystallization of bent dipyridyl type compounds with aromatic dicarboxylic acids: Effect of the geometries of building blocks on hydrogen-bonding supramolecular patterns. *Cryst. Growth Des.,* **2005**, *5*(3), 1199-1208.

(80) Haynes, D. A.; Jones, W.; Motherwell, W. D. S., Cocrystallisation of succinic and fumaric acids with lutidines: a systematic study. *CrystEngcomm.,* **2006**, *8*(11), 830-840.

(81) Lynch, D. E.; Smith, G.; Freney, D.; Byriel, K. A.; Kennard, C. H. L., Molecular cocrystals of carboxylic-Acids .15. Preparation and characterization of heterocyclic base adducts with a series of carboxylic-acids, and the crystal-structures of the adducts of 2-aminopyrimidine with 2,6-dihydroxybenzoic acid, 4-aminobenzoic acid, phenoxyacetic acid, (2,4-dichlorophenoxy)acetic acid, (3,4-dichlorophenoxy)-acetic acid and salicylic-acid, and 2-aminopyridine with 2,6-dihydroxybenzoic acid. *Aust. J. Chem.,* **1994**, *47*(6), 1097-1115.

(82) Papaefstathiou, G. S.; Kipp, A. J.; MacGillivray, L. R., Exploiting modularity in template-controlled synthesis: a new linear template to direct reactivity within discrete hydrogen-bonded molecular assemblies in the solid state. *Chem. Commun.,* **2001**, (23), 2462-2463.

(83) Pedireddi, V. R.; Chatterjee, S.; Ranganathan, A.; Rao, C. N. R., A study of supramolecular hydrogen bonded complexes formed by aliphatic dicarboxylic acids with azaaromatic donors. *Tetrahedron.,* **1998**, *54*(32), 9457-9474.

(84) Thakur, T. S.; Desiraju, G. R., Crystal Structure Prediction of a Co-Crystal Using a Supramolecular Synthon Approach: 2-Methylbenzoic Acid-2-Amino-4-methylpyrimidine. *Cryst. Growth Des.,* **2008**, *8*(11), 4031-4044.

(85) Xiao, J.; Yang, M.; Lauher, J. W.; Fowler, F. W., A supramolecular solution to a long-standing problem: The 1,6-polymerization of a triacetylene. *Angew. Chem. Int. Ed.,* **2000**, *39*(12), 2132.

(86) Aakeroy, C. B.; Hussain, I.; Forbes, S.; Desper, J., Exploring the hydrogen-bond preference of N-H moieties in co-crystals assembled via O-H(acid)center dot center dot center dot N(py) intermolecular interactions. *CrystEngComm.,* **2007**, *9*(1), 46-54.

(87) Santra, R.; Ghosh, N.; Biradha, K., Crystal engineering with acid and pyridine heteromeric synthon: neutral and ionic co-crystals. *New J. Chem.,* **2008**, *32*(10), 1673-1676.

(88) Bis, J. A.; Vishweshwar, P.; Weyna, D.; Zaworotko, M. J., Hierarchy of supramolecular synthons: Persistent hydroxyl···pyridine hydrogen bonds in cocrystals that contain a cyano acceptor. *Mol. Pharm.,* **2007**, *4*(3), 401-416.

(89) Friscic, T.; Drab, D. M.; MacGillivray, L. R., A test for homology: Photoactive crystalline assemblies involving linear templates based on a homologous series of phloroglucinols. *Org. Lett.,* **2004**, *6*(25), 4647-4650.

(90) Papaefstathiou, G. S.; MacGillivray, L. R., Discrete versus infinite molecular self-assembly: Control in crystalline hydrogen-bonded assemblies based on resorcinol. *Org. Lett.,* **2001**, *3*(24), 3835-3838.

(91) MacGillivray, L. R.; Reid, J. L.; Ripmeester, J. A., Supramolecular control of reactivity in the solid state using linear molecular templates. *J. Am. Chem. Soc.,* **2000**, *122*(32), 7817-7818.

(92) Tanaka, T.; Tasaki, T.; Aoyama, Y., Acridinylresorcinol as a self-complementary building block of robust hydrogen-bonded 2D nets with coordinative saturation. Preservation of crystal structures upon guest alteration, guest removal, and host modification. *J. Am. Chem. Soc.,* **2002**, *124*(42), 12453-12462.

(93) Varughese, S.; Pedireddi, V. R., A competitive molecular recognition study: Syntheses and analysis of supramolecular assemblies of 3,5-dihydroxybenzoic acid and its bromo derivative with some N-donor compounds. *Chem. Eur. J.,* **2006**, *12*(6), 1597-1609.

(94) Vishweshwar, P.; Nangia, A.; Lynch, V. M., Supramolecular synthons in phenol-isonicotinamide adducts. *CrystEngComm.,* **2003**, *5*(31), 164-168.

(95) Zeng, Q. D.; Wu, D. X.; Wang, C.; Ma, H. W.; Lu, J.; Liu, C. M.; Xu, S. D.; Li, Y.; Bai, C. L., Supramolecular structures based on bis(2-hydroxy-5-chlorophenyl) sulfide and spirobicromane with bipyridines. *Cryst. Growth Des.,* **2005**, *5*(5), 1889-1896.

(96) Dey, A.; Kirchner, M. T.; Vangala, V. R.; Desiraju, G. R.; Mondal, R.; Howard, J. A. K., Crystal structure prediction of aminols: Advantages of a supramolecular synthon approach with experimental structures. *J. Am. Chem. Soc.,* **2005**, *127*(30), 10545-10559.

(97) Hanessian, S.; Saladino, R.; Margarita, R.; Simard, M., Supramolecular chirons based on enantiodifferentiating self-assembly between amines and alcohols (supraminols). *Chem. Eur. J.,* **1999**, *5*(7), 2169-2183.

(98) Mondal, R.; Howard, J. A. K.; Banerjee, R.; Desiraju, G. R., Crystallographic studies of supramolecular synthons in amine solvates of trans-1,5-dichloro-9,10-diethynyl-9,10-dihydroanthracene-9,10-diol. *Cryst. Growth Des.,* **2006**, *6*(11), 2507-2516.

(99) Vangala, V. R.; Mondal, R.; Broder, C. K.; Howard, J. A. K.; Desiraju, G. R., Dianiline-diphenol molecular complexes based on supraminol recognition. *Cryst. Growth Des.,* **2005**, *5*(1), 99-104.

(100) Childs, S. L.; Chyall, L. J.; Dunlap, J. T.; Smolenskaya, V. N.; Stahly, B. C.; Stahly, G. P., Crystal engineering approach to forming cocrystals of amine hydrochlorides with organic acids. Molecular complexes of fluoxetine hydrochloride with benzoic, succinic, and fumaric acids. *J. Am. Chem. Soc.,* **2004**, *126*(41), 13335-13342.

(101) Remenar, J. F.; Morissette, S. L.; Peterson, M. L.; Moulton, B.; MacPhee, J. M.; Guzmán, H. R.; Almarsson, Ö., Crystal engineering of novel cocrystals of a triazole drug with 1,4-dicarboxylic acids. *J. Am. Chem. Soc.,* **2003**, *125*(28), 8456-8457.

(102) Duggirala, N. K.; Wood, G. P. F.; Fischer, A.; Wojtas, Ł.; Perry, M. L.; Zaworotko, M. J., Hydrogen bond hierarchy: Persistent phenol···chloride

hydrogen bonds in the presence of carboxylic acid moieties. *Cryst. Growth Des.,* **2015**, *15*(9), 4341-4354.

(103) Aakeröy, C. B.; Epa, K.; Forbes, S.; Schultheiss, N.; Desper, J., Ranking relative hydrogen-bond strengths in hydroxybenzoic acids for crystal-engineering purposes. *Chem. Eur. J.,* **2013**, *19*(44), 14998-15003.

(104) Galek, P. T. A.; Pidcock, E.; Wood, P. A.; Bruno, I. J.; Groom, C. R., One in half a million: a solid form informatics study of a pharmaceutical crystal structure. *CrystEngComm.,* **2012**, *14*(7), 2391-2403.

(105) Shattock, T. R.; Arora, K. K.; Vishweshwar, P.; Zaworotko, M. J., Hierarchy of supramolecular synthons: Persistent carboxylic acid···pyridine hydrogen bonds in cocrystals that also contain a hydroxyl moiety. *Cryst. Growth Des.,* **2008**, *8*(12), 4533-4545.

(106) Bis, J. A.; Vishweshwar, P.; Weyna, D.; Zaworotko, M. J., Hierarchy of supramolecular synthons: Persistent hydroxyl···pyridine hydrogen bonds in cocrystals that contain a cyano acceptor. *Mol. Pharm.,* **2007**, *4*(3), 401-416.

(107) Kavuru, P.; Aboarayes, D.; Arora, K. K.; Clarke, H. D.; Kennedy, A.; Marshall, L.; Ong, T. T.; Perman, J.; Pujari, T.; Wojtas, Ł., Hierarchy of supramolecular synthons: persistent hydrogen bonds between carboxylates and weakly acidic hydroxyl moieties in cocrystals of zwitterions. *Cryst. Growth Des.,* **2010**, *10*(8), 3568-3584.

(108) Aakeroy, C. B.; Epa, K. N.; Forbes, S.; Desper, J., Competing hydrogen-bond donors: phenols vs. cyanooximes. *CrystEngComm,* **2013**, *15*(30), 5946-5949.

(109) Metrangolo, P., Resnati, G., Pilati, T. and Biella, S. *Halogen bonding in crystal engineering,* **2008**, Springer.

(110) Corradi, E., Meille, S. V., Messina, M. T., Metrangolo, P. and Resnati, G. Halogen bonding versus hydrogen bonding in driving self-assembly processes', *Angew. Chem., Int. Ed.,* **2000**, 39(10), 1782-1786.

(111) Aakeröy, C. B., Panikkattu, S., Chopade, P. D. and Desper, J. Competing hydrogen-bond and halogen-bond donors in crystal engineering', *CrystEngComm.,* **2013**, 15(16), 3125-3136.

(112) Aaker. y, C. B., Schultheiss, N. C., Rajbanshi, A., Desper, J. and Moore, C. Supramolecular synthesis based on a combination of hydrogen and halogen bonds, *Cryst. Growth Des.,* **2008**, 9(1), 432-441.

(113) F. H Allen; Kennard, O., 3D search and research using the Cambridge Cristallogaphic Database. Chem. *Des. Autom. News.,* **1993**, *8*, 31-37.

(114) Allen, F. H., The Cambridge Structural Database: a quarter of a million crystal structures and rising. *Acta Crystallogr. Sect. B-Struct. Sci.,* **2002**, *B58*(3), 380-388.

(115)

http://www.fda.gov/Food/IngredientsPackagingLabeling/GRAS/SCOGS/default.htm

(116) Fábián, L., Cambridge Structural Database analysis of molecular complementarity in cocrystals. *Cryst. Growth Des.,* **2009**, *9*(3), 1436-1443.

(117) Karamertzanis, P. G.; Kazantsev, A. V.; Issa, N.; Welch, G. W. A.; Adjiman, C. S.; Pantelides, C. C.; Price, S. L., Can the Formation of pharmaceutical cocrystals be computationally predicted? 2. Crystal structure prediction. *J. Chem. Theory Comput.,* **2009**, *5*(5), 1432-1448.

(118) Musumeci, D.; Hunter, C. A.; Prohens, R.; Scuderi, S.; McCabe, J. F., Virtual cocrystal screening. *Chem. Sci.,* **2011**, *2*(5), 883-890.

(119) Abramov, Y. A.; Loschen, C.; Klamt, A., Rational coformer or solvent selection for pharmaceutical cocrystallization or desolvation. *J. Pharm. Sci.,* **2012**, *101*(10), 3687-3697.

(120) James, S. L.; Adams, C. J.; Bolm, C.; Braga, D.; Collier, P.; Friscic, T.; Grepioni, F.; Harris, K. D. M.; Hyett, G.; Jones, W.; Krebs, A.; Mack, J.; Maini, L.; Orpen, A. G.; Parkin, I. P.; Shearouse, W. C.; Steed, J. W.; Waddell, D. C., Mechanochemistry: opportunities for new and cleaner synthesis. *Chem. Soc. Rev.,* **2012**, *41*(1), 413-447.

(121) Shan, N.; Toda, F.; Jones, W., Mechanochemistry and co-crystal formation: effect of solvent on reaction kinetics. *Chem. Commun.,* **2002**, (20), 2372-2373.

(122) Hasa, D.; Schneider Rauber, G.; Voinovich, D.; Jones, W., Cocrystal formation through mechanochemistry: From neat and liquid-assisted grinding to polymer-assisted grinding. *Angew. Chem., Int. Ed.,* **2015**, *54*(25), 7371-7375.

(123) Aher, S.; Dhumal, R.; Mahadik, K.; Paradkar, A.; York, P., Ultrasound assisted cocrystallization from solution (USSC) containing a non-congruently soluble cocrystal component pair: Caffeine/maleic acid. *Eur. J. Pharm. Sci.,* **2010**, *41*(5), 597-602.

(124) Morissette, S. L.; Almarsson, Ö.; Peterson, M. L.; Remenar, J. F.; Read, M. J.; Lemmo, A. V.; Ellis, S.; Cima, M. J.; Gardner, C. R., High-throughput crystallization: polymorphs, salts, co-crystals and solvates of pharmaceutical solids. *Adv. Drug Deliv. Rev.,* **2004**, *56*(3), 275-300.

(125) Kojima, T.; Tsutsumi, S.; Yamamoto, K.; Ikeda, Y.; Moriwaki, T., High-throughput cocrystal slurry screening by use of in situ Raman microscopy and multi-well plate. *Int. J. Pharm.,* **2010**, *399*(1–2), 52-59.

(126) Goyal, S.; Thorson, M. R.; Zhang, G. G. Z.; Gong, Y.; Kenis, P. J. A., Microfluidic approach to cocrystal screening of pharmaceutical parent compounds. *Cryst. Growth Des.,* **2012**, *12*(12), 6023-6034.

(127) Padrela, L.; Rodrigues, M. A.; Velaga, S. P.; Matos, H. A.; de Azevedo, E. G., Formation of indomethacin–saccharin cocrystals using supercritical fluid technology. *Eur. J. Pharm. Sci.,* **2009**, *38*(1), 9-17.

(128) Berry, D. J.; Seaton, C. C.; Clegg, W.; Harrington, R. W.; Coles, S. J.; Horton, P. N.; Hursthouse, M. B.; Storey, R.; Jones, W.; Friščić, T.; Blagden, N., Applying Hot-Stage Microscopy to Co-Crystal Screening: A Study of nicotinamide with seven active pharmaceutical ingredients. *Cryst. Growth Des.,* **2008**, *8*(5), 1697-1712.

(129) McCrone, W. C., Physics and Chemistry of the Organic Solid State, eds. D. Fox, M. M. Labes and A. Weissberger, Interscience Publishers, London, **1965**, 2(725-767).

(130) Lapidus, S. H.; Stephens, P. W.; Arora, K. K.; Shattock, T. R.; Zaworotko, M. J., A comparison of cocrystal structure solutions from powder and single crystal techniques. *Cryst. Growth Des.,* **2010**, *10*(10), 4630-4637.

(131) Mukherjee, A.; Tothadi, S.; Chakraborty, S.; Ganguly, S.; Desiraju, G. R., Synthon identification in co-crystals and polymorphs with IR spectroscopy. Primary amides as a case study. *CrystEngComm.,* **2013**, *15*(23), 4640-4654.

(132) Kojima, T.; Tsutsumi, S.; Yamamoto, K.; Ikeda, Y.; Moriwaki, T., High-throughput cocrystal slurry screening by use of in situ Raman microscopy and multi-well plate. *Int. J. Pharm.,* **2010**, *399*(1), 52-59.

(133) Burley, J. C.; Alkhalil, A.; Bloomfield, M.; Matousek, P., Transmission Raman spectroscopy for quality control in model cocrystal tablets. *Analyst.,* **2012**, *137*(13), 3052-3057.

(134) Vogt, F. G.; Clawson, J. S.; Strohmeier, M.; Edwards, A. J.; Pham, T. N.; Watson, S. A., Solid-State NMR analysis of organic cocrystals and complexes. *Cryst. Growth Des.,* **2009**, *9*(2), 921-937.

(135) Maruyoshi, K.; Iuga, D.; Antzutkin, O. N.; Alhalaweh, A.; Velaga, S. P.; Brown, S. P., Identifying the intermolecular hydrogen-bonding supramolecular synthons in an indomethacin-nicotinamide cocrystal by solid-state NMR. *Chem. Commun.,* **2012**, *48*(88), 10844-10846.

(136) Parrott, E. P. J.; Zeitler, J. A.; Friščić, T.; Pepper, M.; Jones, W.; Day, G. M.; Gladden, L. F., Testing the sensitivity of terahertz Spectroscopy to changes in molecular and supramolecular structure: A study of structurally similar cocrystals. *Cryst. Growth Des.,* **2009**, *9*(3), 1452-1460.

(137) Stevens, J. S.; Newton, L. K.; Jaye, C.; Muryn, C. A.; Fischer, D. A.; Schroeder, S. L. M., Proton transfer, hydrogen bonding, and disorder: Nitrogen near-edge X-ray absorption fine structure and X-ray photoelectron spectroscopy of bipyridine–acid salts and co-crystals. *Cryst. Growth Des.,* **2015**, *15*(4), 1776-1783.

(138) Trask, A. V.; Motherwell, W. D. S.; Jones, W., Pharmaceutical cocrystallization: Engineering a remedy for caffeine hydration. *Cryst. Growth Des.,* **2005**, *5*(3), 1013-1021.

(139) Trask, A. V.; Motherwell, W. D. S.; Jones, W., Physical stability enhancement of theophylline via cocrystallization. *Int. J. Pharm.,* **2006**, *320*, 114-123.

(140) Wang, J.-R.; Zhou, C.; Yu, X.; Mei, X., Stabilizing vitamin D 3 by conformationally selective co-crystallization. *Chem. Commun.,* **2014**, *50*(7), 855-858.

(141) Karki, S.; Friščić, T.; Fábián, L.; Laity, P. R.; Day, G. M.; Jones, W., Improving mechanical properties of crystalline solids by cocrystal formation: new compressible forms of paracetamol. *Adv. Mater.,* **2009**, *21*(38-39), 3905-3909.

(142) Cocrystals of pyrrolidinones. UCB Pharma, WO/2007/141002 A1.

(143) Remenar, J. F.; Peterson, M. L.; Stephens, P. W.; Zhang, Z.; Zimenkov, Y.; Hickey, M. B., Celecoxib: Nicotinamide dissociation: Using excipients to capture the cocrystal's potential. *Mol. Pharm.,* **2007**, *4*(3), 386-400.

(144) Alhalaweh, A.; Ali, H. R. H.; Velaga, S. P., Effects of polymer and surfactant on the dissolution and transformation profiles of cocrystals in aqueous media. *Cryst. Growth Des.,* **2013**, *14*(2), 643-648.

(145) Huang, N.; Rodríguez-Hornedo, N., Effect of micellar solubilization on cocrystal solubility and stability. *Cryst. Growth Des.,* **2010,** *10*(5), 2050-2053.

(146) Abourahma, H.; Urban, J. M.; Morozowich, N.; Chan, B., Examining the robustness of a theophylline cocrystal during grinding with additives. *CrystEngComm.,* **2012**, *14*(19), 6163-6169.

(147) Arora, K. K.; Tayade, N. G.; Suryanarayanan, R., Unintended water mediated cocrystal formation in carbamazepine and aspirin tablets. *Mol. Pharm.,* **2011**, *8*(3), 982-989.

(148) Baldrighi, M.; Cavallo, G.; Chierotti, M. R.; Gobetto, R.; Metrangolo, P.; Pilati, T.; Resnati, G.; Terraneo, G., Halogen bonding and pharmaceutical cocrystals: The case of a widely used preservative. *Mol. Pharm.,* **2013**, *10*(5), 1760-1772.

(149) Shan, N.; Perry, M. L.; Weyna, D. R.; Zaworotko, M. J., Impact of pharmaceutical cocrystals: the effects on drug pharmacokinetics. *Expert Opin. Drug Metab. Toxicol.,* **2014**, *10*(9), 1255-1271.

(150) Amidon, G.; Lennernäs, H.; Shah, V.; Crison, J., A Theoretical basis for a biopharmaceutic drug classification: The correlation of in vitro drug product dissolution and in vivo bioavailability. *Pharm. Res.,* **1995**, *12*(3), 413-420.

(151) Weyna, D. R.; Cheney, M. L.; Shan, N.; Hanna, M.; Zaworotko, M. J.; Sava, V.; Song, S.; Sanchez-Ramos, J. R., Improving solubility and pharmacokinetics of meloxicam via multiple-component crystal formation. *Mol. Pharm.,* **2012**, *9*(7), 2094-2102.

(152) Sheikh, A. Y.; Rahim, S. A.; Hammond, R. B.; Roberts, K. J., Scalable solution cocrystallization: case of carbamazepine-nicotinamide I. *CrystEngComm.,* **2009**, *11*(3), 501-509.

(153) Croker, D. M., Foreman, M. E., Hogan, B. N., Maguire, N. M., Elcoate, C. J., Hodnett, B. K., Maguire, A. R., Rasmuson, Å. C. and Lawrence, S. E. Understanding the p-Toluenesulfonamide/Triphenylphosphine Oxide Crystal Chemistry: A New 1:1 Cocrystal and Ternary Phase Diagram., *Cryst. Growth Des,* **2012**, 12(2), 869-875.

(154) Billot, P.; Hosek, P.; Perrin, M.-A., Efficient purification of an active pharmaceutical ingredient via cocrystallization: From thermodynamics to scale-up. *Org. Process Res. Dev.,* **2013**, *17*(3), 505-511.

(155) Hsi, K. H. Y.; Concepcion, A. J.; Kenny, M.; Magzoub, A. A.; Myerson, A. S., Purification of amoxicillin trihydrate by impurity-coformer complexation in solution. *CrystEngComm.,* **2013**, *15*(34), 6776-6781.

(156) Khan, M.; Enkelmann, V.; Brunklaus, G., Crystal engineering of pharmaceutical co-crystals: Application of methyl paraben as molecular hook. *J. Am. Chem. Soc.,* **2010**, *132*(14), 5254-5263.

(157) Hickey, M. B.; Peterson, M. L.; Scoppettuolo, L. A.; Morrisette, S. L.; Vetter, A.; Guzmán, H.; Remenar, J. F.; Zhang, Z.; Tawa, M. D.; Haley, S.; Zaworotko, M. J.; Almarsson, Ö., Performance comparison of a co-crystal of carbamazepine with marketed product. *Eur. J. Pharm. Biopharm.,* **2007**, *67*(1), 112-119.

(158) Nehm, S. J.; Rodríguez-Spong, B.; Rodríguez-Hornedo, N., Phase solubility diagrams of cocrystals are explained by solubility product and solution complexation. *Cryst. Growth Des.,* **2006**, *6*(2), 592-600.

(159) Jayasankar, A.; Reddy, L. S.; Bethune, S. J.; Rodríguez-Hornedo, N., Role of cocrystal and solution chemistry on the formation and stability of cocrystals with different stoichiometry. *Cryst. Growth Des.,* **2009**, *9*(2), 889-897.

(160) Good, D. J.; Rodríguez-Hornedo, N., Cocrystal eutectic constants and prediction of solubility behavior. *Cryst. Growth Des.,* **2010**, *10*(3), 1028-1032.

(161) Medina, C.; Daurio, D.; Nagapudi, K.; Alvarez-Nunez, F., Manufacture of pharmaceutical co-crystals using twin screw extrusion: A solvent-less and scalable process. *J. Pharm. Sci.,* **2010**, *99*(4), 1693-1696.

(162) am Ende, D. J.; Anderson, S. R.; Salan, J. S., Development and Scale-Up of Cocrystals Using Resonant Acoustic Mixing. *Org. Process Res. Dev.,* **2014**, *18*(2), 331-341.

(163) Alhalaweh, A.; Kaialy, W.; Buckton, G.; Gill, H.; Nokhodchi, A.; Velaga, S., Theophylline cocrystals prepared by spray drying: Physicochemical properties and aerosolization performance. *AAPS PharmSciTech.,* **2013**, *14*(1), 265-276.

(164) Zhao, L.; Raval, V.; Briggs, N. E. B.; Bhardwaj, R. M.; McGlone, T.; Oswald, I. D. H.; Florence, A. J., From discovery to scale-up: [α]-lipoic acid : nicotinamide co-crystals in a continuous oscillatory baffled crystalliser. *CrystEngComm.,* **2014**, *16*(26), 5769-5780.

(165) Almarsson, Ö.; Peterson, M. L.; Zaworotko, M., The A to Z of pharmaceutical cocrystals: a decade of fast-moving new science and patents. *Pharm. Pat. Anal.,* **2012**, *1*(3), 313-327.

(166) Childs, S. L.; Stahly, G. P.; Park, A., The salt−cocrystal continuum: The influence of crystal structure on ionization state. *Mol. Pharm.,* **2007**, *4*(3), 323-338.

(167) Karki, S.; Friščić, T.; Jones, W.; Motherwell, W. D. S., Screening for pharmaceutical cocrystal hydrates via neat and liquid-assisted grinding. *Mol. Pharm.,* **2007**, *4*(3), 347-354.

(168) Sherman, B. C. 6,077,542, **2000**.

(169) Harrison, W. T. A.; Yathirajan, H. S.; Bindya, S.; Anilkumar, H. G.; Devaraju, Escitalopram oxalate: co-existence of oxalate dianions and oxalic acid molecules in the same crystal. *Acta Crystallogr., Sect. C.,* **2007**, *63*(2), o129-o131.

(170) Reflection paper on the use of cocrsytals of active substances in medicinal products,http://www.ema.europa.eu/docs/en_GB/document_library/Scientific_guideline/2015/07/WC500189927.pdf, (accessed on September 16th, **2015**).

(171) Toth, P. E.; Urtis, J., Commonly used muscle relaxant therapies for acute low back pain: a review of carisoprodol, cyclobenzaprine hydrochloride, and metaxalone. *Clin. Ther.,* **2004**, *26*(9), 1355-1367.

(172) Kandasamy, K.; Gowdra, V.; Nammalvar, H.; Govindarajan, A., Bioanalytical method development, validation and quantification of metaxalone in rat plasma

by liquid chromatography tandem mass spectrometry. *J Bioanal Biomed S.,* **2012**, *6*, 2.

(173) Chattopadhyay, J. S., S.; Mahanty. J, S.; Hazra, S.; Mitra, M.; Singh, M. K. US7750165 B2, **2005**.

(174) Lorimer, K. M., K. W.; Sun, T.; Watson, S.; Nielsen, K. US20090163561 A1, **2007**.

(175) Holland, J. F., C.; Chorlton, A.; Gooding, D. US 8,871,793 B2, **2014**.

(176) Childs, S. L.; Kandi, P.; Lingireddy, S. R., Formulation of a danazol cocrystal with controlled supersaturation plays an essential role in improving bioavailability. *Mol. Pharm.,* **2013**, *10*(8), 3112-3127.

(177) Dmowski, W.; Scholer, H.; Mahesh, V.; Greenblatt, R., Danazol--a synthetic steroid derivative with interesting physiologic properties. *Fertil. Steril.,* **1971**, *22*(1), 9-18.

(178) Kaukonen, A. M.; Boyd, B. J.; Charman, W. N.; Porter, C. J., Drug solubilization behavior during in vitro digestion of suspension formulations of poorly water-soluble drugs in triglyceride lipids. *Pharm. Res.,* **2004**, *21*(2), 254-260.

Portions of this chapter have been previously published: Naga, K. Duggirala, Miranda, L. Perry, Ö. Almarsson and Michael, J. Zaworotko, *ChemCommun.,* 2016, Advanced article, DOI: 10.1039/C5CC08216A – Reproduced by permission of the Royal Society of Chemistry.

http://pubs.rsc.org/en/content/articlepdf/2016/cc/c5cc08216a

Chapter 2: Ionic Cocrystals (ICCs)

2.1 Introduction

The current phase of drug development is facing cumulative challenges due to increasing research development costs, patent expiration of several drug products and the poor physicochemical properties of drug candidates. For example, approximately 40% of the marketed drug products and 75% of the new chemical entities are suffering with poor aqueous solubility [1]. When these drug substances are formulated at preclinical stage, the performance of drug is plagued with erratic and highly variable bioavailability. This could be a significant risk factor down the line in drug development that ultimately affects the safety and efficacy of the medicinal product. The main reason for poor physicochemical properties of APIs could be attributed to medicinal chemistry programs shifting towards screening of drug molecules by combinatorial approaches and high-throughput screening modalities that resulted hydrophobic molecules [2]. The issue poor physicochemical properties can be addressed either by covalent i.e. prodrug [3] or by non-covalent modifications of drug molecule. The prodrug approach has a number of challenges including additional work, time and cost associated with synthesis and toxicological assessment. On the other hand with rapid advances of crystal engineering, researchers in pharmaceutical science realized that by non-covalent modification i.e. manipulating the intermolecular interactions of crystal lattice it is possible to create novel crystal forms with improved physiochemical properties. While the early studies were largely focussed upon understanding the intermolecular interactions responsible to hold the crystal structure, now it is more towards the structure-property relationships and thanks to the field of crystal engineering.[4, 5]

Currently there are limited number of pre-formulation approaches to modify the crystal structure and properties of drug molecules that include polymorphs, hydrates, amorphous forms and salts. However in some cases the above approaches could be unsuccessful due to limited property modulation by polymorphs,[9] stability issues associated with amorphous/hydrated forms [6-8] and lack of ionisable functional groups for drug molecules. Therefore alternative pre-formulation approaches are constantly needed to improve the physicochemical properties of a drug substance at early stage of drug development. One of the promising approaches that gained more attention during the last decade to improve the physicochemical properties of drug molecules is pharmaceutical cocrystals.[10] This is mainly due to the fact that cocrystals are amenable to crystal engineering and large number of coformers available to fine tune the properties of APIs. Pharmaceutical cocrystals are proved to modulate the solubility, improve the stability and mechanical properties of APIs by manipulating the intermolecular interaction of API by cocrystallizing with a second molecule i.e. coformer.[11-22]

The definition of cocrystal has been a subject matter of scientific debate for a long time and a recent perspective article clarified cocrystal definition as '*Cocrystals are solids that are crystalline single phase materials composed of two or more crystalline single phase materials composed of two or more different molecular and/or ionic compounds generally in a stoichiometric ration which are neither solvates nor simple salts'*. [23] The history of categorizing the cocrystals containing organic molecules and inorganic molecules dates back to Paul Pfeiffer[24] and a review article by Stahly addressed ICCs containing inorganic salts.[25] The term ionic cocrystal (ICC) was coined by Braga research group in 2010 for the cocrystals containing inorganic metal salt and organic molecules.[26] Our research group categorized cocrystals into two types based on the type of molecules (neutral or ionic) present in the cocrystal; (**I**) when both of the coformers are neutral components (i.e. molecules including zwitterionic molecules), the resulting cocrystal is a *molecular cocrystal* (MCC), (**II**) If at least one of the components is an ionic compound i.e. a salt than the resulting cocrystal is an *ionic cocrystal* (ICC). A schematic representation of ICC is shown in the Scheme 2.1.

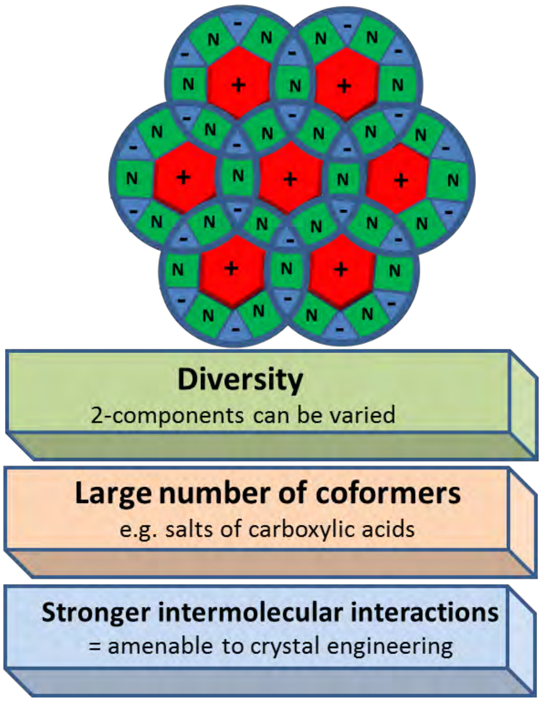

Scheme 2.1. Illustration of ICC containing a cation (+), anion (−) and a neutral molecule (N) or another salt

Compared to MCCs, ICCs are not well explored in terms of design and their applications in relevance to pharmaceutical science. The advantage of ICCs is, can improve the properties of both neutral as well as salt molecules. In an ICC, if at least one of the coformer is an API it can be considered as pharmaceutical ionic cocrystal. The API could be the part of salt (cation or anion) or a neutral molecule (N) or the combination thereof. Few examples of ICCs where the drug molecules are *cations* include (+); tedisamil sesquifumarate, [27] fluoxetine hydrochloride with benzoic acid,[20] *anions* (−); rosuvastatin calcium with sorbitol,[28] raltegravir potassium with cyclamic acid, [29] *neutral molecules* (N); ammonium chloride with carbamazepine[30] and calcium chloride with hydrocortisone.[31] Often ICCs can also be considered as coordination polymers as exemplified in case lithium salts with amino acids.[32]

In this chapter briefly addressed the history and few case studies of ICCs that improved the physicochemical properties and clinical performance of drug molecules.

2.2 Why are ICCs?

- Single component solid forms offer limited opportunities with respect to diversity whereas 2-component solid forms might lead to number of new crystalline forms. ICCs offer even greater diversity than 2-component solid forms since they are based upon 3-components for which two components can be varied without changing the chemical structure of the parent compound. In principle, this provides exponentially even more number of crystalline forms with an opportunity to fine tune wide range of physicochemical properties. For example, lithium ICCs, where lithium is a drug to treat bipolar disorder are the best example to describe how the change of anion and coformer (two variables) impacted the bioavailability and physical stability.[32]
- There are number of salts available from GRAS list that are safe and can be potential ionic coformers for the API; for example salts of citric acid including sodium citrate, potassium citrate, calcium citrate (cation is metal); ammonium citrate, isopropyl citrate and stearyl citrate (cation is organic).
- The components in the ICCs are typically held together by coordination bonds and/or charge assisted interactions. These interactions are strong compared to the traditional hydrogen bonds as seen in MCCs. Therefore understanding and exploiting of these interactions (charge assisted/coordination bonds) permit good control over design of novel crystalline materials. In short, ICCs are amenable to crystal engineering strategies similar to MCCs.

The design of ICCs similar to MCCs can be explained with carbamazepine as a prototypal example. For example Zaworotko and co-workers[18] demonstrated the synthesis of new crystalline phases for carbamazepine by exploiting (I) exo-functional nature of carboxamide dimer (II) disrupting the dimer with carboxylic acids. The same strategies can also be applicable to ICCs and two separate studies were reported in the literature. In case (I) ammonium chloride was used as coformer resulted a 1D chain based on N−H···O and N−H···Cl^- interactions without disrupting the dimer [30] (Figure 2.1 a). In case (II) sodium salts were used as coformer in which sodium cations disrupted the homosynthon to form an ICC based upon Na^+−O=C coordination bonds [33] (Figure 2.1 b).

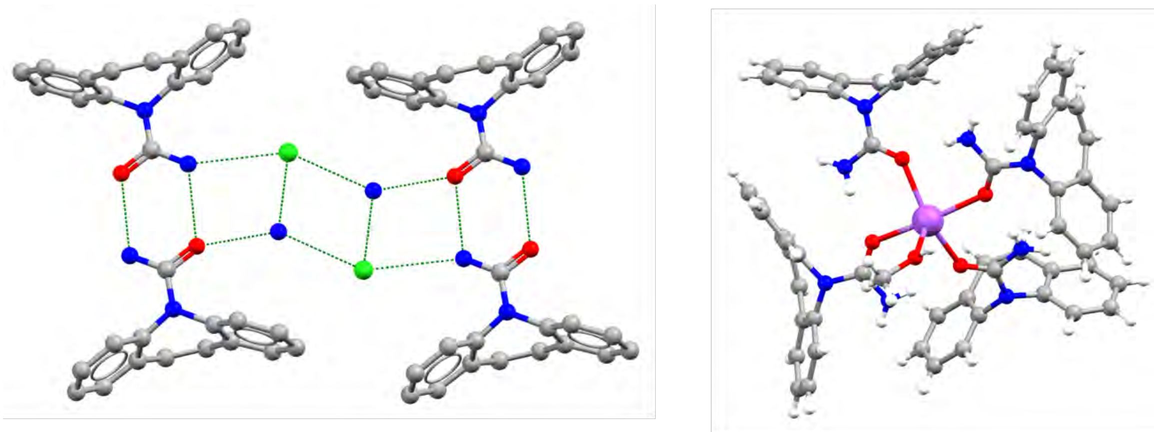

(a) (b)

Figure 2.1. Illustration of (a) Carbamazepine-ammonium chloride ICC formed by utilizing exterior donors and acceptors of amide moiety (hydrogen atoms coordinates are not given in CSD). (b) Coordination environment of sodium cation coordinated by four carbamazepine and one methanol molecules. Charge balancing iodide is removed for clarity.

2.3 History of Ionic Cocrystals (ICCs)

ICC's can be traced back to at least 1783 when Romè de l'Ise observed a habit change in NaCl crystals when crystallised from an aqueous urea solution [34]. Later Bunn (1933) and Seifert (1937) subsequently attributed this habit modification to the adsorption of urea on certain crystal faces of NaCl. Bunn also noted in his article titled that "*There is one complication; in the aqueous system there is a compound NaCl.CO(NH$_2$)$_2$.H$_2$O, the structure of which is not known*". In 1950, Kleber et al. [35] detailed the morphology and optics of this compound before Palm and MacGillivray isolated colourless, transparent crystals from slow evaporation of an equimolar solution of sodium chloride and urea.[36] Single crystal X-ray crystallographic analysis revealed that the compound is a 1:1:1 ICC of NaCl, urea and water (Figure 2.2).

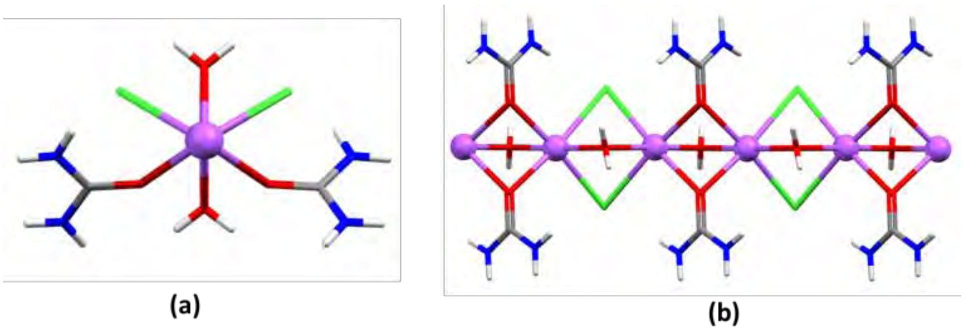

Figure 2.2. (a) Sodium cation coordination environment and (b) 1D chain observed in sodium chloride urea monohydrate

A related family of ICCs is that of sodium and calcium salt ICCs involving sugar coformers. A noteworthy example is the ICC of NaCl with glucose reported by F.V. Kobell in 1843.[37, 38] A well-studied classes of ICCs is based upon carboxylic acids and carboxylate salts. In 1853, Gerhardt reported an ICC of potassium hydrogen benzoate with benzoic acid that was prepared by cooling an alcoholic solution of stoichiometric equivalents of salt and acid.[39] The composition of the ICC was confirmed in 1954.[40] In a subsequent review article by Speakman, this family of ICCs was classified '*acid salts*'[41] and he noted that '*in some cases an acid salt is more easily made than the neutral salt; it may crystallize preferentially when one is trying to prepare the neutral salt*'.[41] Speakman explored acid salts extensively through X-ray and neutron diffraction studies and suggested that they could be further classified into two types depending upon the nature of the carboxylate ion. In type A, the proton is shared between the carboxylates (Figure 2.3 a) whereas in type B the proton is more strongly associated with one of the oxygen atoms, i.e. it is a carboxylic acid (Figure 2.3 b). Speakman salts provided a fundamental understanding about the structural features of short, strong hydrogen bonds.

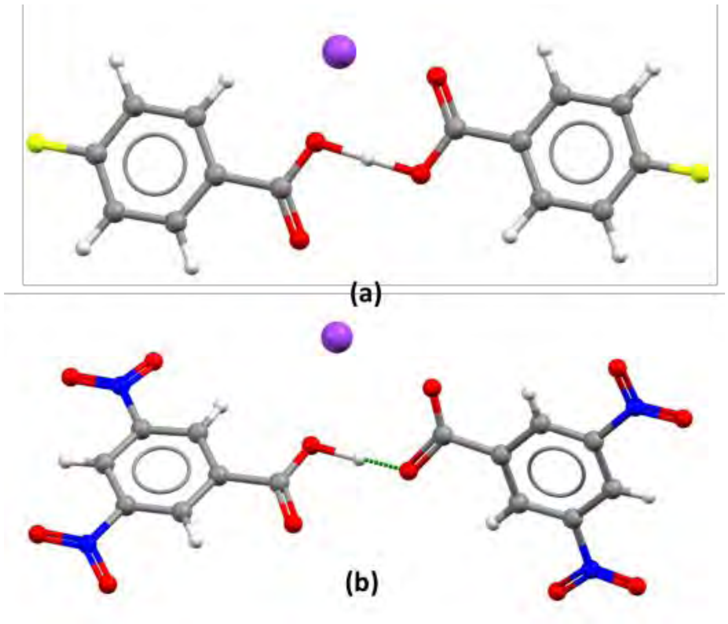

Figure 2.3. Examples of Speakman type A and type B acid salts observed in (a) potassium hydrogen bis (4-flouro benzoate) and (b) potassium hydrogen bis (3,5 dinitrobenzoate)

Improvement in solubility through formation of ICCs was also addressed in early literature: phenylquinoline carboxylic acid with pyrazolones, '*molecular compounds*'[42] streptomycin acid salts with alkaline earth metal halides, '*complex salts;*[43] theophylline with sodium salts such as sodium acetate, sodium salicylate and sodium glycinate.[44, 45] Clinical trials conducted upon theophylline-sodium glycinate involved >300 patients for a period of 18 months and suggested that the ICC produced a typical theophylline response. Pharmacodynamics studies in a rat model revealed that the LD_{50} of theophylline and the ICC were 200 mg/kg and 350 mg/kg, respectively, suggesting decreased toxicity for ICC. Hoffmann-La Roche Inc. subsequently reported the ICC of theophylline (Tp) and magnesium (Mg) salicylate (S) with the formula $Tp_2MgS_2.5H_2O$.[46] This ICC can be crystallized using magnesium salicylate (0.5−2.0 moles) with 1.0 mole of theophylline.

An ICC that demonstrates improved performance of a drug product was reported for tetracyclines, broad spectrum polyketide antibiotics that tend to exhibit low solubility. Reverin, a derivative of tetracycline, exhibited increased solubility but also increased toxicity.[47] Two ICCs or '*additional complexes'*, tetracycline-sodium methylene salicylate and chlorotetracycline-sodium methylene salicylate were administered as distilled water solutions to albino mice. The ICC was found to be less toxic (LD_{50}: 375 mg/kg) when compared to Reverin (225 mg/kg).

A 1971 patent filed by George and Ernest claimed 56 ICCs formed by 3-isothiazolones and metal halides as '*metal salt complexes'* and reported improved thermal stability compared to the corresponding isothiazoles.[48] For instance, 5-chloro-2-methyl-3-isothiazole and its hydrochloride salt undergo 30% and 58% decomposition, respectively, at 50 ^{0}C whereas the $CaCl_2$ ICC was found to be thermally stable.

ICCs based upon organic cation halides are also reported in the literature. Childs et al. patented fluoxetine hydrochloride ICCs with a series of carboxylic acid coformers. [20] An ICC of fluoxetine hydrochloride with benzoic acid is shown in Figure 2.4. Modulation of dissolution rate with respect to the parent fluoxetine hydrochloride salt was reported for this family of ICCs. Saxagliptin hydrochloride, Onglyza®, exists as a monohydrate and that converts to a chemically unstable dihydrate during a coating process. To overcome this problem, Enantia synthesized and patented novel ICCs of saxagliptin hydrochloride.[49]

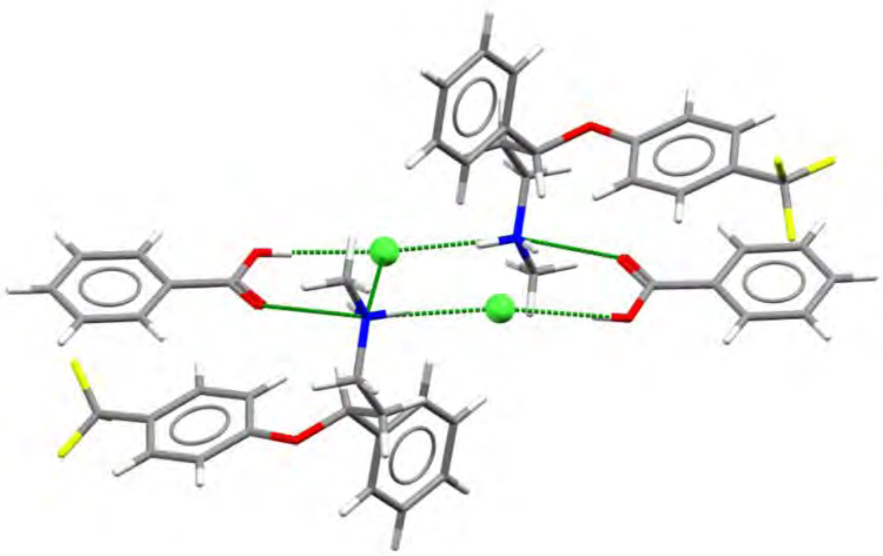

Figure 2.4. The discrete assembly that is sustained by charge assisted hydrogen bond interaction in fluoxetine-hydrochloride benzoic acid ICC

In summary, ICCs have been known as *acid salts, molecular compound, complex salt, additional complexes, metal salt complexes and adduct*.

2.4 Case Studies on Ionic Cocrystals

2.4.1 Tramadol hydrochloride with Celecoxib

Tramadol is a centrally acting synthetic opioid analgesic used to treat moderate to severe pain.[50] Tramadol has two chiral centres and, in the marketed drug, is a racemic mixture of the hydrochloride salt. The dosage of tramadol required to treat pain can be as low as 25 mg/day and is increased as needed, potentially building up to a dose of 100 mg every 4 to 6 hours. Unfortunately, such high doses of tramadol can cause severe side effects. Thus there is a need for a more efficacious low dose formulation. The combination treatments with other COX inhibitors, however, have shown greater efficacy (measured through reductions in pain scores) than with the tramadol paracetamol combination.[51] With a goal to develop an effective combination dosage form, Esteve reported an ICC of tramadol HCl with celecoxib.[52] Celecoxib is a cyclooxygenase-2 inhibitor selective non-steroidal anti-inflammatory drug (NSAID) used to treat osteoarthritis and acute pain.[53] Celecoxib belongs to BCS class II, i.e. low solubility (7 ug/ml in water) and high permeability. The slow dissolution rate of celecoxib also contributes to its low bioavailability. Variations in the excipients used in the formulation of the ICC provided further enhancement in PK when compared to the marketed drug products Celebrex® and Aldonta® (celecoxib and tramadol HCl, respectively). Type A tablets consisted of Kollidon® VA 64, type B contained Soloplus® and type C contained Kollidon® VA 64 without Sepitrap® 80 & 4000. A single dose PK study involving tablets A, B, C and concomitant administration of celecoxib and tramadol HCl was conducted on beagle dogs. The PK profile revealed that, when compared to Adolonta®, the overall exposure ($AUC_{0-\infty}$) values had reduced for the formulations A, B and C by factors of 0.3, 0.4 and 0.9, respectively. However, similar T_{max} values were observed for all formulations, suggesting that the novel formulations could have a better safety profile compared to Adolonta®. For celecoxib, PK parameters were much more variable with respect to formulation with type C tablets providing the greatest AUC_{0-t} and shortest T_{max}, 37780.2 ng.h/mL and 2.3 hours, respectively. Celebrex® tablets had a much longer T_{max} (14.5 hours) and reached a maximum concentration of 1048.5 ng/ml. Therefore, the novel formulations of the ICC achieved higher plasma concentrations and greater exposure of celecoxib vs. Celebrex®. Thus, the ICC provides two key benefits not attainable when the components are administered separately: (1) the safety of tramadol is improved and (2) the bioavailability of celecoxib is increased.

2.4.2 Sodium valproate with Valproic acid

Valproic acid is an anticonvulsant and is also used for the treatment of manic episodes associated with bipolar disorder.[54, 55] Valproic acid (Depakene®) is a liquid at room temperature and is therefore difficult to develop as a solid dosage form. Therefore various salts of valproic acids have been isolated including the sodium, calcium and magnesium salts of valproic acid.[56] The use of calcium valproate has been discouraged due to adverse toxicological effects.[57] The magnesium and sodium valproate salts were found to have similar pharmacological properties to that of valproic acid.[58] Sodium valproate is a solid at room temperature with a substantially high melting point but it is hygroscopic in nature. An alternative solid form, sodium valproate with valproic acid in a 1:1 stoichiometric ratio (sodium valproate: valproic acid) was isolated by cooling an acetone solution of sodium valproate and valproic acid.[59] A stability test (conducted at room temperature by exposing samples to 80% RH for 45 mins) revealed that sodium valproate gained 17-24% by weight whereas sodium divalproate exhibited no appreciable weight gain. Thus, due to its improved stability and comparable PK behaviour, sodium divalproate, marketed as Depakote®, is the leading marketed form of valproic acid. More recently, another solid form containing sodium valproate was reported.[60] The asymmetric unit of the new crystal form, shown in Figure 2.5, contains 3 sodium cations, 3 valproate anions, 1 valproic acid and a water molecule. Reports indicate that even more crystalline forms exist (characterized by PXRD and FTIR) for the three component ICCs of sodium valproate and valproic acid.[61]

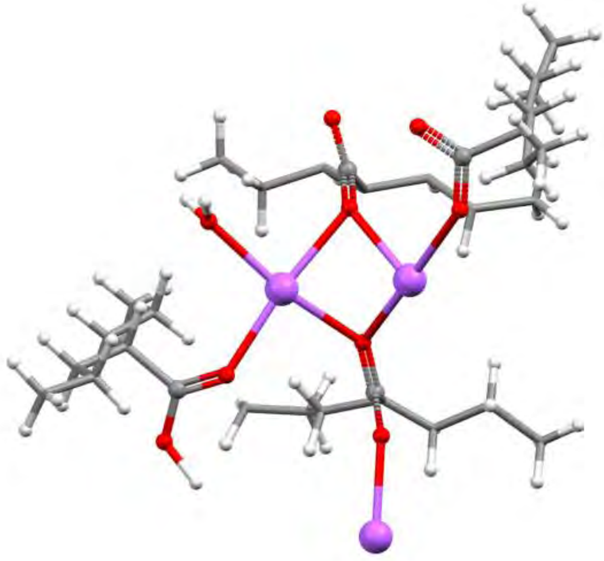

Figure 2.5. Illustration of asymmetric unit of ICC containing three sodium cations, three valproates, one valproic acid and one water molecule. Hydrogen atoms of valporoat near to the carboxylates are removed for clarity.

2.4.3 Lithium ICCs

Lithium salts have a long history in medication; in the mid-1800s lithium was used in the treatment of gout and rheumatic disorders.[62, 63] The modern revival of lithium began in 1949 with an Australian scientist, John Cade, who demonstrated the clinical importance of lithium for mania.[64] To date, lithium is the only drug indicated for bipolar disorder that can also reduce suicidal tendencies.[65] Unfortunately, the more widespread use of lithium is hindered by its low bioavailability and physical stability. To address these issues, the Zaworotko and Braga research groups have synthesised a series of novel ICCs of lithium .[32, 66] Braga and co-workers synthesised novel ICCs as co-drugs of racetams.[66] Our research group has explored lithium-carboxylate[32] and lithium-hydroxyl bonds[67] with various anions to synthesize novel ICCs. Simple inorganic anions such as chloride, bromide or nitrate afforded ICCs with square grid, diamondoid and ABW topologies. Organic anions tend to exhibit square grid networks with lithium and carboxylates in 1:2 stoichiometric ratios. To determine if ICCs of lithium can improve the bioavailability of lithium, a rat PK study was commissioned.[68] The ICC lithium salicylate-proline (LISPRO) was administered as a single oral dose to a Sprague-Dawley rat and resulted in 39% and 56% plasma and brain relative bioavailability compared to lithium carbonate (Li_2CO_3). Although the relative bioavailabilities were lower from LISPRO than from the reference, the attenuated plasma and brain concentrations extended the lithium presence for 48 hours post dose. This low, steady concentration could be advantageous as the risk of toxicity associated with high serum levels of lithium is likely to be reduced. To address the poor physical stability of some lithium salts an ICC of lithium chloride was prepared.[67] Lithium chloride was found to deliquesce at ca. 11% RH. The recently reported ICC of lithium chloride with glucose was found to improve the physical stability of lithium chloride, making it stable past 11% RH but it gained 4% by weight at 30% RH and the ICC is hygroscopic at higher RH. These studies further demonstrate the diversity of ICCs (changing anions and coformers systematically) and their ability to modulate properties such as bioavailability and physical stability.

2.5 Conclusions

Ionic cocrystals (ICCs) are recently emerging class of crystal forms for the new fundamental science in the context of crystal engineering and have been barely studied in relevance to the pharmaceutical science. Ionic cocrystals offer greater diversity than two component solid forms since they are based upon three components in which two components can be varied without changing the chemical structure of the parent compound. As there is large number of ionic coformers available (salts), there are more opportunities to create number of novel crystal forms for a given API compared to single component crystals. In short, this chapter highlights the ionic cocrystals from the perspective of history and structural diversity. Three case studies of ICCs are presented in the context of Active Pharmaceutical Ingredients (APIs) for the improvement of physicochemical properties and clinical performance highlighted the importance in pre-formulation screening of the drug development.

2.6 References

(1) Di, L.; Fish, P. V.; Mano, T., Bridging solubility between drug discovery and development. *Drug Discovery Today.,* **2012**, *17*(9–10), 486-495.

(2) Gardner, C. R.; Walsh, C. T.; Almarsson, Ö., Drugs as materials: valuing physical form in drug discovery. *Nat. Rev. Drug Discov.,* **2004,** *3*(11), 926-934.

(3) Stella, V.; Borchardt, R.; Hageman, M.; Oliyai, R.; Maag, H.; Tilley, J., *Prodrugs: challenges and rewards*. ed.; Springer Science & Business Media: **2007**.

(4) Moulton, B.; Zaworotko, M. J., From molecules to crystal engineering: supramolecular isomerism and polymorphism in network solids. *Chem. Rev.,* **2001**, *101*(6), 1629-1658.

(5) Desiraju, G. R.; Parshall, G. W., Crystal engineering: the design of organic solids. *Materials science monographs.,* **1989**, *54*.

(6) Pikal, M.; Lukes, A.; Lang, J. E.; Gaines, K., Quantitative crystallinity determinations for β-lactam antibiotics by solution calorimetry: Correlations with stability. *J. Pharm. Sci.,* **1978**, *67*(6), 767-773.

(7) Yoshioka, M.; Hancock, B. C.; Zografi, G., Crystallization of indomethacin from the amorphous state below and above its glass transition temperature. *J. Pharm. Sci.,* **1994**, *83*(12), 1700-1705.

(8) Khankari, R. K.; Grant, D. J., Pharmaceutical hydrates. *Thermochimica Acta.,* **1995**, *248*, 61-79.

(9) Pudipeddi, M.; Serajuddin, A., Trends in solubility of polymorphs. *J. Pharm. Sci.,* **2005**, *94*(5), 929-939.

(10) Almarsson, Ö.; Zaworotko, M. J., Crystal engineering of the composition of pharmaceutical phases. Do pharmaceutical co-crystals represent a new path to improved medicines? *Chem. Commun.,* **2004**, (17), 1889-1896.

(11) Vishweshwar, P.; McMahon, J. A.; Bis, J. A.; Zaworotko, M. J., Pharmaceutical co-crystals. *J. Pharm. Sci.,* **2006**, *95*(3), 499-516.

(12) Shan, N.; Zaworotko, M. J., The role of cocrystals in pharmaceutical science. *Drug Discovery Today.,* **2008**, *13*(9–10), 440-446.

(13) Aakeroy, C. B.; Desper, J.; Helfrich, B. A., Heteromeric intermolecular interactions as synthetic tools for the formation of binary co-crystals. *CrystEngComm.,* **2004**, *6*(5), 19-24.

(14) Trask, A. V.; Motherwell, W. D. S.; Jones, W., Pharmaceutical cocrystallization: Engineering a remedy for caffeine hydration. *Cryst. Growth Des.,* **2005**, *5*(3), 1013-1021.

(15) Trask, A. V.; Motherwell, W. D. S.; Jones, W., Physical stability enhancement of theophylline via cocrystallization. *Int. J. Pharm.,* **2006**, *320*(1–2), 114-123.

(16) Karki, S.; Friščić, T.; Fábián, L.; Laity, P. R.; Day, G. M.; Jones, W., Improving mechanical properties of crystalline solids by cocrystal formation: new compressible forms of paracetamol. *Adv. Mater.,* **2009**, *21*(38-39), 3905-3909.

(17) Thakuria, R.; Delori, A.; Jones, W.; Lipert, M. P.; Roy, L.; Rodríguez-Hornedo, N., Pharmaceutical cocrystals and poorly soluble drugs. *Int. J. Pharm.,* **2013**, *453*(1), 101-125.

(18) Fleischman, S. G.; Kuduva, S. S.; McMahon, J. A.; Moulton, B.; Bailey Walsh, R. D.; Rodríguez-Hornedo, N.; Zaworotko, M. J., Crystal engineering of the composition of pharmaceutical phases: Multiple-component crystalline solids involving carbamazepine. *Cryst. Growth Des.,* **2003**, *3*(6), 909-919.

(19) Good, D. J.; Rodríguez-Hornedo, N., Solubility Advantage of Pharmaceutical Cocrystals. *Cryst. Growth Des.,* **2009**, *9*(5), 2252-2264.

(20) Childs, S. L.; Chyall, L. J.; Dunlap, J. T.; Smolenskaya, V. N.; Stahly, B. C.; Stahly, G. P., Crystal Engineering Approach To Forming Cocrystals of Amine Hydrochlorides with Organic Acids. Molecular Complexes of Fluoxetine Hydrochloride with Benzoic, Succinic, and Fumaric Acids. *J. Am. Chem. Soc.,* **2004**, *126*(41), 13335-13342.

(21) Childs, S. L.; Kandi, P.; Lingireddy, S. R., Formulation of a Danazol Cocrystal with Controlled Supersaturation Plays an Essential Role in Improving Bioavailability. *Mol. Pharm.,* **2013**, *10*(8), 3112-3127.

(22) Shan, N.; Perry, M. L.; Weyna, D. R.; Zaworotko, M. J., Impact of pharmaceutical cocrystals: the effects on drug pharmacokinetics. *Expert Opin. Drug Metab. Toxicol.,* **2014**, *10*(9), 1255-1271.

(23) Aitipamula, S.; Banerjee, R.; Bansal, A. K.; Biradha, K.; Cheney, M. L.; Choudhury, A. R.; Desiraju, G. R.; Dikundwar, A. G.; Dubey, R.; Duggirala, N.; Ghogale, P. P.; Ghosh, S.; Goswami, P. K.; Goud, N. R.; Jetti, R. R. K. R.; Karpinski, P.; Kaushik, P.; Kumar, D.; Kumar, V.; Moulton, B.; Mukherjee, A.; Mukherjee, G.; Myerson, A. S.; Puri, V.; Ramanan, A.; Rajamannar, T.; Reddy, C. M.; Rodriguez-Hornedo, N.; Rogers, R. D.; Row, T. N. G.; Sanphui, P.; Shan, N.; Shete, G.; Singh, A.; Sun, C. C.; Swift, J. A.; Thaimattam, R.; Thakur, T. S.; Kumar Thaper, R.; Thomas, S. P.; Tothadi, S.; Vangala, V. R.; Variankaval, N.; Vishweshwar, P.; Weyna, D. R.; Zaworotko, M. J., Polymorphs, Salts, and Cocrystals: What's in a Name? *Cryst. Growth Des.,* **2012**, *12*(5), 2147-2152.

(24) Pfeiffer, P., Organische Molekulverbindungen; Verlag von Ferdinand Enke: Stuttgart, **1922**.

(25) Stahly, G. P., A Survey of Cocrystals Reported Prior to 2000. *Cryst. Growth Des.,* **2009**, *9*(10), 4212-4229.

(26) Braga, D.; Grepioni, F.; Maini, L.; Prosperi, S.; Gobetto, R.; Chierotti, M. R., From unexpected reactions to a new family of ionic co-crystals: the case of barbituric acid with alkali bromides and caesium iodide. *Chem. Commun.,* **2010**, *46*(41), 7715-7717.

(27) Jones, P. G.; Schon, U.; Finner, E., Tedisamil sesquifumarate. *Acta Crystallogr. Sect. E:,* **2004**, *60*(8), o1285-o1287.

(28) Andreas Hafner, F. B., Martin Szelagiewicz, Bernd Siebenhaar, Multicomponent system of resuvastatin calcium salt and sorbitol. US 2013/0237553.

(29) Chiodo, T., Dr. Cocrystals of raltegravir potassium. 131740508, 2015.

(30) Reck, G. T., W., *Pharmazie.,* **1991**, (46), 509.

(31) Hauser, M. R.; Doxsee, K. M.; Hope, H., Calcium complexation by corticosteroids. *Inorg. Chem.,* **2009**, *48*(22), 10780-10788.

(32) Ong, T. T.; Kavuru, P.; Nguyen, T.; Cantwell, R.; Wojtas, Ł.; Zaworotko, M. J., 2:1 Cocrystals of homochiral and achiral amino acid zwitterions with Li^+ salts: Water-stable zeolitic and diamondoid metal–organic materials. *J. Am. Chem. Soc.,* **2011**, *133*(24), 9224-9227.

(33) Buist, A. R.; Kennedy, A. R., Ionic cocrystals of pharmaceutical compounds: Sodium complexes of carbamazepine. *Cryst. Growth Des.,* **2014**, *14*(12), 6508-6513.

(34) De Rome De LIsle, J. B. L., *Crystallographie, 2nd ed. Paris,* **1783**.

(35) Kleber, M., von Stackelberg, M., Wallraf, M., *Neues Jb. Miner., Mh.,* **1950**, *241*, 11.

(36) Palm, J. H.; MacGillavry, C., Habit modification in the system rocksalt–urea–water. *Acta Crystallogr.,* **1963**, *16*(10), 963-968.

(37) Kobell, F. V., *J. Prakt. Chem.,* **1843**, *28*.

(38) Ferguson, G.; Kaitner, B.; Connett, B.; Rendle, D., Structure of the α-d-glucose–sodium chloride–water complex (2/1/1). *Acta Crystallogr. Sect. B-Struct. Sci.,* **1991**, *47*(4), 479-484.

(39) Gerhardt, *Jahresber.,* **1852**, *450*.

(40) Skinner, J. M.; Stewart, G. M. D.; Speakman, J. C., The crystal structure of the acid salts of some monobasic acids. Part III. Potassium hydrogen dibenzoate. *J. Chem. Soc.,* **1954**, *185*(0), 180-184.

(41) Speakman, J. C., Acid salts of carboxylic acids, crystals with some 'very short' hydrogen bonds. *Structure and bonding.,* **1972**, *12*, 141.

(42) Oscar Adler., Rudolf Alder., Process for the producing of molecular compounds of the salts of phenyl-quinoline carboxylic acids with alkylated pyrazolones and alkykated amino-pyrazolodones. 1,954,909*,* **1934**.

(43) Robert, L. P. Complex salts of streptothricin. 2,474,758, **1949**.

(44) J. C. Krantz Pharmaceutical compositions containing theophylline. 2,433,765, **1945**.

(45) Krantz, J. C.; Holbert, J. M.; Iwamoto, H. K.; Carr, C. J., Sodium theophylline glycinate. *J. Am. Pharm. Assoc.,* **1947,** *36*(8), 248-250.

(46) Richard Barry., H. R. Theophylline magnesium salicyalte. 4,198,507, 1980.

(47) Marcus, I. Water soluble tetracyclines. 3,846,486, **1974**.

(48) Metal salt complexes of 3-isothiazolones. George A. Miller and Ernest D. Weiler, 4,150,026, **1979**.

(49) T. Nicolas; T. C. Montserrat; C. R. Lydia; Liorenc, R. J. Crystalline forms of Saxagliptin. WO 2013/160354 A1.

(50) Leppert, W., Tramadol as an analgesic for mild to moderate cancer pain. *Pharmacol. Rep.,* **2009**, *61*(6), 978-992.

(51) Chandanwale, A. S.; Sundar, S.; Latchoumibady, K.; Biswas, S.; Gabhane, M.; Naik, M.; Patel, K., Efficacy and safety profile of combination of tramadol-diclofenac versus tramadol-paracetamol in patients with acute musculoskeletal conditions, postoperative pain, and acute flare of osteoarthritis and rheumatoid arthritis: a Phase III, 5-day open-label study. *J. Pain Res.,* **2014**, *7*, 455.

(52) Ranzani, L. S. A., A. F. US 2013/0109659 A1.

(53) McCormack, P., Celecoxib. *Drugs.,* **2011**, *71*(18), 2457-2489.

(54) Phiel, C. J.; Zhang, F.; Huang, E. Y.; Guenther, M. G.; Lazar, M. A.; Klein, P. S., Histone deacetylase is a direct target of valproic acid, a potent anticonvulsant, mood stabilizer, and teratogen. *J. Biol. Chem.,* **2001**, *276*(39), 36734-36741.

(55) Macritchie, K.; Geddes, J.; Scott, J.; Haslam, D.; Goodwin, G., Valproic acid, valproate and divalproex in the maintenance treatment of bipolar disorder. *The Cochrane Library.,* **2001**.

(56) W. C. Chuo, W. Wong, Y. L. Wu, US 8,729,300 B2, 2009.

(57) Watkins, J. R.; Gough, A. W.; McGuire, E. J.; Goldenthal, E.; de la Iglesia, F. A., Calcium valproate-induced uterine adenocarcinomas in Wistar rats. *Toxicology.,* **1992**, *71*(1–2), 35-47.

(58) D. J. Nelson, W. C. Holberg, US 2007/0083063 A1.

(59) Sherman, B. C. 6,077,542, **2000**.

(60) Petruševski, G.; Naumov, P.; Jovanovski, G.; Ng, S. W., Unprecedented sodium–oxygen clusters in the solid-state structure of trisodium hydrogentetravalproate monohydrate: A model for the physiological activity of the anticonvulsant drug Epilim®. *Inorg. Chem. Commun.,* **2008**, *11*(1), 81-84.

(61) Petruševski, G.; Naumov, P.; Jovanovski, G.; Bogoeva-Gaceva, G.; Ng, S. W., Solid-state forms of sodium valproate, active component of the anticonvulsant drug epilim. *ChemMedChem.,* **2008**, *3*(9), 1377-1386.

(62) Garrod, A. B., *The nature and treatment of gout and rheumatic gout*. ed.; Walton and Maberly: **1859**.

(63) Shorter, E., The history of lithium therapy. *Bipolar disorders.,* **2009**, *11*(s2), 4-9.

(64) Cade, J. F., Lithium salts in the treatment of psychotic excitement. Bulletin-world health organization*,* **2000**, *78*(4), 518-520.

(65) Goodwin, F. K.; Fireman, B.; Simon, G. E.; Hunkeler, E. M.; Lee, J.; Revicki, D., Suicide risk in bipolar disorder during treatment with lithium and divalproex. *JAMA,* **2003**, *290*(11), 1467-1473.

(66) Braga, D.; Grepioni, F.; Maini, L.; Capucci, D.; Nanna, S.; Wouters, J.; Aerts, L.; Quéré, L., Combining piracetam and lithium salts: ionic co-crystals and co-drugs? *Chem. Commun.,* **2012**, *48*(66), 8219-8221.

(67) Duggirala, N. K.; Smith, A. J.; Wojtas, Ł.; Shytle, R. D.; Zaworotko, M. J., Physical stability enhancement and pharmacokinetics of a lithium ionic cocrystal with glucose. *Cryst Growth. Design,* **2014**, *14*(11), 6135-6142.

(68) Smith, A. J.; Kim, S.-H.; Duggirala, N. K.; Jin, J.; Wojtas, L.; Ehrhart, J.; Giunta, B.; Tan, J.; Zaworotko, M. J.; Shytle, R. D., Improving lithium therapeutics by crystal engineering of novel ionic cocrystals. *Mol. Pharm.,* **2013**, *10*(12), 4728-4738.

Hydrogen Bond Hierarchy: Persistent Phenol···Chloride Hydrogen Bonds in the Presence of Carboxylic Acid Moieties

"Reprinted (adapted) with permission from (*Crystal Growth & Design*, **2015,** *10.1021/acs.cgd.5b00628*). Copyright (2015) American Chemical Society."

The link to the publication is http://pubs.acs.org/doi/abs/10.1021/acs.cgd.5b00628

Copyright Clearance Center RightsLink® Home Account Info Help Live Chat

ACS Publications Most Trusted. Most Cited. Most Read.

Title:	Hydrogen Bond Hierarchy: Persistent Phenol···Chloride Hydrogen Bonds in the Presence of Carboxylic Acid Moieties
Author:	Naga Kiran Duggirala, Geoffrey P. F. Wood, Addison Fischer, et al
Publication:	Crystal Growth and Design
Publisher:	American Chemical Society
Date:	Jul 1, 2015

Copyright © 2015, American Chemical Society

Logged in as:
Naga Duggirala
LOGOUT

PERMISSION/LICENSE IS GRANTED FOR YOUR ORDER AT NO CHARGE

This type of permission/license, instead of the standard Terms & Conditions, is sent to you because no fee is being charged for your order. Please note the following:

- Permission is granted for your request in both print and electronic formats, and translations.
- If figures and/or tables were requested, they may be adapted or used in part.
- Please print this page for your records and send a copy of it to your publisher/graduate school.
- Appropriate credit for the requested material should be given as follows: "Reprinted (adapted) with permission from (COMPLETE REFERENCE CITATION). Copyright (YEAR) American Chemical Society." Insert appropriate information in place of the capitalized words.
- One-time permission is granted only for the use specified in your request. No additional uses are granted (such as derivative works or other editions). For any other uses, please submit a new request.

BACK CLOSE WINDOW

Chapter 3: Hydrogen bond hierarchy: Persistent phenol···chloride hydrogen bonds in the presence of carboxylic acid moieties

3.1 Introduction

The term crystal engineering was coined by R. Pepinsky in 1955[1] in the context of metal complexes and was further developed by G. M. J. Schmidt to enable the field of solid-state topochemical reactions such as those of cinnamic acids.[2] Crystal engineering has subsequently evolved into a paradigm for materials design through exploiting intermolecular interactions in order to design new crystalline substances with desirable structures and properties.[3-6] The impact of crystal engineering is broad since, in principle, any structure-dependent property can be addressed in a systematic manner. This includes nonlinear optical performance (NLO),[7] electrical and proton conductivity,[8] energetic materials,[9, 10] and porosity,[11] all of which have advanced through application of crystal engineering principles.

However, perhaps the area of greatest immediate impact lies in the field of pharmaceutical science where crystalline materials lie at the heart of drug products. This is because active pharmaceutical ingredients (APIs or "drug substances") enable the efficacy of orally delivered drug products. Further, APIs are inherently amenable to crystal engineering as they almost invariably contain functional groups with multiple hydrogen bond donors and acceptors. These molecular features are what drive biological activity, but they also mean APIs can exist in multiple crystalline forms such as polymorphs,[12] solvates,[13] salts,[14] and cocrystals.[15-19] These solid forms are potential drug substances, and they can exhibit subtly or dramatically different materials properties that could ultimately enable the efficacy of a medicine. The range of intermolecular interactions in a drug substance can include coordination bonds, charge-assisted interactions, hydrogen bonds, and, for aromatics, C–H···π, π···π, and cation···π interactions.[20]

The diversity of intermolecular interactions possible in drug substances thereby offers an opportunity to gain a better fundamental understanding of crystal design as well as improving the performance of drug products. With respect to crystal design, the patterns of intermolecular interactions in crystal structures have been rationalized using the concepts of motifs and synthons. Etter developed graph-set theory[13] and denoted the repetitive hydrogen bonding in crystal structures as a motif and developed the notation $G^a_d(r)$ where "G" is pattern designator, "r" is its degree, "d" denotes the number of donors, and "a" is the number of acceptors. However, graph theory does not take into account the functional groups that are involved in the motif; e.g., $R^2_2(8)$ represents both an acid and an amide dimer. To better understand the functional groups that are involved in intermolecular interactions, Desiraju developed the concept of supramolecular synthons.[5] Zaworotko categorized supramolecular synthons into supramolecular homosynthons (interactions between identical functional groups)[21] and supramolecular heterosynthons (interactions between two different, but complementary functional groups).[22] Commonly observed supramolecular homosynthons include carboxylic acid···carboxylic acid[23-28] and amide···amide,[29-34] whereas systematic supramolecular heterosynthon studies for the cocrystal formation include carboxylic acid···amide,[35-39] amine···hydroxyl,[40-43] carboxylic acid···pyridine,[44-50] and hydroxyl···pyridine.[50-55] Supramolecular synthons between various combinations of functional groups have been subjected to study for well over a decade,[56-63] but these studies are complicated by the presence of competing functional groups and/or the lack of statistics in the Cambridge Structural Database (CSD).[64, 65] Thus far, only a few supramolecular heterosynthons have been found to be persistent in the presence of competing functional groups, e.g., pyridine··· carboxylic acid.[46, 50] However, even persistent supramolecular synthons between two functional groups can be disrupted by the presence of relatively strong hydrogen bond donors/ acceptors, and so systematic delineation of hierarchy of synthons remains an important aspect of crystal design. Delineating supramolecular synthon hierarchy is a multistep process as presented in Scheme 3.1.

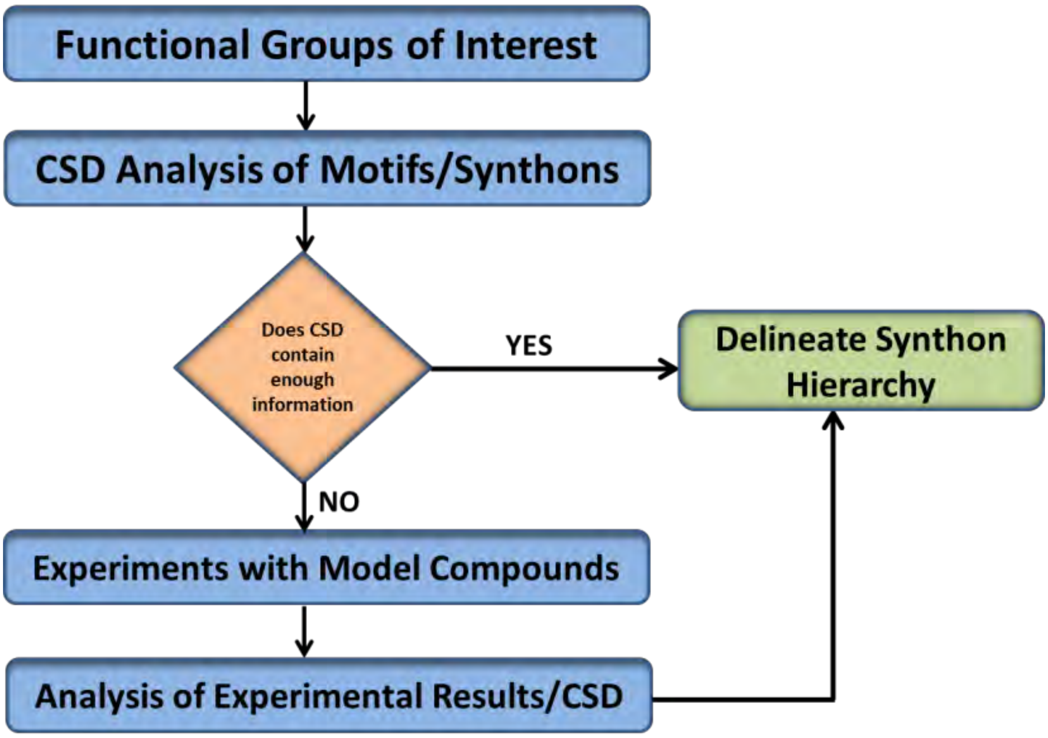

Scheme 3.1. Flow Chart to Determine Supramolecular Synthon Hierarchy

The first step is to identify the functional groups that are of interest. The next step is to retrieve all relevant crystal structures from the Cambridge Structural Database (CSD) and conduct a statistical analysis of the motifs and supramolecular synthons that exist within those crystal structures. Should the CSD contain enough information to draw valid conclusions then the hierarchy of the selected functional groups can be delineated without the need for further experimentation. If not, it is necessary for systematic experiments with model compounds to be conducted. Analysis of experimental results together with the CSD then enables delineation of supramolecular synthon hierarchy. Multicomponent crystals such as cocrystals are ideally suited to serve as model compounds to investigate the hierarchy of particular supramolecular synthons because the components can be carefully selected to systematically address the question at hand. Although the Cambridge Structural Database (CSD) contains >700 000 entries including ~307 000 organic compounds (~91 000 multicomponent crystals including ~24 000 hydrates, ~29 000 solvates[66] and ~9000 cocrystals), even permutations of common functional groups can be underrepresented. This situation impacts all classes of cocrystals but especially ICCs, which must necessarily be comprised of at least three components.

Cocrystals have been classified according to whether their components are neutral or ionic: (1) molecular cocrystals (MCCs) contain only neutral cocrystal formers; (2) ionic cocrystals (ICCs) are comprised of at least one cocrystal former that is a salt.[67] In an ICC, if the salt is an alkali or alkaline earth metal salt, then coordination bonds typically direct the crystal packing.[68] If the ICC is based upon an organic salt then the crystal structure is generally sustained by charge-assisted hydrogen bonds.[69] Perhaps the first ICC, NaCl, urea, and water, was reported in 1783 by De Romé De L'Isle.[70] However, despite the discovery of ICCs in the 18th century and high profile studies on NaCl/sugars in the 19th and 20th centuries,[71-74] ICCs have been barely studied in the context of drug substances. In an ICC, the API can be a cation, anion, or neutral molecule. ICCs where APIs are neutral cocrystal formers are exemplified by ammonium chloride-carbamazepine[75] and magnesium chloride-norfloxacin.[76] More recently, Braga et al.[77] and Zaworotko et al.[78] have reported ICCs of lithium salts where the lithium cation is the API and the neutral molecule is a zwitterion such as amino acid. Lithium ICCs have been shown to exhibit improved thermal stability[77] and modulated pharmacokinetic properties.[79] ICCs that contain a chloride salt of an API are of particular interest because ~50% of basic APIs are marketed as chloride salts.[80-82] Further, there are numerous reports concerning solubility and/or stability problems with respect to chloride salts.[83] The hygroscopicity of lithium chloride and the low aqueous solubility of fluoxetine hydrochloride salts are two such examples. With respect to solubility and bioavailability, cocrystals are well-known to control performance,[84] and an early example of an ICC was reported by Childs et al. who modulated the dissolution rate of fluoxetine hydrochloride (Prozac) using carboxylic acid coformers.[85] Lowering the deliquescence of lithium chloride by cocrystallizing it with glucose was also recently reported.[86]

In chloride salts, the chloride anions are recognized as being "strong" hydrogen bond acceptors and can accommodate multiple hydrogen bond donors.[87] Therefore, to follow Etter's hydrogen bond principle: "the best proton donor and acceptors remaining after intramolecular hydrogen-bond formation form intermolecular hydrogen bonds to one another"[32] the molecule with the best hydrogen bond donor capability would preferentially hydrogen bond to the chloride anion. One widely accepted method for determining the best hydrogen bond donor is to consider the pK_a/pK_b of the molecule.[88] Carboxylic acids exhibit pK_a values ~2−5 and are well suited to form the carboxylic acid···chloride supramolecular heterosynthon.[85, 89] Phenols are more weakly acidic (pK_a ≈ 8−11), and thus one would not intuitively expect them to be better hydrogen bond donors when compared to carboxylic acids. Two earlier synthon hierarchy studies, reported by Zaworotko and Aakeröy suggest, however, that phenol is a competitive, if not better, hydrogen bond donor than a carboxylic acid. The Zaworotko group studied model cocrystals and found that phenol moieties are equally likely to form supramolecular synthons to aromatic nitrogens.[50] In a separate study, conducted by

Aakeröy's research group, it was found that cocrystallizing 3-hydroxybenzoic acid and 4-hydroxybenzoic acid with molecules containing two acceptor sites of different strengths resulted in phenol moieties preferentially hydrogen bonding to the strongest acceptor.[90] The strongest acceptor was not based upon its pK_a but instead upon molecular electrostatic potential calculations. In this contribution, we further consider the hierarchy of hydrogen bonding interactions of carboxylic acids versus phenols by using ICCs. Model compounds were selected to provide a variety of substituted carboxylic acids, phenols, and chloride salts. Ammonium chloride salts were used as a source of chloride anion for several ICCs because the ammonium cation is widely present in the pharmaceutical and biological sciences and can serve as a strong hydrogen donor.[91] In addition; we used computationally determined hydrogen bond and lattice energies to support our analysis.

3.2 Experimental Section

Sixteen entries were retrieved from the CSD in which a chloride anion is present with both phenol and carboxylic acid moieties (ConQuest Version 5.36 with November updates, search parameters: organic compounds with 3D coordinates, R < 7.5%, not disordered and no errors). However, the presence of competing hydrogen bond donors and acceptors in several of these compounds makes it difficult to draw valid conclusions about hierarchy with such a limited number of data points. We therefore prepared and structurally characterized 12 novel ICCs: pyridine hydrochloride: 4-hydroxybenzoic acid (PHC4HBA); pyridine hydrochloride:3,5-dihydroxybenzoic acid (PHCDBA); pyridine hydrochloride:gallic acid (PHCGAL); pyridine hydrochloride:6- hydroxy-2-naphthoic acid (PHC6HNA); tetramethylammonium chloride:4-hydroxybenzoic acid (TMA4HBA); tetramethylammonium chloride: 3,5-dihydroxybenzoic acid (TMADBA); tetramethylammonium chloride:gallic acid (TMAGAL), tetramethylammonium chloride: protocatechuic acid (TMAPCA); tetraethylammonium chloride: 5- hydroxyisophthalic acid (TEAHPA); tetraethylammonium chloride:3-hydroxybenzoic acid (TEA3HBA); tetraethylammonium chloride:coumaric acid (TEACOU); and tetraethylammonium chloride:protocatechuic acid (TEAPCA). The chemical structure of the cocrystal formers used herein are presented in Scheme 3.2. Although we tried all the combinations, i.e., chloride anion containing coformers with carboxylic acid-phenol containing coformers (24 ICCs possible), we could successfully crystallized 12 ICCs, and the remaining combinations turned out either gummy or crystallized as pure materials within the experimental conditions that we have explored.

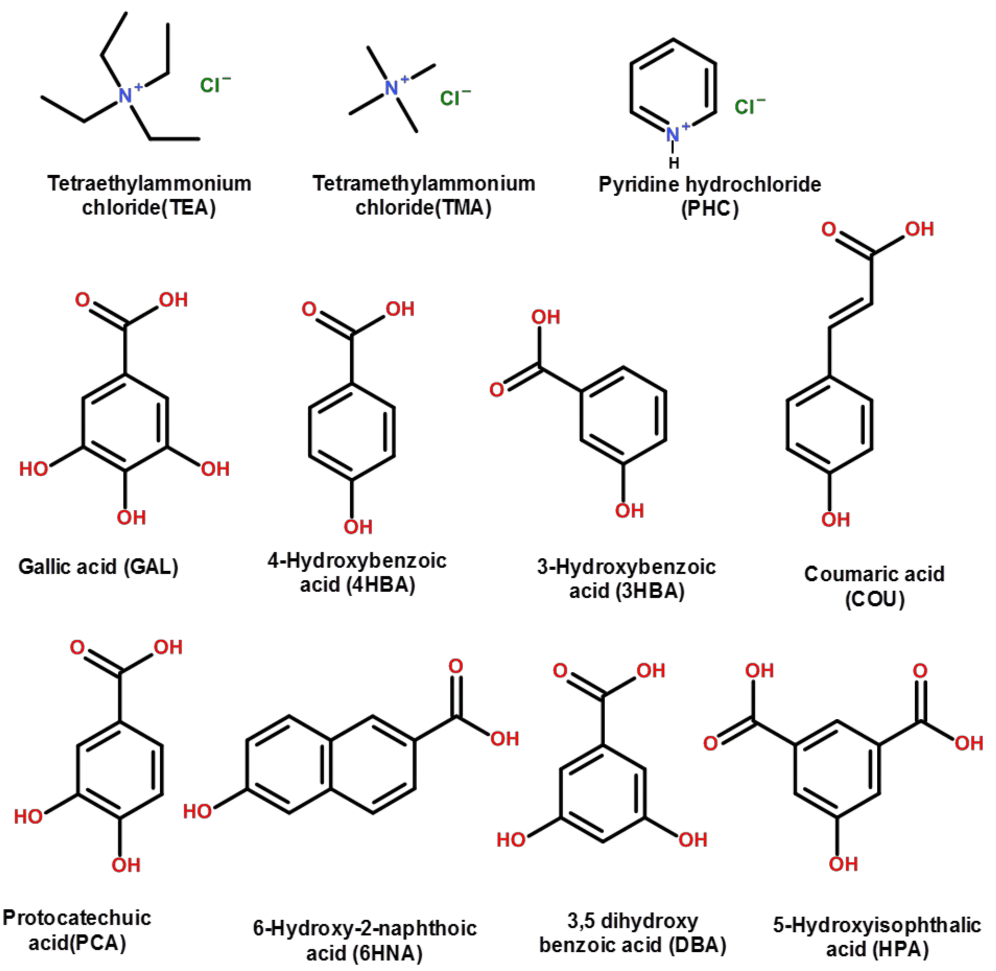

Scheme 3.2. Cocrystal Formers and Their Corresponding Abbreviations

3.2.1 Syntheses of Cocrystals.

First set of experiments, methanol was chosen as a solvent because most of the coformers are soluble in methanol. At this point only few crystallization experiments were successful and yielded ICCs. The remaining experiments turned out either gummy or crystallized as input materials. In second set of experiments two variables were employed (1) stoichiometry of input materials and (2) mixture of solvents instead of pure methanol. The rationale behind this is to minimize the solubility differences between coformers so that cocrystal would be supersaturated in solution compared to the individual components that would eventually crystallize. With the combination of TEA, TMA and PHC along with 8 acid-phenols a total number of 24 possible structures exist (1:1 stoichiometry) and with variable stoichiometry even more ICCs possible. Here in this study we have obtained only 12 ICCs and did not attempt to obtain all the possible ICCs as our aim was to delineate the hydrogen bond hierarchy. The specific methods of preparation for each of the ICC were given in the following section.

All reagents were obtained from commercial suppliers and used without further purification. Single crystals were grown using slow solvent evaporation. Synthetic details are presented in the following. Cocrystals were harvested through filtration before complete evaporation of the solvent had occurred.

PHCGAL: pyridine hydrochloride (0.115g, 1mmol) and gallic acid acid (0.170g, 1mmol) were dissolved in methanol. Slow evaporation of the solvent yielded slightly tan, needle shaped crystals.

PHC4HBA: Pyridine hydrochloride (0.115g, 1mmol) and 4-hydroxybenzoicacid (0.138g, 1mmol) were dissolved in methanol. The solvent was evaporated at room temperature, thin white needle shaped crystals were afforded.

PHC6HNA: Pyridine hydrochloride (0.115g, 1mmol) and 6-hydroxy-2-naphthoic acid (0.188, 1mmol) were dissolved in methanol. Slow evaporation of the solvent yielded slightly yellow rod shaped crystals.

PHCDBA: Pyridine hydrochloride (0.115g, 1mmol) and 3,5-dihydroxybenzoic acid (0.154, 1mmol) were dissolved in methanol. After slow evaporation of the solvent, diamond shaped crystals with a slightly tan hue were afforded.

TEA3HBA: Tetraethylammonium chloride (0.183g, 1mmol) and 3-hydroxybenzoic acid (0.138g, 1mmol) were dissolved in a in a 1:1 solution of acetone/methanol. Slow evaporation of the solvent yielded colourless block crystals.

TEACOU: Tetraethylammonium chloride (0.183g, 1mmol) and para-coumaric acid (0.164g, 1mmol) were dissolved in methanol. Upon slow evaporation of the solvent, tan needle shaped crystals were obtained.

TEAGAL: Tetraethylammonium chloride (0.183g, 1mmol) and gallic acid (0.170g, 1mmol) and both compounds were dissolved in 2-propanol. Slow evaporation of the solvent yielded white diamond shaped crystals.

TEAHPA: Tetraethylammonium chloride (0.183g, 1mmol) and 5-hydroxyisophthalic acid (0.182g, 1mmol) were dissolved in methanol. After slow evaporation of the solvent, colorless rod shaped crystals were afforded.

TEAPCA: Tetraethylammonium chloride (0.183g, 1mmol) and protocatechoic acid (0.154g, 1mmol) were dissolved in methanol. Upon slow evaporation of the solvent, colorless needle shaped crystals were obtained.

TMA4HBA: Tetramethylammonium chloride (0.109g, 1mmol) and 4-hydroxybenzoic acid (0.138g, 1mmol) were both dissolved in methanol. Slow evaporation of the solvent yielded, very fine white needle shaped crystals.

TMAGAL: Tetramethylammonium chloride (0.109g, 1mmol) and gallic acid (0.170g, 1mmol) were dissolved in methanol. Slow evaporation of the solvent yielded slightly tan clusters of rod shaped crystals.

TMAHPA: Tetramethylammonium chloride (0.109g, 1mmol) and 5-hydroxyisophthalic acid (0.182g, 1mmol) were dissolved in a 1:1 solution containing ethyl acetate/methanol. Upon slow evaporation of the solvent, white clusters of needle shaped crystals were obtained.

TMAPCA: Tetramethylammonium chloride (0.109g, 1mmol) and protocatechoic acid (0.154g, 1mmol) were dissolved in methanol. After slow evaporation of the solvent, colorless diamond shaped crystals were afforded.

TMADBA: Tetramethylammonium chloride (0.109g, 1mmol) and 3,5-dihydroxybenzoic acid (0.154g, 1mmol) were dissolved in a 1:1 solution of ethyl acetate and methanol. Slow evaporation of the solvent yielded colorless crystals with needle morphology.

3.2.2 Powder X-ray Diffraction (PXRD). A Bruker advance D8 X-ray powder diffractometer was used for all PXRD measurements with experimental parameters as follows: Cu Kα radiation (λ =1.54056 Å); 40 kV and 30 mA; detector type: scintillation; scanning interval: 3−40° 2θ; time per step: 0.5 s. The experimental PXRD patterns and calculated PXRD patterns from single crystal structures were compared to confirm the composition of bulk materials (Appendix 2).

3.2.3 Differential Scanning Calorimetry (DSC). Thermal analysis was conducted on a TA Instruments DSC Q20 differential scanning calorimeter. Aluminum pans were used for all samples, and the instrument was calibrated using an indium standard. An empty pan, sealed in the same way as the sample, was used as the reference pan. Samples were heated in the DSC cell under a nitrogen blanket from ca. 30 °C to the melting point of the ICCs at a rate of 10 °C/min.

3.2.4 Fourier Transform Infrared Spectroscopy (FT-IR). ICCs were analyzed by infrared spectroscopy with a Nicolet Avatar 320 FT-IR instrument over the range of 500−4000 cm^{-1}. Sample amounts of 4−5 mg were used along with EZ Omnic software.

3.2.5 Single-Crystal X-ray Data Collection and Structure Determination. The X-ray intensity data for PHC4HBA, PHCDBA, PHCGAL, TMA4HBA, TMADBA, TMAGAL, TEAHPA, and TEACOU were collected on a Bruker D8 Venture PHOTON 100 CMOS system equipped with a Cu Kα INCOATEC Imus microfocus source (λ = 1.54178 Å) at 100(2), 268(2), or 296(2) K. The X-ray diffraction data for PHC6HNA, TMAPCA, TEAPCA, and TEA3HBA were collected using a Bruker-AXS SMART-APEXII[92] CCD diffractometer (CuKα, λ = 1.54178 Å) at 228(2) K. Data integration and reduction were performed using SaintPlus 6.01.[93] Absorption correction was performed by the multi-scan method as implemented in SADABS.[93] Space groups were determined using XPREP as implemented in APEX2.[92] Structures were solved using SHELXS-97 (direct methods) and refined using SHELXL-97 (full-matrix least squares on F2) contained in OLEX2[94] and WinGX v1.70.01 programs.[95] All non-hydrogen atoms were refined anisotropically. Hydrogen atoms of −CH groups were placed in geometrically calculated positions and included in the refinement process using a riding model with isotropic thermal parameters: $U_{iso}(H) = 1.2U_{eq}(-CH)$. Hydrogen atoms on water molecules were refined using DFIX and DANG restraints and $U_{iso}(H) = 1.5U_{eq}(-OH)$. The disordered hydrogen atoms of carboxylic acids have been found from electron density difference maps and included in the refinement process using the riding model (AFIX 3) with fixed occupancies (0.5) and $U_{iso}(H) = 1.0U_{eq}(-OH)$. H_2 and H_5 disordered hydrogen atoms have been found from electron density difference maps and refined with $U_{iso}(H) = 1.0U_{eq}(-OH)$. Occupancies of disordered H atoms have been refined using free variable FVAR 2 (= 0.64) and −2 (= 0.36). The rest of hydrogen atoms have been freely refined.

PHCDBA: All non-hydrogen atoms were refined anisotropically. Hydrogen atoms of –CH groups were placed in geometrically calculated positions and included in the refinement process using riding model with isotropic thermal parameters: $U_{iso}(H) = 1.2U_{eq}(\text{-CH})$. Hydrogen atoms of water molecule have been refined using DFIX and DANG restraints and $U_{iso}(H) = 1.5U_{eq}(\text{-OH})$. H4 and H1 disordered hydrogen atoms have been found from el. density difference map and included in the refinement process using riding model (AFIX 3) with fixed occupancies (0.5) and $U_{iso}(H) = 1.0U_{eq}(\text{-OH})$. H_2 and H_5 disordered hydrogen atoms have been found from el. density difference map and refined with $U_{iso}(H) = 1.0U_{eq}(\text{-OH})$. Occupancies of those two disordered H atoms have been refined using free variable FVAR 2 (=0.64) and -2 (=0.36). The rest of hydrogen atoms have been freely refined.

PHCGAL: All non-hydrogen atoms were refined anisotropically. Hydrogen atoms of –CH groups were placed in geometrically calculated positions and included in the refinement process using riding model with isotropic thermal parameters: $U_{iso}(H) = 1.2Ue_q(\text{-CH})$. Disordered hydrogen atoms (H_6, H_7, H_9, H_{19}, H_{12a}, H_{13}) have been found from el. density difference map and included in the refinement process using riding model (AFIX 3) with $U_{iso}(H) = 1.5U_{eq}(\text{-OH})$. Occupancies of disordered H atoms have been refined using free variables. The rest of hydrogen atoms have been freely refined.

TEA3HBA: All non-hydrogen atoms were refined anisotropically. Hydrogen atoms of -CH, -CH_2, -CH_3 groups were placed in geometrically calculated positions and included in the refinement process using riding model with isotropic thermal parameters: $U_{iso}(H)$

= $1.2U_{eq}$(-CH,-CH_2), U_{iso}(H) = $1.5U_{eq}$(-CH_3). Hydrogen atoms of hydroxyl groups have been found from el. density difference map and were freely refined.

TMAPCA: All non-hydrogen atoms were refined anisotropically. Hydrogen atoms of –CH and –CH3 groups were placed in geometrically calculated positions and included in the refinement process using riding model with isotropic thermal parameters: U_{iso}(H) = $1.2U_{eq}$(-CH), U_{iso}(H) = 1.5Ueq(-CH_3) . Hydrogen atoms of hydroxyl groups have been found from el. density difference map and were freely refined.

TMA4HBA: All non-hydrogen atoms were refined anisotropically. Hydrogen atoms of –CH and –CH_3 groups were placed in geometrically calculated positions and included in the refinement process using riding model with isotropic thermal parameters: U_{iso}(H) = $1.2U_{eq}$(-CH), U_{iso}(H) = $1.5U_{eq}$(-CH_3) . Hydrogen atoms of hydroxyl groups have been found from el. density difference map and were freely refined. Water molecules have been refined using distance restraints (DFIX, DANG). Disordered hydrogen atoms (H_2, H_3, H_4, H_{15}) have been found from density difference map and included in the refinement process using riding model (AFIX 3) with freely refined U_{iso}(H).

TMADBA: All non-hydrogen atoms were refined anisotropically. Hydrogen atoms of –CH and –CH_3 groups were placed in geometrically calculated positions and included in the refinement process using riding model with isotropic thermal parameters: U_{iso}(H) = $1.2U_{eq}$(-CH), U_{iso}(H) = $1.5U_{eq}$(-CH_3) . Hydrogen atoms of hydroxyl groups have been found from el. density difference map and were freely refined or refined using DFIX=0.88A restraint (H_6). Disordered hydrogen atoms (H_1, H_2) have been found from el. density difference map and included in the refinement process using riding model (AFIX 3) with freely refined U_{iso}(H).

TMAGAL: All non-hydrogen atoms were refined anisotropically. Hydrogen atoms of –CH and –CH_3 groups were placed in geometrically calculated positions and included in the refinement process using riding model with isotropic thermal parameters: $U_{iso}(H) = 1.2U_{eq}(-CH)$, $U_{iso}(H) = 1.5U_{eq}(-CH_3)$. Hydrogen atoms of hydroxyl groups have been found from el. density difference map and were freely refined. Water molecules have been refined using distance restraints (DFIX, DANG). Disordered hydrogen atoms (H_2, H_4, H_9, H_{10}) have been found from density difference map and included in the refinement process using riding model (AFIX 3) with $U_{iso}(H) = 1.5U_{eq}(-OH)$. Occupancies of disordered H atoms have been refined using free variable (0.66 H_9/H_{10}:0.33 H_2/H_4).

TEACOU: All non-hydrogen atoms were refined anisotropically. Hydrogen atoms of –CH and $–CH_3$ groups were placed in geometrically calculated positions and included in the refinement process using riding model with isotropic thermal parameters: $U_{iso}(H) = 1.2U_{eq}(-CH,-CH_2)$, $U_{iso}(H) = 1.5U_{eq}(-CH_3)$. Hydrogen atoms of hydroxyl groups have been found from el. density difference map and were freely refined.

TEAHPA: All non-hydrogen atoms were refined anisotropically. Hydrogen atoms of –CH and $–CH_3$ were freely refined with isotropic thermal parameters: $U_{iso}(H) = 1.2U_{eq}(-CH,-CH_2)$, $U_{iso}(H) = 1.5Ueq(-CH_3)$. Hydrogen atoms of hydroxyl groups have been found from density difference map and were freely refined or refined using DFIX=0.88A restraint (H_4).

TEAPCA: All non-hydrogen atoms were refined anisotropically. Hydrogen atoms of –CH and $–CH_3$ groups were placed in geometrically calculated positions and included in the refinement process using riding model with isotropic thermal parameters: $U_{iso}(H) = 1.2U_{eq}(-CH,-CH_2)$, $U_{iso}(H) = 1.5U_{eq}(-CH_3)$. Hydrogen atoms of hydroxyl groups have been found from el. density difference map and were freely refined.

PHC4HBA: All non-hydrogen atoms were refined anisotropically. Hydrogen atoms of –CH and groups were placed in geometrically calculated positions and included in the refinement process using riding model with isotropic thermal parameters: $U_{iso}(H) = 1.2U_{eq}(\text{-CH})$. Hydrogen atoms of hydroxyl groups have been found from el. density difference map and were freely refined or refined using DFIX=0.88A restraint (H002).

PHC6HNA: All non-hydrogen atoms were refined anisotropically. Hydrogen atoms of –CH groups were placed in geometrically calculated positions and included in the refinement process using riding model with isotropic thermal parameters: $U_{iso}(H) = 1.2U_{eq}(\text{-CH})$. Hydrogen atoms of hydroxyl groups have been found from el. density difference map and were freely refined. Disordered hydrogen atoms (H_1,H_4) have been found from el. density difference map and included in the refinement process using riding model (AFIX 3) with $U_{iso}(H) = 1.5U_{eq}(\text{-OH})$. Occupancies of disordered H atoms have been refined using free variable (0.7 H_4:0.3 H_1).

All the single crystal data can be found in Table 3.1 and the hydrogen bond parameters can be found in Appendix 1.

Table 3. 1. Crystallographic Data and Structure Refinement Parameters for the ICCs Reported Herein.

Code	PHC4HBA	PHC6HNA	PHCDBA	PHCGAL	TEA3HBA	TEACOU
Formula	$C_{12}H_{12}ClNO_3$	$C_{27}H_{22}ClNO_6$	$C_{24}H_{26}Cl_2N_2O$	$C_{36}H_{38}Cl_3N_3O_1$	$C_{15}H_{26}ClNO_3$	$C_{26}H_{36}ClNO$
MW	253.68	491.91	557.37	875.04	303.82	494.01
Crystal	Monoclinic	Monoclinic	Triclinic	Triclinic	Orthorhombic	Triclinic
Space group	$P2_1/n$	$C2/c$	P-1	P-1	$P2_12_12_1$	P-1
a (Å)	12.4053(3)	24.8495(9)	9.242(3)	10.685(2)	11.2329(2)	8.505(12)
b (Å)	6.7701(2)	11.3672(4)	10.157(3)	13.595(2)	11.9856(2)	10.144(1)
c (Å)	14.9514(2)	8.5460(3)	14.593(4)	16.500(2)	12.5798(3)	15.638(2)
α (deg)	90	90	108.077(1)	113.934(1)	90	83.028(4)
β (deg)	106.374(1)	106.166(2)	101.343(1)	105.063(1)	90	74.421(5)
γ (deg)	90	90	95.392(10)	91.573(1)	90	86.909(5)
V /Å^3	1204.77(5)	2318.53(1)	1259.15(7)	1970.79(5)	1693.66(6)	1289.7(3)
D_c/mg m^{-3}	1.399	1.409	1.470	1.475	1.192	1.272
Z	4	4	2	2	4	2
Nref./Npara	2148/200	2131/170	4374/371	7242/577	3067/194	4553/327
T /K	228(2)	228(2)	100(2)	228(2)	296(2)	100(2)
R_1	0.0297	0.0371	0.0345	0.0356	0.0320	0.0406
wR_2	0.0792	0.0975	0.0903	0.09000	0.0865	0.1031
GOF	1.047	1.040	1.103	1.043	1.050	1.063

Abs coef.	2.793	1.842	2.817	2.777	2.052	1.643

code	TEAHPA	TEAPCA	TMA4HBA	TMADBA	TMAGAL	TMAPCA
Formula	$C_{24}H_{32}ClNO_1$	$C_{15}H_{26}ClNO_4$	$C_{18}H_{26}ClNO_7$	$C_{11}H_{18}ClNO_4$	$C_{18}H_{26}ClNO_1$	$C_{18}H_{24}ClNO$
MW	529.96	319.82	403.85	263.71	467.85	417.83
Crystal	Triclinic	Orthorhombi	Monoclinic	Triclinic	Triclinic	Monoclinic
Space group	P-1	$P2_12_12_1$	$P2_1$/n	P-1	P-1	$C2$/c
a (Å)	9.953(1)	8.436(1)	9.311(5)	6.169(5)	7.151(2)	22.227(6)
b (Å)	10.703(1)	10.961(2)	7.919(4)	9.4614(8)	12.264(2)	13.688(4)
c (Å)	12.983(1)	18.402(3)	28.529(1)	13.2542(10)	12.832(2)	11.460(3)
α (deg)	81.478(4)	90	90	71.370(4)	73.930(1)	90
β (deg)	74.616(3)	90	99.185(2)	77.094(3)	75.339(1)	101.941(10)
γ (deg)	74.498(3)	90	90	76.917(4)	87.319(1)	90
V/Å^3	1280.7(2)	1701.54(5)	2081.24(2)	704.40(10)	1061.91(4)	4025.34(2)
D_c/g cm^{-3}	1.374	1.248	1.289	1.243	1.459	1.379
Z	2	4	4	2	2	8
Nref./Npara	4499/353	1808/206	3659/268	2467/171	3904/318	3704/283
T/K	100(2)	228(2)	100(2)	268(2)	100(2)	293(2)
R_1	0.0433	0.0280	0.0350	0.0497	0.0361	0.0391
wR_2	0.1125	0.0739	0.0968	0.1380	0.0991	0.1122
GOF	1.069	1.039	1.037	1.061	1.025	1.023
Abs coef.	1.816	2.114	1.956	2.450	2.140	2.083

3.2.6 CSD Analysis. A CSD search was conducted using CSD v5.36 (with 2014 November update) for structures that contain carboxylic acids, phenols, and chloride anions. The following parameters were addressed by the search: (1) # of structures that contain both a chloride anion and either a carboxylic acid or phenol group, irrespective of other functional groups. (2) # of structures that form supramolecular heterosynthons between a chloride anion and either a carboxylic acid or phenol. Hydrogen bond distances were analyzed by Vista. Restrictions on the searches included: 3D-coordinates present; only organics; R factor ≤7.5%, no errors and no disorder. All searches were considered as one of two categories: "raw" or "refined". Raw searches were aimed toward determining the existence of specific supramolecular synthons irrespective of other functional groups. Refined searches addressed the reliability of particular supramolecular synthons when only the specified functional groups are present. Each hit was checked manually to facilitate removal of structures containing intramolecular hydrogen bonds, disordered structures, calixarenes, and crown ethers.

3.2.7 Computational Methods. Standard ab initio molecular orbital theory[96] and density functional theory (DFT)[97] calculations were carried out using the GAUSSIAN 09 computer program.[98] Mixed Gaussian plane-wave (GPW) DFT calculations were carried out using the Cp2K program package.[99-101] The interaction energies between molecular synthons were calculated by the supermolecule approach. This involves taking the initial coordinates of the supramolecular assembly containing the synthon of interest from the X-ray crystal structure and carrying out a geometry optimization in the gas-phase using the M06/6-311G(d,p) level of theory.[102] Optimizations were followed by vibrational frequency analyses to ensure that the selected structures corresponded to minima on the potential energy surface (no imaginary frequencies). Each supramolecular assembly was then decomposed into its fragments, all of which were also subjected to geometry optimizations using the same protocol. Following this, single-point energy calculations were carried out on the resultant structures using the M06/6-311+G(3df,2p) level of theory. Energies of interaction are computed by taking the difference in energy between the assembly and its constituent fragments. Zero-point vibrational energy and other vibrational corrections have not been included in the present calculations. Prior to analysing the relative energetic differences between synthons, we carried out a benchmarking study of theoretical techniques in order to establish the approximate error associated with the M06/6-311+G(3df,2p) level of theory. This was achieved by analyzing the energy of interaction of a small subset of "simple" synthons (see Results and Discussion for details) using the high-level CBS-QB3 methodology[103] and comparing the result to a series of DFT functionals. It was found that the M06 energies gave a mean absolute deviation (MAD) from the CBS-QB3 energies on this subset of structures of just 2.6 kJ mol^{-1}. This can be compared against the PBE0/6-311+G(3df,2p) level of theory, which also performed very well, giving a MAD(CBS-QB3) of 2.8 kJ mol^{-1}. Although the benchmarking was not extensive it serves to give us a relative amount of confidence using the indicated protocol. The results of this assessment are presented in Table 3.2 of the Supporting Information section.

Table 3.2. Comparison of gas-phase binding energies (in kJ mol^{-1}) computed with a number of levels of theory for various of supramolecular synthons.

Synthon	**CBS-QB3**[a]	**M06**[b]	**PBE0**[c]	**M06L**[d]	**PBE**[e]
$CH_3CH_2OH \cdots Cl^-$	-72.7	-75.8	-70.9	-76.9	-74.1
$CH_3CH_2COOH \cdots Cl^-$	-80.5	-81.4	-83.8	-81.5	-89.1
$PheOH \cdots Cl^-$	-104.2	-106.2	-105.5	-106.3	-111.3
$PheCOOH \cdots Cl^-$	-90.1	-89.4	-93.0	-88.8	-98.8
$HOOCPheOH \cdots Cl^-$	-126.5	-131.7	-132.0	-133.1	-140.7
$Cl^- \cdots HOOCPheOH$	-88.4	-85.1	-88.8	-87.9	-94.7
PheCOOH···HOOCPhe	-75.1	-73.2	-73.4	-72.9	-72.0
HOPheCOOH···HOOCPheOH	-75.5	-73.3	-73.6	-74.2	-73.7
$(CH_3CH_2)_4N^+ \cdots Cl^-$	-368.9	-371.5	-363.6	-372.2	-367.1
MD[f]		–0.6	–0.3	–1.3	–4.4
MAD[g]		2.4	2.7	2.5	5.9
LAD[h]		5.5	5.5	6.6	14.5

[a] Molecular geometry optimized using M06/6-311(d,p). [b] M06/6-311+G(3df,2p)//M06/6-311(d,p). [c] PBE0/6-311+G(3df,2p)//M06/6-311(d,p). [d] M06L using GPW method, Gaussian basis set was TZVP-MOLOPT-GTH and plane wave basis set had a 500 Ry cutoff, long range electrostatics were treated with the wavelet method and the box size was increased until convergence was reached typically 16 angstroms in most cases except for PheCOOH···HOOCPhe and HOPheCOOH···HOOCPheOH where 19 was used. [e] Same parameters as for note *d* except the PBE functional was used. [f] Mean deviation from the CBS-QB3 results. [g] Mean absolute value from the CBS-QB3 results. [h] Largest Absolute Deviation from the CBS-QB3 results.

Lattice energies were computed by performing lattice optimizations on the crystal structures found from the single crystal X-ray studies using the M06L functional. A full relaxation of the molecular geometry is also taken into account. However, the lattice symmetry, as determined from the X-ray crystal structure experiments was kept constant throughout the optimizations. The Gaussian and Plane Wave (GPW) implementation of DFT was used throughout,[103] employing the TZP-MOLOPT Gaussian basis set.[104] The plane-wave basis set was converged using a density cutoff of 300 Ry, while the Goedecker-Teter-Hutter (GTH) pseudopotentials constructed from the PBE functional[105, 106] have been used to describe the core electrons. The final energies used for lattice energy determinations were computed by single-point energy calculations using the same protocol except that the density was converged using a cutoff of 500 Ry. To compute the final lattice energies of the molecular and ionic components are also required, which were found using the same computational protocol described above but in the absence of periodic boundary conditions. The box size for these calculations was varied until the energy converged to within 10−5 Hartrees. The long-range electrostatics was solved using the wavelet numerical algorithm for solving Poisson's equation.[107]

Since the M06L functional has not been widely used in the context of lattice energy calculations using the parameters described above, we have assessed its ability to reproduce the lattice energies of some pharmaceutically relevant compounds as well as some ICCs. The results of this study can be found in the Supporting Information Table 3.3. As the table shows this computational protocol is extremely robust in both areas. The mean absolute deviation form experiment is very low at 13.4 kJ mol^{-1} with only KF being somewhat problematic, which gives confidence in the lattice energies of the ICCs computed in the present study. In addition, as shown in Table 3.3 of the

Supporting Information very good agreement with CBS-QB3 is also found for binding energies in the gas-phase using this method with a MAD of just 2.5 kJ mol^{-1}.

Table 3.3. Lattice energies (kJ mol^{-1}) for a number of compounds computed using M06L and the GPW method (see text for details).

Compound	Experimental	Computed	dE
NaCl	-770.3	-782.7	-12.4
NaF	-914.2	-903.4	10.8
KCl	-701.2	-695.1	6.1
KF	-812.1	-858.3	-46.2
aspirin Form 1	-114.7	-123.6	-8.9
aspirin Form 2		-122.5	
ibuprofen	-120.8	-128.2	-7.5
paracetamol I	-122.9	-130.7	-7.8
paracetamol II	-120.9	-128.5	-7.6

3.3 Results and Discussions

3.3.1 CSD Analysis of Carboxylic Acid···Chloride Interaction. The CSD contains 302 entries that include both a carboxylic acid moiety and a chloride anion. Of these entries, 208/302 (69%) exhibit the carboxylic acid···chloride supramolecular heterosynthon (2.89−3.10 Å, mean 2.99 (1) Å). With respect to the remaining crystal structures where the heterosynthon is not observed, 57% (53/94) of the entries contain water molecules in the crystal lattice. Examination of these hydrates revealed that the water molecules are hydrogen bonded to the chloride anion in all cases. Further, the $R^2_4(8)$ ring motif is observed in 12 crystal structures. The carboxylic acid···water supramolecular synthon was observed in 83% (44/53) of the crystal structures.

3.3.2 CSD Analysis of Phenol···Chloride Anion Interaction. There are only 50 structures containing phenols and chloride anions in the absence of competing hydrogen bonding groups. The OH···Cl^{-} supramolecular heterosynthon exists in all structures (2.95−3.21 Å, mean 3.066(2) Å). When the search was relaxed to allow other functional groups, the OH···Cl^{-} heterosynthon was found to occur at 74% frequency (214/290). In the remaining 76 entries other donors and/or acceptors were observed to disrupt the OH···Cl^{-} supramolecular heterosynthon. In 40 of these 76 structures the disruption can be attributed to water molecules with the phenol moiety being bound to water 95% (38/40) of the time and to chloride in 93% (37/40) of the structures. This association with chloride and phenol in most of the crystal structures might be attributable to the diverse hydrogen bonding capability of water molecules.[108] The $R^2_4(8)$ ring motif is observed in 24% (11/40) of these crystal structures. The types of supramolecular synthons likely for a chloride anion, carboxylic acid moiety, phenolic group, and water molecules are presented in Scheme 3.3.

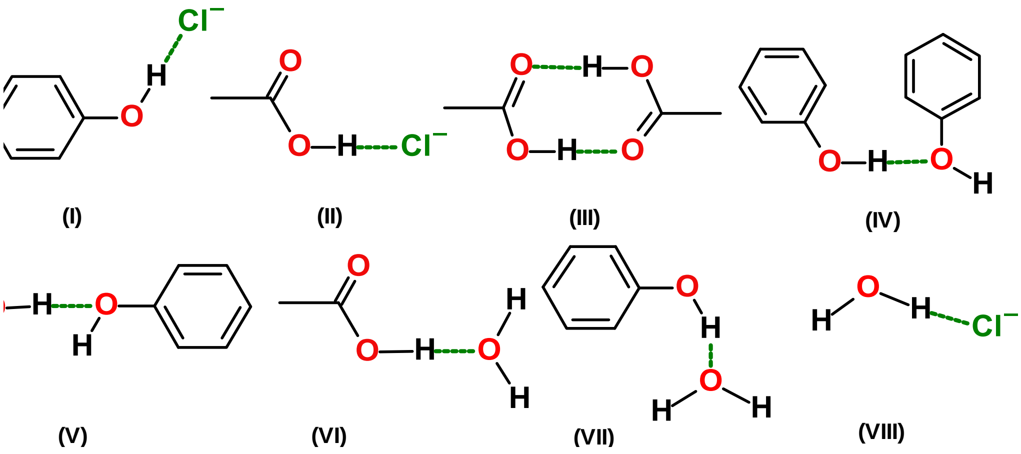

Scheme 3.3. (I) PhOH···Cl⁻ Supramolecular Heterosynthon (II) COOH···Cl⁻ Supramolecular Heterosynthon (III) COOH···COOH Supramolecular Homosynthon (IV) PhOH···PhOH Supramolecular Homosynthon (V) PhOH···COOH Supramolecular Heterosynthon (VI) COOH···H_2O Supramolecular Heterosynthon (VII) PhOH···H_2O Supramolecular Heterosynthon (VIII) Cl⁻···H_2O Supramolecular Heterosynthon

3.3.3 CSD Analysis of Structures That Contain Carboxylic Acids, Phenolic Groups, and Chloride Salts. There are only 16 hits archived in the CSD[109] in which a carboxylic acid, phenol, and chloride anion are present (regardless of whether there are other hydrogen bond donors or acceptors). Fourteen out of the 16 compounds are the chloride salt or hydrated chloride salt of the target compound. Quite surprisingly, even though the CSD contains >700 000 crystal structures there are no cocrystals reported in which the only hydrogen bonding groups present are a carboxylic acid, a phenolic group and a chloride anion. The 16 archived crystal structures includes 6 compounds which are hydrates[110] and contain the water to chloride anion supramolecular synthon (6/6, synthon VIII). In addition, water molecules also facilitate the formation of supramolecular synthons VI (5/6) and VII (4/6). In 14/16 crystal structures, the chloride-phenol supramolecular heterosynthon (synthon I) is observed. In the remaining two crystal structures; synthon I is disrupted by water (synthon VII) in 3-amino tyrosine dihydrochloride monohydrate (refcode: FAPKEN) and L-DOPA hydrochloride (refcode: LDOPAC01) exhibit catechols that are disrupted by the other phenol moiety (synthon IV) and a carboxylic acid (synthon IV). The carboxylic acid···chloride anion supramolecular heterosynthon (synthon II) is observed in only five cases (refcodes: XOHTUL, WISJOX, LDOPAC01, OTROSC, and TEJPIH). In two structures the carboxylic acid forms supramolecular homosynthons: a catemer (refcode: GERCEL) or a dimer (refcode: SUZTAJ). In the remaining nine crystal structures, synthon II is disrupted by other hydrogen bond donors and acceptors that include carboxylate, carbonyl, hydroxyl, water, and protonated amines. Only five entries contain carboxylic acid, phenolic, and chloride moieties in the absence of competing functional groups. As discussed in the above section, CSD analysis of carboxylic acids and phenolic groups with chloride anions revealed that water can be disruptive and including hydrates there are nine relevant crystal structures.

3.3.4 Description of Crystal Structures. The novel ICCs reported in the present study are analyzed in terms of the supramolecular synthons given in Scheme 3.3. Weak interactions such as C−H···O, C−H···Cl^-, π−π, and C−H···π are not discussed. These crystal structures are subsequently grouped according to the synthon hierarchy, and the observed synthons (I and III) are highlighted by green and red boxes, respectively.

PHC4HBA is a 1:1 ICC that crystallizes in the space group $P2_1/n$. The crystal structure is sustained by three distinct hydrogen bonded supramolecular synthons; the carboxylic acid dimer (synthon III), the phenol-chloride heterosynthon (synthon I) and the protonated pyridyl cation to chloride anion hydrogen bond. The carboxylic acid dimer O···O distance is 2.638(1), the phenol to chloride anion O···Cl^-distance is 3.079(1) Å, and the protonated pyridyl to the chloride anion N···Cl^- bond distance is 3.081(1) Å that result a discrete adduct (Figure 3.1).

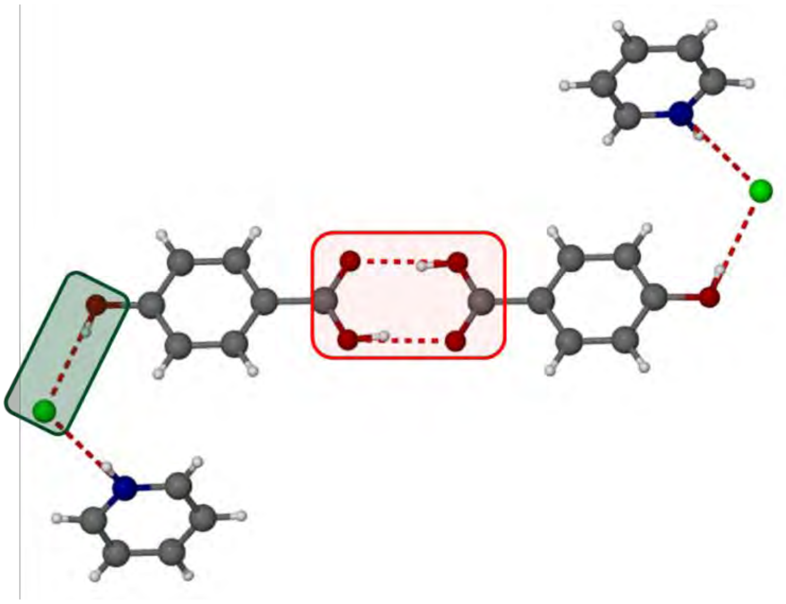

Figure 3.1. Discrete supramolecular structure in PHC4HBA

PHC6HNA, TEACOU, and TEA3HBA exist as 1D network (Figure 3.2). The three crystal structures are sustained by synthon I with O···Cl^{-} distances ranging from 2.985(1) to 3.121(1) Å. In addition to synthon I, synthon III is observed in TEACOU and PHC6HNA. Synthon III is not formed in TEA3HBA. Instead the chain is sustained by a phenol to chloride to carboxylic acid interaction wherein the chloride anion is inserted between the phenol and acid moieties. In PHC6HNA, the protonated hydrogen of the pyridyl cation is hydrogen bonded to chloride with N···Cl^{-} distance of 3.037(2) Å.

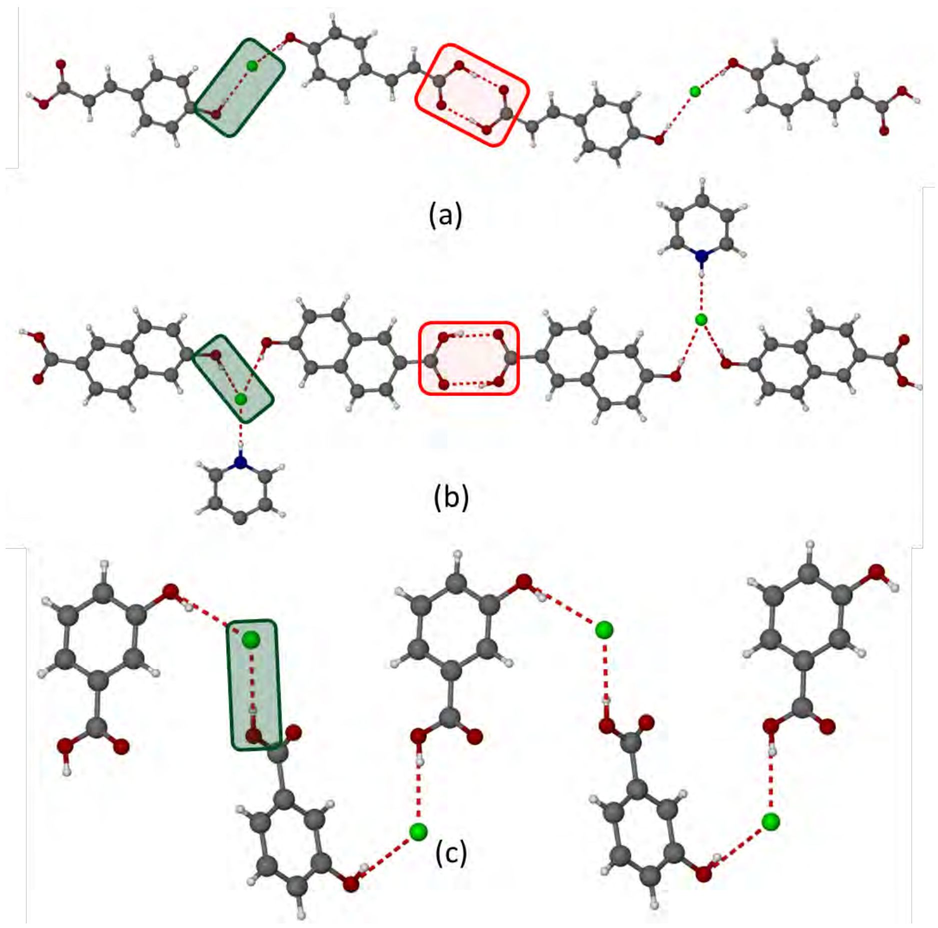

Figure 3.2. One-dimensional networks in TEACOU (a), PHC6HNA (b), and TEA3HBA (c). TEA cations in (a) and (c) are omitted for clarity.

TMADBA, TEAHPA, TEAPCA, TMAPCA, TMAGAL, and TMA4HBA form 2D networks. TMADBA and TEAHPA crystallize in the centrosymmetric space group $P_{1.}$ TMADBA contains two TMA and two DBA molecules per unit cell, whereas TEAHPA contains two molecules of HPA and one molecule of TEA in the asymmetric unit. In both crystal structures chloride anions form synthon I (3.001(2) to 3.050(2) Å) and synthon III, which together facilitate the observed 2D hydrogen bonded networks. The pores in these nets are occupied by the charge balancing cations as shown in Figure 3.3.

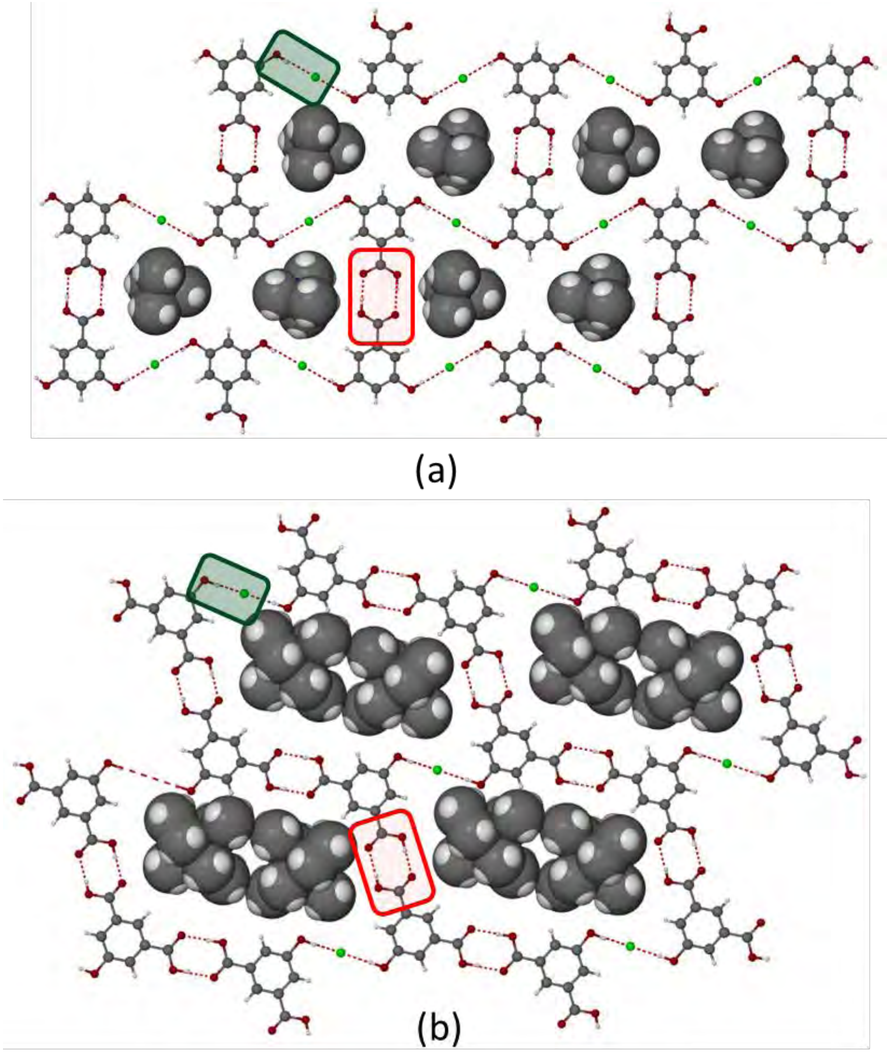

Figure 3.3. 2D hydrogen bonded networks observed in (a) TMADBA and (b) TEAHPA. TMA and TEA cations are shown in spacefill mode.

TEAPCA crystallizes in the noncentrosymmetric space group $P2_12_12_1$, whereas TMAPCA crystallizes in the space group $C2/c$ with 1:1 and 1:2 stoichiometry, respectively. In both crystal structures, the phenolic moieties from the catechol moiety of PCA form supramolecular synthon I with chloride anions (O··· Cl^- bond distances range from 3.029 (1) to 3.151(1) Å). In TEAPCA the chloride anion accepts two phenol donors, whereas in TMAPCA, the chloride anion interacts with four phenols from two catechol moieties. The carboxylic acid dimer (synthon III, O···O distances 2.636(2) and 2.601(2) Å) is also observed in TMAPCA. However, in TEAPCA, this synthon is disrupted by the insertion of a phenol (synthon V). The carboxylic acid···phenol heterosynthon forms chains and these chains are cross-linked by synthon I to form a 2D hydrogen bonded network in TEAPCA. Synthons I and III enable the generation of the 2D hydrogen bonded networks in TMAPCA as shown in the Figure 3.4.

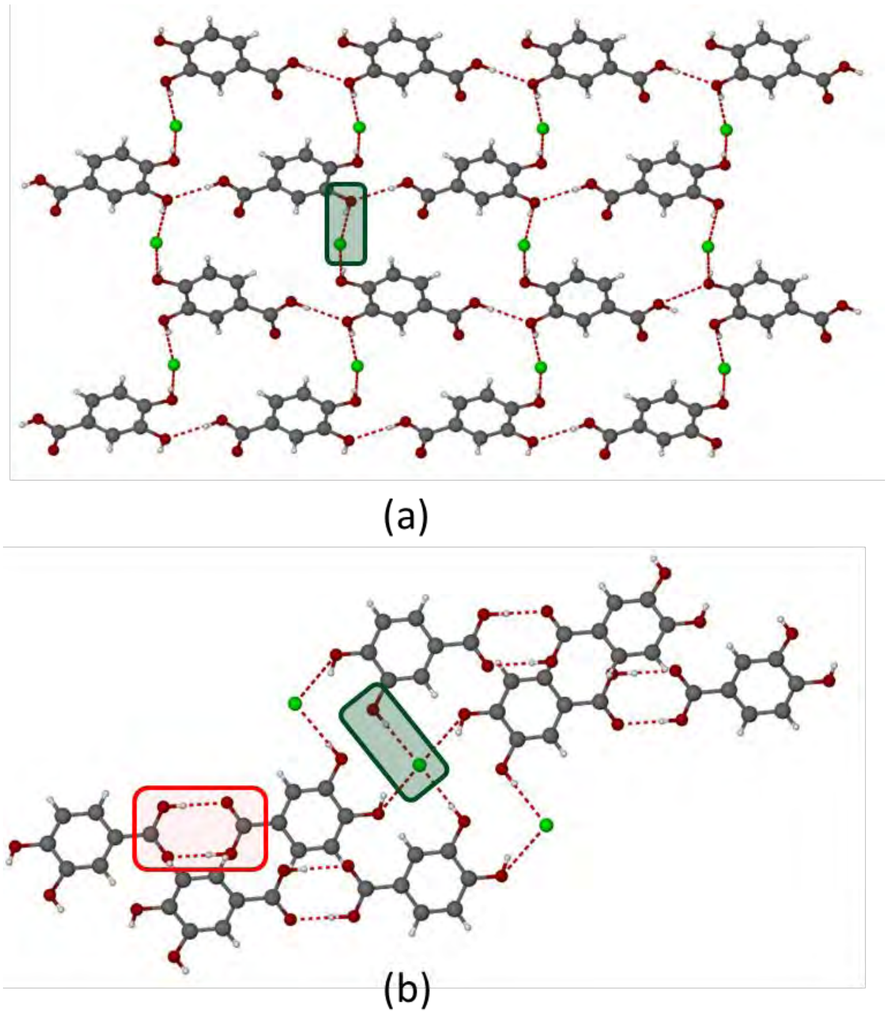

Figure 3.4. Intermolecular hydrogen bonding in (a) TEAPCA and (b) TMAPCA. TMA and TEA cations are omitted for clarity.

TMAGAL and TMA4HBA crystallize as hydrates sustained by synthons I, III, IV, VII, and VIII. The catechol moiety in TMAGAL forms a dimer, and the phenol forms homosynthon (IV) and also hydrogen bonds with water molecules (synthon VII) resulting in a double layer hydrogen bonded network, Figure 3.5a. In TMA4HBA, water molecules form helical chains with chloride anions (synthon VIII) that run along the crystallographic c-axis (Figure 3.5b). 4HBA molecules on either side are hydrogen bonded to these water and chloride moieties by synthon VII (O···O: 2.693(1)) and synthon I (O···Cl^-: 3.020(1) Å). 4HBA molecules are further connected through synthon III to afford 2D network structures as illustrated in Figure 3.5b.

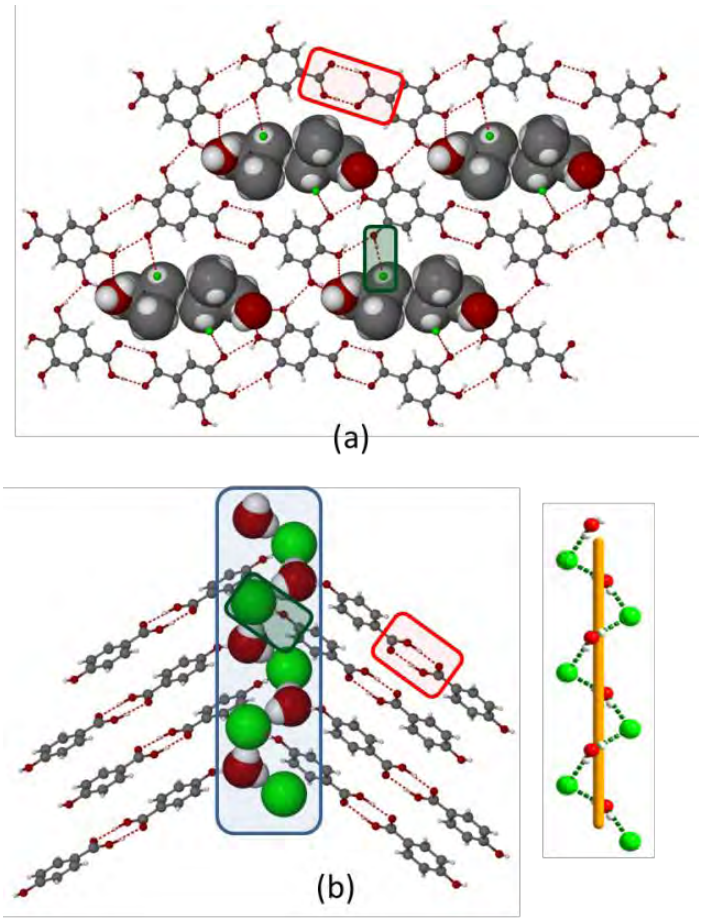

Figure 3.5. Intermolecular hydrogen bonding in (a) TMAGAL and (b) TMA4HBA. Catechol dimers and supramolecular synthons IV and VII are in TMAGAL whereas VII and VIII are observed in TMA4HBA. Ammonium cations are given in space filling model in TMAGAL and omitted for clarity in TMA4HBA. (c) Helical chain of chloride anions and water molecules lie along a 2_1 screw axis.

PHCDBA and PHCGAL form 3D networks. PHCGAL is a 1:1 ICC that is also a 0.33 hydrate. It contains two independent chloride anions in the asymmetric unit. One chloride anion forms synthon I, with O···Cl^- 3.002(1), 3.009(1), and 2.953(2) Å, whereas the other chloride anion is involved in both synthon I and synthon VIII. Phenol homosynthon (IV) is observed in PHCDBA, whereas a catechol dimer and synthon VII are observed in PHCGAL. The chloride anions and water, further hydrogen bonded by synthon I, III, and VIII, collectively afford 3D networks. The crystal structure of PHCDBA contains two pyridine hydrochlorides, two dihydroxybenzoic acids, and one water molecule in the asymmetric unit. One chloride anion forms synthon I and is additionally involved in hydrogen bonding to a protonated nitrogen (N···Cl^-: 3.092(2) Å), whereas the second chloride anion forms synthons I and VIII (O···O bond: 3.222(1) Å), shown in Figure 3.6.

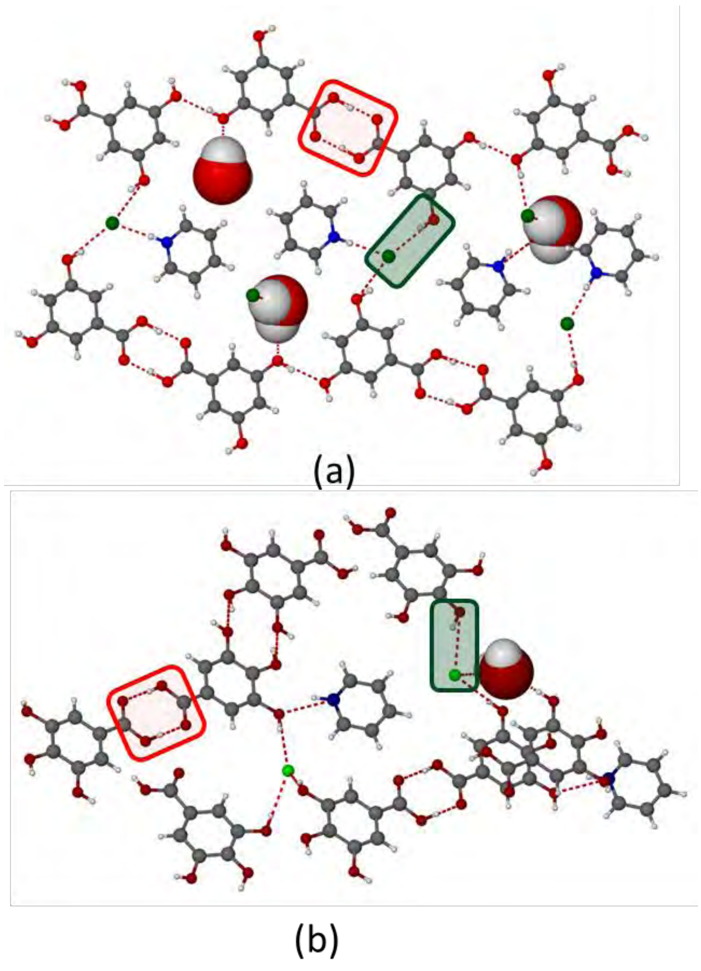

Figure 3.6. Illustration of hydrogen bonding networks and different types of supramolecular synthons observed (a) PHCDBA and (b) PHCGAL.

Overall, out of 12 ICCs, in (12/12) synthon I, in only one case synthon II and in (10/12) cases synthon III are observed. A summary of the supramolecular synthons observed in the nine most relevant published crystal structures along with the newly reported crystal structures is presented in Table 3.4.

Table 3.4. Summary of Supramolecular Synthons Observed in Related Compounds Archived in the CSD and in the Compounds Reported Herein

Compound	***I***	***II***	***III***	***IV***	***V***	***VI***	***VII***	***VIII***
Entries retrieved from CSD								
LDOPAC01		✔		✔	✔			
LTYRHC10	✔				✔			
OTROSC	✔	✔						
SUZTAJ	✔		✔					✔
TEJPIH	✔	✔						
FAPKEN (H)						✔	✔	✔
IJUKAA (H)	✔					✔		✔
SEDDEM (H)	✔					✔	✔	✔
WAPYOC (H)	✔					✔	✔	✔
Novel ICCs								
PHC4HBA	✔		✔					
PHC6HNA	✔		✔					
TEA3HBA	✔	✔						
TEACOU	✔		✔					
TEAHPA	✔		✔					
TEAPCA	✔				✔			
TMADBA	✔		✔					
TMAPCA	✔		✔					
PHCDBA (H)	✔		✔				✔	✔
PHCGAL (H)	✔		✔	✔				✔
TMA4HBA (H)	✔		✔				✔	✔
TMAGAL (H)	✔		✔	✔			✔	✔

3.4 Computational Studies

3.4.1 Hydrogen Bond Strengths. In Table 3.5 we give the gas-phase hydrogen bond strengths for the synthons that are the main focus of the present study, i.e., COOH···COOH, OH··· Cl^-, and COOH···Cl^-. The interaction energy for each synthon has been computed for a variety of different species. These include some "simple" synthons such as benzoic acid (COOHPh), phenol (Ph−OH), ethanol (CH3CH2OH), propanoic acid (CH3CH2COOH), 2 -methyl propanoicacid ((CH3) 2CH2COOH), and 2-methy l propan-1-ol ((CH3)2CHCH2OH). In addition, we have also computed the interaction energies between the different molecules forming the synthons examined in the present study, these include 3HBA, 6HNA, COU, HPA, PCA, and DBA (see Scheme 3.1). Table 3.5 includes the synthons observed in the resolved crystal structures and also those that could potentially form but are not observed. In a number of cases the cocrystal former has more than one possible means of forming the synthon. In these cases we have computed all non-symmetry equivalent possibilities. For example, PCA has two phenol groups, one that is meta and the other that is para to the carboxyl group; these are non-equivalent and therefore the OH···Cl^- synthon has been computed twice. For DBA on the other hand, which also has two phenol groups, only one OH··· Cl^- synthon has been computed due to their symmetry equivalence. Furthermore, there are two different ICCs containing the PCA cocrystal former that have different conformations. For TEAPCA the phenol groups on the PCA molecule are pointing away from one other (see Figure 3.4a), whereas in the TMAPCA the para-phenol group is rotated toward the meta-phenol group (see Figure 3.4b). Taking the conformational diversity into account result in four OH···Cl^- interaction energies for PCA, these are all given in Table 3.5.

Table 3.5. Hydrogen bond energies[a] (in kJ mol^{-1}) computed using M06/6-311+G(3df,2p)//M06/6-311G(d,p) of three different synthons formed with a number of alternative substrates (see Scheme 1).

R-COOH···COOH-R		**R-COOH···Cl$^-$**		**R-OH···Cl$^-$**	
species	ΔE	species	ΔE	species	ΔE
CH_3CH_2COOH	−70.5	CH_3CH_2COOH	−81.4	CH_3CH_2OH	−75.8
$(CH_3)_2CHCOOH$	−70.6	$(CH_3)_2CHCOOH$	−82.5	$(CH_3)_2CHCH_2OH$	−74.5
HOOC-Ph	−73.2	HOOC-Ph	−89.4	Ph-OH	−106.2
3HBA	−72.4	3HBA	−92.5	3HBA	−108.3
4HBA	−73.4	4HBA	−85.0	4HBA	−131.7
6HNA	−72.6	6HNA	−88.6	6HNA	−131.5
COU	−72.5	COU	−79.1	COU	−138.4
HPA	−75.7	HPA	−97.2	HPA	−135.2
DBA	−73.2	DBA	−97.6	DBA	−107.9
PCA	−73.1	PCA[d]	−87.3	PCA[b,d]	−142.6
		PCA[e]	−91.6	PCA[c,d]	−127.0
				PCA[b,e]	−127.8
				PCA[c,e]	−104.0
Ave.	−72.8	Ave.	−88.1	Ave.	−116.2
Std.	1.3	Std.	5.7	Std.	21.5

[a] Computed in the gas-phase with no correction for vibrational contributions added. [b] OH group is para to the carboxyl group. [c] OH group is meta to the carboxyl group. [d] The conformation of the PCA molecule as found in the TMAPCA ICC. [e] The conformation of the PCA molecule as found in the TEAPCA ICC.

Table 3.5 shows that the COOH···COOH synthon is typically the weakest of the three synthons examined, with an average energy of interaction of −72.8 kJ mol^{-1} across all the substrates. It also has very low variability with a standard deviation of 1.3 kJ mol^{-1}. This low variability demonstrates that substituent effects are only small with the majority of the stabilization energy (2−3 kJ mol^{-1}) due the weak resonance assistance from the aromatic ring. This is clearly demonstrated by the difference in dimer strengths between propanoic acid (−70.5 KJ mol^{-1}), 2-methyl propanoic acid (−70.6 kJ mol^{-1}), and benzoic acid (−73.2 kJ mol^{-1}). An additional minor meta-effect from the carboxyl group present in HPA is also observed with an interaction of −75.7 kJ mol^{-1}. This has been rationalized in terms of the smaller partial negative charge induced on the carboxyl group.[111]

The carboxylic acid to chloride anion synthon ($COOH\cdots Cl^-$) is on average 15.3 kJ mol^{-1} stronger than that of the carboxylic acid dimer synthon. This increase in strength comes primarily from the increased electrostatic effect of a carboxyl group interacting with an anion as compared with a neutral species. For example, in the absence of aromatic functionalities the interaction energy is approximately 11−12 kJ mol^{-1} greater. The standard deviation is also higher at 5.7 kJ mol^{-1}. This variability is due to the larger resonance assistance from the aromatic ring, which amounts to an additional 8 kJ mol^{-1} on top of the charge assistance. The increased resonance assistance is clearly demonstrated by the different interaction energies for propanoic acid (−81.4 kJ mol^{-1}), 2-methyl propanoic acid (−82.5 kJ mol^{-1}) and benzoic acid (−89.4 kJ mol^{-1}).

Table 3.5 shows that the strongest synthon on average is the alcohol to chloride interaction ($OH\cdots Cl^-$) at −120.6 kJ mol^{-1}. In this case resonance stabilization plays a key role in stabilizing the hydrogen bond with the formally charged anion. Without this additional stabilization the phenol group would normally be a weaker donor than the carboxyl group. This is clearly demonstrated by comparing the differences in interaction energies in the presence and absence of a phenyl group. For example, the simple alkyl carboxylic acids have interaction energies of approximately 81 kJ mol^{-1} compare with approximately 75 kJ mol^{-1} for simple alkyl alcohols. However, the introduction of a phenyl group dramatically increases the −OH interaction energy by more than ~25 kJ mol^{-1} but for −COOH interactions the benefit of the aromatic group is at most ~15 kJ mol^{-1}. The resonance stabilization dramatically increases the effect of a para-phenol group with the highest hydrogen bond interaction found for the PCA molecule at −142.6

kJ mol^{-1}. These results also cause the OH...Cl^{-} synthon to have the highest variability of 18.1 kJ mol^{-1}. When considering the average hydrogen bond strengths for the three synthons described above, then the prevalence of the phenol OH···Cl^{-} synthon in the ICCs examined in the present study seem to be justified. However, the chemistry of the attached groups needs to be carefully considered when drawing conclusions about general synthon hierarchies. For example, whereas the strength of the carboxylic acid dimer is not affected by the identity of the attached group in the present study the OH···Cl^{-} synthon may show a wide range of interaction energies (−75.8 to 142.6 kJ mol^{-1}).

3.4.2 Lattice Energies. Using the synthon hierarchy described above (COOH···COOH < COOH···Cl^{-} < Ph−OH···Cl^{-}) it might be tempting to predict the order of lattice energies for the various ICCs synthesized in the present study. To test this hypothesis we present in Table 3.6 the lattice energies for all the ICCs that do not contain water. The table also gives the numbers and types of synthons present in the lattice according to Scheme 3.5 along with the calculated strengths as determined from Table 3.5. Synthon II and V were not considered in Scheme 3.5, so additional calculations using the same methodology were used to determine the strengths of interaction.

We first note that the lattice energies in Table 3.6 are much higher than lattices containing neutral organic components, which reflects their ionic nature. Moreover, in some cases the lattice energies even exceed that of common salts; for example, NaCl, has a calculated lattice energy of −782.0 kJ mol^{-1} when using the same protocol as that used for Table 3.6. At first sight Table 3.6 suggests that if the lattice contains a higher number of Ph−OH···Cl^{-} synthons then the lattice energy is more negative. This is agreement in with the general trend of their relative strengths. For example, the weakest lattices generally only have one Ph−OH···Cl⁻ synthon per chloride anion, whereas the strongest lattices have two Ph−OH···Cl⁻ synthons per chloride atom. Furthermore, if the lattice contains a particularly strong Ph−OH···Cl⁻ synthon, like that of HPA, than the lattice energy tends to be more negative. However, there are some obvious difficulties with this analysis. For example, PHC4HBA contains only one Ph−OH···Cl⁻ synthon per chloride, but its lattice energy is lower than that of TEAPCA, which contains two. In order to reconcile these differences, we might want to invoke the argument of different packing efficiencies. However, if the strength of the ionic interaction is also considered then the synthon hierarchies tend to follow the chemistry fairly closely. Table 3.6 contains ICCs with three different counterions, i.e., PHC, TMA, and TEA. The strengths of these interactions calculated with the same protocol as Table 3.6 are −481.3, −412.9, and −371.5 kJ mol^{-1}, for PHC, TMA, and TEA, respectively. As the table shows, within each counterion series the calculated interaction energies of the synthons correlates well with the lattice energy. The only exception to this trend is the lattice energy of TEAHPA, which seems to be much lower than what is indicated by the synthons.

Table 3.6. Lattice Energies in kJ mol^{-1} for various ICCs along with the number and types[a] of synthons present in the lattice (per molecule) and the gas-phase energies (in kJ mol^{-1}) of each of the indicated synthon.

			strengths[b]				
Compound	ΔE_{latt}	Synthons[a,c]	I	I	II	V	III
PHC4HBA	-749.9	I(1),III(1)	-85.0				-73.4
PHC6HNA	-935.9	I(2),III(1)	-131.5	-131.5			-72.6
TMADBA	-764.1	I(2),III(1)	-108.3	-108.3			-73.2
TMAPCA	-870.0	I(2),III(1)	-127.8	-127.8			-72.9

TEA3HBA	-703.2	I(1),II(1)	-108.3		-92.5		
TEAPCA	-738.8	I(2),V(1)	-127.8	-104.0		-45.1	
TEACOU	-882.1	I(2),III(1)	-138.4	-138.4			-72.5
TEAHPA	-938.2	I(2),III(1)	-135.2	-135.2			-75.7

[a] See Scheme 3 for the synthon definition and associated Roman numeral. [b] The gas-phase association energy in kJ mol^{-1} calculated using M)6/6-311G(3df,2p)//M06/6-311G(d,p) for each of the indicated synthons. [c] The number of synthons of the particular type present in the lattice per molecule is indicated brackets.

3.5 Conclusions

Crystal structure analyses reveal that the majority of carboxylic acid and phenol groups form charge-assisted hydrogen bonds with chloride anions (ca. 70% of the time) even when in the presence of competing functional groups. Furthermore, in the absence of other hydrogen bond donors and acceptors, both functional groups persistently form charge-assisted hydrogen bonds with chloride anions. However, the CSD does not contain sufficient information to address the hierarchy of the chloride anion supramolecular heterosynthon in a competitive environment containing carboxylic acid and phenol moieties. To address the hierarchy of these interactions, we analyzed 9 crystal structures from the CSD along with 12 novel ICCs. Our analysis and a parallel computational study strongly suggest that phenol···chloride hydrogen bonds (synthon I) are persistent even when in the presence of a carboxylic acid moiety (in 19/21 cases). Indeed, the carboxylic acid to chloride supramolecular synthon occurs in a mere 4/21 in the presence of phenols. The carboxylic acid dimer is instead more prevalent as it occurs in 11 of the 21 structures. The computational studies of the reported synthons further suggest that the phenol···chloride supramolecular heterosynthon is preferred vs the carboxylic acid···chloride interaction. Furthermore, synthon I is not disrupted even in the presence of water molecules. Thus, our data show that the relative preference of supramolecular synthon is synthon I > III > II when carboxylic, phenol, and chloride anions are present. This crystal engineering study exemplifies a new category of hierarchy of supramolecular synthons via ICCs. Furthermore, synthon I, suggests that polyphenols can be used as cocrystal formers for the synthesis of novel ICCs of chloride salt. These supramolecular synthon principles can be employed to implement a broadly based design strategy to synthesize novel materials and are most pertinent to ingredients of pharmaceutical and nutraceutical science. Future studies will focus upon exploring this crystal engineering strategy to address issues such as physicochemical stability for hydrochloride salts of APIs and to improve the solubility of nutraceuticals containing phenol moieties through ionic cocrystallization. Finally, this study points out that relying upon pKa values to predict the hierarchy of hydrogen bonds between competing supramolecular synthons is a rule of thumb that does not always lead to the expected outcome.

3.6 References:

(1) Pepinsky, R., *Phys. Rev.,* **1955**, (100), 971.

(2) Schmidt, G., Photodimerization in the solid state. *Pure Appl. Chem.,* **1971**, *27*(4), 647-678.

(3) Moulton, B.; Zaworotko, M. J., From molecules to crystal engineering: supramolecular isomerism and polymorphism in network solids. *Chem. Rev.,* **2001**, *101*(6), 1629-1658.

(4) Desiraju, G. R.; Parshall, G. W., Crystal engineering: the design of organic solids. *Materials science monographs.,* **1989**, *54*.

(5) Desiraju, G. R., Supramolecular synthons in crystal engineering – a new organic synthesis. *Angew. Chem. Int. Ed.,* **1995**, *34*(21), 2311-2327.

(6) Seddon, K. R.; Zaworotko, M., *Crystal engineering: the design and application of functional solids*. ed.; Springer Science & Business Media: 1999; Vol. 539.

(7) Huang, K.-S.; Britton, D.; Byrn, S. R., A novel class of phenol–pyridine co-crystals for secondharmonic generation. *J. Mater. Chem.,* **1997**, *7*(5), 713-720.

(8) Murata, T.; Morita, Y.; Yakiyama, Y.; Fukui, K.; Yamochi, H.; Saito, G.; Nakasuji, K., Hydrogen bond interaction in organic conductors: Redox activation, molecular recognition, structural regulation, and proton transfer in donor−acceptor charge-transfer complexes of TTF-Imidazole. *J. Am. Chem. Soc.,* **2007**, *129*(35), 10837-10846.

(9) Bolton, O.; Simke, L. R.; Pagoria, P. F.; Matzger, A. J., High power explosive with good sensitivity: A 2:1 Cocrystal of CL-20:HMX. *Cryst. Growth Des.,* **2012**, *12*(9), 4311-4314.

(10) Landenberger, K. B.; Bolton, O.; Matzger, A. J., Two isostructural explosive cocrystals with significantly different thermodynamic stabilities. *Angew. Chem. Int. Ed.,* **2013**, *52*(25), 6468-6471.

(11) Kitagawa, S.; Kitaura, R.; Noro, S. i., Functional porous coordination polymers. *Angew. Chem. Int. Ed.,* **2004**, *43*(18), 2334-2375.

(12) Haleblian, J.; McCrone, W., Pharmaceutical applications of polymorphism. *J. Pharm. Sci.,* **1969**, *58*(8), 911-929.

(13) Brittain, H. G., Polymorphism and solvatomorphism 2010. *J. Pharm. Sci.,* **2012**, *101*(2), 464-484.

(14) Pudipeddi, M.; Serajuddin, A., Trends in solubility of polymorphs. *J. Pharm. Sci.,* **2005**, *94*(5), 929-939.

(15) Almarsson, Ö.; Zaworotko, M. J., Crystal engineering of the composition of pharmaceutical phases. Do pharmaceutical co-crystals represent a new path to improved medicines? *Chem. Commun.,* **2004**, (17), 1889-1896.

(16) Vishweshwar, P.; McMahon, J. A.; Bis, J. A.; Zaworotko, M. J., Pharmaceutical co-crystals. *J. Pharm. Sci.,* **2006**, *95*(3), 499-516.

(17) Jones, W.; Motherwell, W. D. S.; Trask, A. V., Pharmaceutical cocrystals: An emerging approach to physical property enhancement. *MRS Bull.,* **2006**, *31*(11), 875-879.

(18) Shan, N.; Zaworotko, M. J., The role of cocrystals in pharmaceutical science. *Drug Discovery Today.,* **2008**, *13*(9–10), 440-446.

(19) Schultheiss, N.; Newman, A., Pharmaceutical cocrystals and their physicochemical properties. *Cryst. Growth Des.,* **2009**, *9*(6), 2950-2967.

(20) Maitland, G.; Rigby, M.; Smith, E.; Wakeham, W., Intermolecular forces–Their origin and determination. Oxford University Press. In ed.; Oxford: **1981**.

(21) Walsh, R. D. B.; Bradner, M. W.; Fleischman, S.; Morales, L. A.; Moulton, B.; Rodriguez-Hornedo, N.; Zaworotko, M. J., Crystal engineering of the composition of pharmaceutical phases. *Chem. Commun.,* **2003**, (2), 186-187.

(22) Bis, J. A.; Zaworotko, M. J., The 2-Aminopyridinium-carboxylate supramolecular heterosynthon: A robust motif for generation of multiple-component crystals. *Cryst. Growth Des.,* **2005**, *5*(3), 1169-1179.

(23) Duchamp, D. J.; Marsh, R. E., The crystal structure of trimesic acid (benzene-1, 3, 5-tricarboxylic acid). *Acta Crystallogr. Sect. B-Struct. Sci.,* **1969**, *25*(1), 5-19.

(24) Berney, C., Spectroscopy of CF_3COZ compounds. V. Vibrational spectra and structure of solid trifluoroacetic acid. *J. Am. Chem. Soc.,* **1973,** *95*(3), 708-716.

(25) Leiserowitz, L., Molecular packing modes. Carboxylic acids. *Acta Crystallogr. Sect. B-Struct. Sci.,* **1976**, *32*(3), 775-802.

(26) Etter, M. C., A new role for hydrogen-bond acceptors in influencing packing patterns of carboxylic acids and amides. *J. Am. Chem. Soc.,* **1982**, *104*(4), 1095-1096.

(27) Pinkus, A. G.; Subramanian, T. S., Isolation and characterization of 1 : 1 crystalline substituted benzoic acid heterodimers resulting from intermolecular hydrogen bonding. *J. Chem. Soc., Chem.Commun.,* **1986**, (18), 1439-1439.

(28) Ermer, O., Five-fold diamond structure of adamantane-1,3,5,7-tetracarboxylic acid. *J. Am. Chem. Soc.,* **1988**, *110*(12), 3747-3754.

(29) Leiserowitz, L.; Schmidt, G. M. J., Molecular packing modes. Part III. Primary amides. *J. Chem. Soc. A.,* **1969**, (0), 2372-2382.

(30) Huang, C. M. L., L.; Schmidt, G. M. J., *J.Chem. Soc. Perkin. Trans. 2,* **1973**.

(31) Weinstein, S.; Leiserowitz, L.; Gil-Av, E., Chiral secondary amides. 2. Molecular packing and chiral recognition. *J. Am. Chem. Soc.,* **1980**, *102*(8), 2768-2772.

(32) Etter, M. C., Encoding and decoding hydrogen-bond patterns of organic compounds. *Acc. Chem. Res.,* **1990**, *23*(4), 120-126.

(33) Nguyen, T. L.; Fowler, F. W.; Lauher, J. W., Commensurate and incommensurate hydrogen bonds. An exercise in crystal engineering. *J. Am. Chem. Soc.,* **2001**, *123*(44), 11057-11064.

(34) McMahon Jennifer, A.; Bis Joanna, A.; Vishweshwar, P.; Shattock Tanise, R.; McLaughlin Olga, L.; Zaworotko Michael, J., Crystal engineering of the composition of pharmaceutical phases. 3. Primary amide supramolecular

heterosynthons and their role in the design of pharmaceutical co-crystals. In *Z. Kristallogr.*, **2005**, *220*, 340.

(35) Leiserowitz, L.; Nader, F., The molecular packing modes and the hydrogen-bonding properties of amide:dicarboxylic acid complexes. *Acta Crystallogr. Sect. B-Struct. Sci.,* **1977**, *33*(9), 2719-2733.

(36) Videnova-Adrabińska, V.; Etter, M., Urea-glutaric acid (2:1) structural aggregates as building blocks for crystal engineering. *J. Chem. Crystallogr.,* **1995**, *25*(12), 823-829.

(37) Fleischman, S. G.; Kuduva, S. S.; McMahon, J. A.; Moulton, B.; Bailey Walsh, R. D.; Rodríguez-Hornedo, N.; Zaworotko, M. J., Crystal Engineering of the composition of pharmaceutical phases: Multiple-component crystalline solids involving carbamazepine. *Cryst. Growth Des.,* **2003**, *3*(6), 909-919.

(38) Aakeröy, C. B.; Beatty, A. M.; Helfrich, B. A.; Nieuwenhuyzen, M., Do polymorphic compounds make good cocrystallizing agents? A structural case study that demonstrates the importance of synthon flexibility. *Cryst. Growth Des.,* **2003**, *3*(2), 159-165.

(39) Vishweshwar, P.; Nangia, A.; Lynch, V. M., Molecular complexes of homologous alkanedicarboxylic acids with isonicotinamide: X-ray crystal structures, hydrogen bond synthons, and melting point alternation. *Cryst. Growth Des.,* **2003**, *3*(5), 783-790.

(40) Copp, S. B.; Subramanian, S.; Zaworotko, M. J., Supramolecular chemistry of manganese complex $[Mn(CO)_3(\mu_3\text{-}OH)]4$: assembly of a cubic hydrogen-bonded diamondoid network with 1,2-diaminoethane. *J. Am. Chem. Soc.,* **1992**, *114*(22), 8719-8720.

(41) Loehlin, J. H.; Etter, M. C.; Gendreau, C.; Cervasio, E., Hydrogen-bond patterns in several 2: 1 amine-phenol cocrystals. *Chem. Mater.,* **1994**, *6*(8), 1218-1221.

(42) Loehlin, J.; Franz, K.; Gist, L.; Moore, R., Supramolecular alcohol–amine crystals and their hydrogen-bond patterns. *Acta Crystallogr. Sect. B-Struct. Sci.,* **1998**, *54*(5), 695-704.

(43) Vangala, V. R.; Mondal, R.; Broder, C. K.; Howard, J. A.; Desiraju, G. R., Dianiline-diphenol molecular complexes based on supraminol recognition. *Cryst. Growth Des.,* **2005**, *5*(1), 99-104.

(44) Sharma, C. V. K.; Zaworotko, M. J., X-Ray crystal structure of $C_6H_3(CO_2H)_3$-1,3,5[middle dot]1.5(4,4[prime or minute]-bipy): a 'super trimesic acid' chicken-wire grid. *Chem. Commun.,* **1996**, (23), 2655-2656.

(45) Steiner, T., Competition of hydrogen-bond acceptors for the strong carboxyl donor. *Acta Crystallogr. Sect. B-Struct. Sci.,* **2001,** *57*(1), 103-106.

(46) Aakeröy, C. B.; Beatty, A. M.; Helfrich, B. A., A High-yielding supramolecular reaction. *J. Am. Chem. Soc.,* **2002**, *124*(48), 14425-14432.

(47) Aakeröy, C. B.; Beatty, A. M.; Helfrich, B. A., "Total synthesis" supramolecular style: Design and hydrogen-bond-directed assembly of ternary supermolecules. *Angew. Chem. Int. Ed.,* **2001**, *40*(17), 3240-3242.

(48) Bond, A. D., In situ co-crystallisation as a tool for low-temperature crystal engineering. *Chem. Commun.,* **2003**, (2), 250-251.

(49) Bhogala, B. R.; Basavoju, S.; Nangia, A., Three-component carboxylic acid−bipyridine lattice inclusion host. supramolecular synthesis of ternary cocrystals. *Cryst. Growth Des.,* **2005**, *5*(5), 1683-1686.

(50) Shattock, T. R.; Arora, K. K.; Vishweshwar, P.; Zaworotko, M. J., Hierarchy of supramolecular synthons: Persistent carboxylic acid···pyridine hydrogen bonds

in cocrystals that also contain a hydroxyl moiety. *Cryst. Growth Des.,* **2008**, *8*(12), 4533-4545.

(51) MacGillivray, L. R.; Reid, J. L.; Ripmeester, J. A., Supramolecular control of reactivity in the solid state using linear molecular templates. *J. Am. Chem. Soc.,* **2000**, *122*(32), 7817-7818.

(52) MacGillivray, L. R.; Atwood, J. L., Cavity-containing materials based upon resorcin [4] arenes by discovery and design. *J. Solid State Chem.,* **2000**, *152*(1), 199-210.

(53) Papaefstathiou, G. S.; MacGillivray, L. R., Discrete versus infinite molecular self-assembly: control in crystalline hydrogen-bonded assemblies based on resorcinol. *Org. Lett.,* **2001**, *3*(24), 3835-3838.

(54) Vishweshwar, P.; Nangia, A.; Lynch, V. M., Supramolecular synthons in phenol-isonicotinamide adducts. *CrystEngComm.,* **2003**, *5*(31), 164-168.

(55) Bis, J. A.; Vishweshwar, P.; Weyna, D.; Zaworotko, M. J., Hierarchy of supramolecular synthons: Persistent hydroxyl···pyridine hydrogen bonds in cocrystals that contain a cyano acceptor. *Mol. Pharm.,* **2007**, *4*(3), 401-416.

(56) Lynch, D. E.; Smith, G.; Freney, D.; Byriel, K. A.; Kennard, C. H., Molecular cocrystals of carboxylic acids. XV. Preparation and characterization of heterocyclic base adducts with a series of carboxylic acids, and the crystal structures of the adducts of 2-aminopyrimidine with 2, 6-dihydroxybenzoic acid, 4-aminobenzoic acid, phenoxyacetic acid,(2, 4-Dichlorophenoxy) acetic acid,(3, 4-dichlorophenoxy)-acetic acid and salicylic acid, and 2-aminopyridine with 2, 6-dihydroxybenzoic acid. *Aust. J. Chem.,* **1994**, *47*(6), 1097-1115.

(57) Papaefstathiou, G. S.; Kipp, A. J.; MacGillivray, L. R., Exploiting modularity in template-controlled synthesis: a new linear template to direct reactivity within

discrete hydrogen-bonded molecular assemblies in the solid state. *Chem. Commun.,* **2001**, (23), 2462-2463.

(58) Vishweshwar, P.; Nangia, A.; Lynch, V. M., Recurrence of carboxylic acid−pyridine supramolecular synthon in the crystal structures of some pyrazinecarboxylic acids. *J. Org. Chem.,* **2002**, *67*(2), 556-565.

(59) Aakeroy, C. B.; Desper, J.; Helfrich, B. A., Heteromeric intermolecular interactions as synthetic tools for the formation of binary co-crystals. *CrystEngComm.,* **2004**, *6*(5), 19-24.

(60) Reddy, L. S.; Nangia, A.; Lynch, V. M., Phenyl-perfluorophenyl synthon mediated cocrystallization of carboxylic acids and amides. *Cryst. Growth Des.,* **2004**, *4*(1), 89-94.

(61) Bhogala, B. R.; Basavoju, S.; Nangia, A., Tape and layer structures in cocrystals of some di- and tricarboxylic acids with 4,4[prime or minute]-bipyridines and isonicotinamide.From binary to ternary cocrystals. *CrystEngComm.,* **2005**, *7*(90), 551-562.

(62) Vishweshwar, P.; McMahon, J. A.; Peterson, M. L.; Hickey, M. B.; Shattock, T. R.; Zaworotko, M. J., Crystal engineering of pharmaceutical co-crystals from polymorphic active pharmaceutical ingredients. *Chem. Commun.,* **2005**, (36), 4601-4603.

(63) Edwards, M. R.; Jones, W.; Motherwell, W. D. S., Cocrystal formation of 4-methyl and 4-chlorobenzamide with carboxylic acids: Chloro/methyl interchange and crystal structure. *CrystEngComm.,* **2006**, *8*(7), 545-551.

(64) F. H Allen; Kennard, O., 3D search and research using the Cambridge Cristallogaphic Database. Chem. *Des. Autom. News.,* **1993**, *8*, 31-37.

(65) Allen, F. H., The Cambridge Structural Database: a quarter of a million crystal structures and rising. *Acta Crystallogr. Sect. B-Struct. Sci.,* **2002**, *B58*(3), 380-388.

(66) Solvates that included in the search are; methanol, ethanol, propanol, butanol, DCM, DMSO, DMF, formamide, IPA, ethyl acetate, THF, acetic acid, formic acid, acetone, chloroform, ethylene glycol, propylene glycol, N-methyl pyrrolidine, N-methyl pyrrolidone, pyrdine, 1,4 dioxane, acetonitrile.

(67) Braga, D.; Grepioni, F.; Maini, L.; Prosperi, S.; Gobetto, R.; Chierotti, M. R., From unexpected reactions to a new family of ionic co-crystals: the case of barbituric acid with alkali bromides and caesium iodide. *Chem. Commun.,* **2010**, *46*(41), 7715-7717.

(68) Braga, D.; Grepioni, F.; Lampronti, G. I.; Maini, L.; Turrina, A., Ionic co-crystals of organic molecules with metal halides: A new prospect in the solid formulation of active pharmaceutical ingredients. *Cryst. Growth Des.,* **2011**, *11*(12), 5621-5627.

(69) Rodríguez-Cuamatzi, P.; Arillo-Flores, O.; Bernal-Uruchurtu, M.; Höpfl, H., Experimental and theoretical analysis of the hydrogen-bonding motifs formed between the carboxyl and the carboxylate group: towards a systematic classification of their supramolecular motifs. *Supramol. Chem.,* **2007**, *19*(8), 559-578.

(70) De Rome De LIsle, J. B. L., *Crystallographie, 2nd ed. Paris,* **1783**.

(71) Kobell, F. V., *J. Prakt. Chem.,* **1843**, *28*.

(72) Beevers, C.; Cochran, W., X-ray examination of sucrose. *Nature.,* **1946**, *157*, 872.

(73) Wood, R.; James, V.; Mills, J., 2, 5, 0-methylene-D-mannitol sodium chloride $C_{17}O_6O_{14}$·NaCl. *Cryst. Struct. Comm.,* **1976**, *5*, 207.

(74) Ferguson, G.; Kaitner, B.; Connett, B.; Rendle, D., Structure of the α-D-glucose–sodium chloride–water complex (2/1/1). *Acta Crystallogr. Sect. B-Struct. Sci.,* **1991**, *47*(4), 479-484.

(75) Reck, G. T., W., *Pharmazie.,* **1991**, (46), 509.

(76) Chen, Z.-F.; Xiong, R.-G.; Zuo, J.-L.; Guo, Z.; You, X.-Z.; Fun, H.-K., X-Ray crystal structures of Mg^{2+} and Ca^{2+} dimers of the antibacterial drug norfloxacin. *Dalton Trans.,* **2000**, (22), 4013-4014.

(77) Braga, D.; Grepioni, F.; Maini, L.; Capucci, D.; Nanna, S.; Wouters, J.; Aerts, L.; Quéré, L., Combining piracetam and lithium salts: ionic co-crystals and co-drugs? *Chem. Commun.,* **2012**, *48*(66), 8219-8221.

(78) Ong, T. T.; Kavuru, P.; Nguyen, T.; Cantwell, R.; Wojtas, Ł.; Zaworotko, M. J., 2:1 Cocrystals of homochiral and achiral amino acid zwitterions with Li^+ salts: Water-stable zeolitic and diamondoid metal–organic materials. *J. Am. Chem. Soc.,* **2011**, *133*(24), 9224-9227.

(79) Smith, A. J.; Kim, S.-H.; Duggirala, N. K.; Jin, J.; Wojtas, L.; Ehrhart, J.; Giunta, B.; Tan, J.; Zaworotko, M. J.; Shytle, R. D., Improving lithium therapeutics by crystal engineering of novel ionic cocrystals. *Mol. Pharm.,* **2013**, *10*(12), 4728-4738.

(80) Stahl, P. H.; Wermuth, C. G., *Handbook of pharmaceutical salts: properties, selection, and use*. ed.; Wiley-Vch Weinheim, Germany: **2002**; Vol. 2.

(81) Berge, S. M.; Bighley, L. D.; Monkhouse, D. C., Pharmaceutical salts. *J. Pharm. Sci.,* **1977**, *66*(1), 1-19.

(82) Bighley, L.; Berge, S.; Monkhouse, D., Salt forms of drugs and absorption. *Encyclopedia of Pharmaceutical Technology.,* **1996**, *13*, 453-499.

(83) Isabel Kalofonos, G. P. S., William Martin-Doyle, Dimitris Kalofonos, Jeffrey S. Stults, Jason A. Hanko, Rex A. Shipplett, Flupirtine hydrochloride maleic acid cocrystal. WO2010017343 A2, **2010**.

(84) Shan, N.; Perry, M. L.; Weyna, D. R.; Zaworotko, M. J., Impact of pharmaceutical cocrystals: the effects on drug pharmacokinetics. *Expert Opin. Drug Metab. Toxicol.,* **2014**, *10*(9), 1255-1271.

(85) Childs, S. L.; Chyall, L. J.; Dunlap, J. T.; Smolenskaya, V. N.; Stahly, B. C.; Stahly, G. P., Crystal engineering approach to forming cocrystals of amine hydrochlorides with organic acids. Molecular complexes of fluoxetine hydrochloride with benzoic, succinic, and fumaric Acids. *J. Am. Chem. Soc.,* **2004**, *126*(41), 13335-13342.

(86) Duggirala, N. K.; Smith, A. J.; Wojtas, Ł.; Shytle, R. D.; Zaworotko, M. J., Physical stability enhancement and pharmacokinetics of a lithium ionic cocrystal with glucose. *Cryst. Growth Des.,***2014**, *14*(11), 6135-6142.

(87) Thallapally, P. K.; Nangia, A., A Cambridge Structural Database analysis of the C–HCl interaction: C–HCl^{-} and C–HCl–M often behave as hydrogen bonds but C–HCl–C is generally a van der Waals interaction. *CrystEngComm.,* **2001**, *3*(27), 114-119.

(88) Gilli, P.; Pretto, L.; Bertolasi, V.; Gilli, G., Predicting hydrogen-bond strengths from acid−base molecular properties. The pK_a slide rule: Toward the solution of a long-lasting problem. *Acc. Chem. Res.,* **2008**, *42*(1), 33-44.

(89) Sládková, V.; Cibulková, J.; Eigner, V.; Šturc, A.; Kratochvíl, B.; Rohlíček, J., Application and comparison of cocrystallization techniques on trospium chloride cocrystals. *Cryst. Growth Des.,* **2014**, *14*(6), 2931-2936.

(90) Aakeroy, C. B.; Epa, K. N.; Forbes, S.; Desper, J., Competing hydrogen-bond donors: phenols vs. cyanooximes. *CrystEngComm.,* **2013**, *15*(30), 5946-5949.

(91) Steiner, T., Hydrogen-bond distances to halide ions in organic and organometallic crystal structures: Up-to-date database study. *Acta Crystallogr. Sect. B-Struct. Sci.,* **1998**, *54*(4), 456-463.

(92) Bruker, A. V., 0 Data collection and processing software. *Bruker AXS Inc., Madison, Wisconsin, USA,* **2008**.

(93) SAINT, P., Data reduction software, version 7.34 a. *Bruker AXS Inc., Madison, WI,* **2005**.

(94) Dolomanov, O. V.; Bourhis, L. J.; Gildea, R. J.; Howard, J. A.; Puschmann, H., OLEX2: a complete structure solution, refinement and analysis program. *J. Appl. Crystallogr.,* **2009**, *42*(2), 339-341.

(95) Farrugia, L., WinGX suite for small-molecule single-crystal crystallography. *J. Appl. Crystallogr.,* **1999**, *32*(4), 837-838.

(96) Hehre, W. J., *Ab initio molecular orbital theory*. ed.; Wiley-Interscience: 1986.

(97) Holthausen, M.; Koch, W., A Chemist's guide to density functional theory. In ed.; Wiley-VCH: Weinheim, Germany: **2000**.

(98) Frisch, M.; Trucks, G.; Schlegel, H.; Scuseria, G.; Robb, M.; Cheeseman, J.; Scalmani, G.; Barone, V.; Mennucci, B.; Petersson, G., Gaussian 09, revision A. 1; Gaussian, Inc: Wallingford, CT, **2009**.

(99) Released under GPL license and freely available at the URL http://www.cp2k.org (accessed August 1, **2013**).

(100) Lippert, G.; Hutter, J.; Parrinello, M., The Gaussian and augmented-plane-wave density functional method for ab initio molecular dynamics simulations. *Theor. Chem. Acc.,* **1999**, *103*(2), 124-140.

(101) VandeVondele, J.; Krack, M.; Mohamed, F.; Parrinello, M.; Chassaing, T.; Hutter, J., Quickstep: Fast and accurate density functional calculations using a mixed gaussian and plane waves approach. *Comput. Phys. Commun.,* **2005**, *167*(2), 103-128.

(102) Zhao, Y.; Truhlar, D. G., The M06 suite of density functionals for main group thermochemistry, thermochemical kinetics, noncovalent interactions, excited states, and transition elements: two new functionals and systematic testing of four M06-class functionals and 12 other functionals. *Theor. Chem. Acc.,* **2008**, *120*(1-3), 215-241.

(103) Wood, G. P.; Radom, L.; Petersson, G. A.; Barnes, E. C.; Frisch, M. J.; Montgomery Jr, J. A., A restricted-open-shell complete-basis-set model chemistry. *J. Chem. Phys.,* **2006**, *125*(9), 094106.

(104) VandeVondele, J.; Hutter, J., Gaussian basis sets for accurate calculations on molecular systems in gas and condensed phases. *J. Chem. Phys.,* **2007**, *127*(11), 114105.

(105) Goedecker, S.; Teter, M.; Hutter, J., Separable dual-space Gaussian pseudopotentials. *Phys. Rev. B.,* **1996**, *54*(3), 1703.

(106) Hartwigsen, C.; Gœdecker, S.; Hutter, J., Relativistic separable dual-space gaussian pseudopotentials from H to Rn. *Phys. Rev. B.,* **1998**, *58*(7), 3641.

(107) Genovese, L.; Deutsch, T.; Neelov, A.; Goedecker, S.; Beylkin, G., Efficient solution of Poisson's equation with free boundary conditions. *J. Chem. Phys.,* **2006**, *125*(7), 074105.

(108) Gillon, A. L.; Feeder, N.; Davey, R. J.; Storey, R., Hydration in molecular crystals a cambridge structural database analysis. *Cryst. Growth Des.,* **2003**, *3*(5), 663-673.

(109) *16 entries from CSD (Refcodes:* XOHTUL, BERVOJ, DIVBIV, FAPKEN, GERCEL, IJUKAA, LDAPOC01, LTYRHC10, OTROSC, SEDDEM, SUZTAJ, TEJPIH, YUSMOJ, WAPYOC, WISJOX, XPSERC*).*

(110) *Hydrated form Refcodes from CSD:* FAPKEN, IJUKAA, SEDDEM, WAPYOC, WISJOX, XPSERC.

(111) Hollingsworth, C. A.; Seybold, P. G.; Hadad, C. M., Substituent effects on the electronic structure and pK_a of benzoic acid. *Int. J. Quantum Chem.,* **2002**, *90*(4-5), 1396-1403.

Physical Stability Enhancement and Pharmacokinetics of a Lithium Ionic Cocrystal with Glucose

"Reprinted (adapted) with permission from (*Crystal Growth & Design*, **2014,** *14* (11), 6135–6142). Copyright (2014) American Chemical Society."

The link to the publication is http://pubs.acs.org/doi/abs/10.1021/cg501310d

Copyright Clearance Center RightsLink® Home Account Info Help Live Chat

ACS Publications Most Trusted. Most Cited. Most Read.

Title: Physical Stability Enhancement and Pharmacokinetics of a Lithium Ionic Cocrystal with Glucose

Author: Naga Kiran Duggirala, Adam J. Smith, Łukasz Wojtas, et al

Publication: Crystal Growth and Design

Publisher: American Chemical Society

Date: Nov 1, 2014

Copyright © 2014, American Chemical Society

Logged in as:
Naga Duggirala
LOGOUT

PERMISSION/LICENSE IS GRANTED FOR YOUR ORDER AT NO CHARGE

This type of permission/license, instead of the standard Terms & Conditions, is sent to you because no fee is being charged for your order. Please note the following:

- Permission is granted for your request in both print and electronic formats, and translations.
- If figures and/or tables were requested, they may be adapted or used in part.
- Please print this page for your records and send a copy of it to your publisher/graduate school.
- Appropriate credit for the requested material should be given as follows: "Reprinted (adapted) with permission from (COMPLETE REFERENCE CITATION). Copyright (YEAR) American Chemical Society." Insert appropriate information in place of the capitalized words.
- One-time permission is granted only for the use specified in your request. No additional uses are granted (such as derivative works or other editions). For any other uses, please submit a new request.

BACK CLOSE WINDOW

Chapter 4: Physical stability enhancement and pharmacokinetics of a lithium ionic cocrystal with glucose

4.1 Introduction

Crystalline forms of drug substances are generally preferred in orally delivered drug products because of their relative ease of purification and manufacture. Their stability versus corresponding amorphous forms can also offer advantages.[1, 2] The pharmaceutical industry employs a variety of unit operations during processing and in situations where the physical stability of a drug substance is affected by water. If this occurs, then the drug substance is designated to be a hygroscopic material.[3,4] Hygroscopicity in a drug substance must be addressed because it could affect physicochemical properties such as dissolution rate, solubility, compactability, and shelf life, any of which could in turn impact drug product performance [5-7]. Conventional approaches to address hygroscopicity include formulation of the drug substance with appropriate excipients, coating the drug product with enteric polymers, or limiting moisture contact with the drug product by proper packaging. If the drug substance undergoes dissolution in water at a critical relative humidity (RHc), it is termed a deliquescent material, which is an extreme case of hygroscopicity. Deliquescence has implications for chemical stability, as seen in the thiamine hydrochloride and sodium ascorbate systems.[8]

Deliquescence can be mitigated by mixing two or more individual deliquescent materials, as demonstrated in common food ingredients such as sugars and organic acids.[9] However, although such a technique has been successfully employed in the food and agricultural industries, only limited studies have addressed the matter in pharmaceuticals.[10, 11] Furthermore, it is difficult to lower the deliquescence of an active pharmaceutical ingredient (API) by conventional formulation techniques. Consequently, there is a general need for new technologies to address hygroscopicity during the formulation of deliquescent drug substances. Cocrystallization affords multiple-component materials that involve incorporation of a second molecule, the coformer, in the crystal lattice with a molecule or ion.[12, 13] Cocrystallization has become a widely studied phenomenon in the context of the pharmaceutical industry because cocrystallization of drug molecules or salts has been found to impact solubility[14, 15] and bioavailability.[16-19] However, cocrystallization could also offer an opportunity to address other physicochemical properties such as hygroscopicity, thereby eliminating the need for formulation approaches to address the matter. Indeed, there are already studies that demonstrate improved physical stability of a molecular compound with respect to hydration.[20, 21] Furthermore, Braga and co-workers have shown that the deliquescence of magnesium chloride can be shifted from 35% RH to 60−70% RH by cocrystallization with racetams, although their objective was to improve the melting point of racetams, which are nonhygroscopic.[22]

Cocrystals in which at least one of the coformers is a drug molecule or ion are termed pharmaceutical cocrystals.[23] Since most drug molecules and ions contain functional groups with hydrogen bonding propensity, pharmaceutical cocrystals are amenable to crystal engineering.[24, 25] They are now recognized for their clinical, legal, and regulatory importance in the context of pharmaceutical science.[26] Most pharmaceutical cocrystals studied to date are molecular cocrystals, i.e., they are composed of two molecular compounds. However, recently a subclass of pharmaceutical cocrystals that offers exceptional diversity in terms of composition and properties has emerged: ionic cocrystals (ICCs). Our research group defines an ICC as a multicomponent material containing at least one salt in a crystal lattice. Their general formula is A^+B^-N (A^+ = cation, B^- = anion, N = neutral molecule or another salt), and they can be regarded as three-component systems. This means that if an ICC is formed in which one of the coformers is an API, and then there are two other variables that can be changed in a modular fashion to alter the physicochemical properties of the solid form of an API. Perhaps the first ICC was that formed from sodium chloride and glucose and reported in the scientific literature by Kobell in 1843 [27]. Sodium iodide with sucrose was isolated in 1871[28] and in 1946 the crystal structure of sodium chloride complexed with sucrose and water was studied by Beevers and Cochran[29]. Subsequently, sodium chloride−mannitol was reported in 1976[30] and sodium chloride−glucose hydrate in 1991,[31] and the term "ionic cocrystal" was coined by Braga for the sodium bromide−barbituric acid cocrystal in 2010.[32] However, even today ICCs are not that well explored and studied compared with molecular cocrystals, and it is reasonable to assert that ICCs are a long known but underexplored class of compounds.

Lithium salts are among the oldest inorganic compounds used as drug products. For example, lithium bromide was used in the treatment of gout and rheumatic disorders as described by Garrod in 1859[33]. The Australian scientist Cade introduced lithium salts for the treatment of manic psychosis in 1949[34]. Subsequently Schou demonstrated the clinical value of lithium salts in manic patients.[35-37] Furthermore; a recent preliminary experimental study indicated that lithium is effective for decreasing some of the pathological consequences of traumatic brain injury[38]. However, the most established use of lithium therapeutics is as mood stabilizers in bipolar disorder. In this context, a major limitation of the use of lithium salts is their narrow therapeutic index, which necessitates frequent blood tests and close supervision by a physician. Despite this safety problem, lithium salts have been used in neuropsychiatric disorders and are the only drug products that have consistently reduced suicidality in patients[39, 40] The well-established efficacy of lithium as a mood stabilizer and the more recent interest in its potential for treating various neurodegenerative disorders [41] has driven recent attempts to generate new solid forms of lithium with improved safety and clinical performance through the use of crystal engineering approaches. Zaworotko and co-workers reported lithium ICCs in a synthetic and structural study of a family of inorganic anion lithium salts with amino acids (cation = Li^+; anion = Cl^-, Br^-, $NO3^-$; cocrystal former = amino acid zwitterion).[42] Braga et al.[43] subsequently reported new ICCs of inorganic anion lithium salts with racetam coformers. Moreover, these investigators suggested that such racetam ICCs might also be “co-drugs” since racetams are biologically active. Even more recently, we reported the first organic anion (B^- = salicylate, nicotinate) lithium ICCs with L-proline as a coformer. [44] Moreover, we reported that the blood and brain pharmacokinetics (PK) of one ICC, that formed from lithium salicylate and proline (LISPRO), are drastically different than those of the most commonly prescribed FDA-approved lithium salt, lithium carbonate, in rats. Importantly, we also demonstrated that this new speciation of lithium did not negatively affect the bioactivity of lithium in clinically relevant in vitro models. These studies laid the groundwork for the further development of a crystal engineering approach to improve lithium therapeutics as detailed herein.

Lithium chloride (LIC) is hygroscopic and rapidly deliquesces under low-RH conditions (11.30%) when exposed to air. This makes LIC unsuitable for development as a drug substance.[45] Even though LIC ICCs have been described in other studies; they focused primarily on the crystal engineering aspects of the solid forms, i.e., rational coformer selection, design, and crystallographic characterization.[46] To our knowledge the ability to modulate the deliquescent nature of LIC via cocrystallization has not yet been studied. Herein we describe a new ICC formed from lithium chloride and glucose

(LICGLU) and report on its physical stability and pharmacokinetics. Glucose was selected because it is a safe coformer that is already used as a diluent and filler in the formulation of drug products. We chose not to study the physical stability and bioavailability of LIBGLU because of the potential for bromide intoxication, chronic side effects, and the past history of bromism reported in patients.[47-49]

4.2 Experimental Section

4.2.1 Reagents and Materials. Lithium chloride (≥99% purity), lithium bromide (≥99% purity), and α-D-glucose (≥96% purity) were purchased from Sigma-Aldrich (St. Louis, MO, USA) and used as received.

4.2.2 ICC Syntheses.

The ICC of lithium bromide (LIB) with D-glucose was prepared by slow evaporation of water. Different experimental conditions (different temperatures, concentration, stoichiometry) were explored to isolate single crystals. Only in one attempt we could successfully isolated single crystals. Therefore alternative method such as solution mediated transformation was explored. As LIBGLU and D-glucose solubility's are very high in water, alcohols were chose as solvent system. The slurry of both the components in 1:1 stoichiometric ratio in isopropyl alcohol (IPA) resulted mixture of LIBGLU ICC and D-glucose. To prepare pure composition of ICC various stoichiometries were investigated and finally 2:1 stoichiometric ratio of LIB: GLU resulted pure phase of cocrystal. The time to convert input materials to pure ICC was measured by taking samples at regular intervals of time characterized by PXRD and TGA. As many attempts to prepare single crystals of LICGLU ICC were unsuccessful, the slurry approach was followed and PXRD indicated that isostructural with LIBGLU. The slurry method was successful to prepare 10.0 gms of LICGLU ICC for the bioavailability studies.

Lithium bromide (1.00 g, 11.5 mmol) and α-D glucose (1.80 g, 10.0 mmol) were dissolved in 5 mL of deionized water and slowly evaporated. Colorless needle like crystals were harvested after 6 months. Bulk samples of LIBGLU and LICGLU were prepared by slurrying lithium bromide or lithium chloride, respectively, and α-Dglucose in ethanol for 2 days.

4.2.3 Single-Crystal X-ray Diffraction. X-ray diffraction data were collected using a Bruker AXS SMART-APEXII [50] CCD diffractometer (Cu Kα radiation, λ = 1.54178 Å). Indexing was performed using APEX2 (difference vectors method). Data integration and reduction were performed using SaintPlus 6.01 [51]. An absorption correction was performed by a multi-scan method as implemented in SADABS [52]. The space group was determined using XPREP as implemented in APEX2. The structure was solved using SHELXS-97 (direct methods) and refined using SHELXL-97 (full-matrix least-squares on F2) contained in the OLEX2 [53] and WinGX v1.70.01 programs [54]. All non-hydrogen atoms were refined anisotropically. Hydrogen atoms of −CH and $-CH_2$ groups were placed in geometrically calculated positions and were included in the refinement process using a riding model with isotropic thermal parameters given by $U_{iso}(H) = 1.2[1.5]\ U_{eq}(-CH_2[-CH_3])$. For −OH groups, atoms H_{4A}, H_{9A}, H_{12}, H_{16}, H_6, H_{3A}, H_{18A}, H_{21A}, H_{24A}, H_{29}, H_{27A}, H_{34}, and H_{31} were placed in geometrically calculated positions and included in the refinement process using a riding model with isotropic thermal parameters given by $U_{iso}(H) = 1.5U_{eq}(-OH)$. The remaining H atoms of −OH groups were found from difference Fourier map inspection and were included in the refinement process using distance restraints (DFIX = 0.88 for $O_{14}–H_{14}$, $O_{13}–H_{13}$, $O_2–H_{2a}$, $O_1–H_{1a}$, $O_{26}–H_{26a}$, $O_{25}–H_{25a}$, $O_{20}–H_{20a}$, $O_{19}–H_{19a}$, $O_{35}–H_{35a}$, $O_{36}–H_{36a}$, $O_7–H_{7a}$,

O_8–H_{8a}, O_{22}–H_{22}, and O_{33}–H_{33}), and the isotropic thermal parameters for atoms H_{14} and H_{35A} were calculated as $U_{iso}(H) = 1.5U_{eq}(H_2O)$.

4.2.4 Differential Scanning Calorimetry. Differential scanning calorimetry (DSC) analysis was performed on a TA Instruments DSC Q20 differential scanning calorimeter. An aluminum pan was used for the sample, and the instrument was calibrated using an indium standard. For reference, an empty pan sealed in the same way as the sample was used. Under an inert atmosphere of nitrogen, the sample was heated in the DSC cell from 30 °C to the melting point of the ICC at a rate of 10 °C/min.

4.2.5 Fourier Transform Infrared Spectroscopy. The ICC was analyzed by Fourier transform infrared spectroscopy (FT-IR) with a Nicolet Avatar 320 FT-IR instrument. The sample size was 4−5 mg, and the spectrum was analyzed using EZ Omnic software over the range of 500−4000 cm^{-1}.

4.2.6 Thermogravimetric Analysis. Thermogravimetric analysis (TGA) was performed on a Q50 thermogravimetric analyser (TAInstruments-Waters LLC) in the range of 30−300 °C with a ramp rate of 10 °C/min.

4.2.7 Dynamic Vapor Sorption Analysis. The water sorption study on the ICC was conducted on an automated vapor sorption analyser (VTI SGA100; VTI Scientific/TA Instruments). The microbalance was calibrated using a 100 mg standard weight. The relative humidity sensor was calibrated at 5.0, 11.3, 32.8, 52.8, 75.3, and 84.3% RH (25 °C) using saturated salt solutions as well as at 80% RH (25 °C) using poly(vinylpyrrolidone). Approximately 8−10 mg of the powder sample was placed in the platinum sample pan and dried at ≤3% RH at 25 °C. The attainment of equilibrium was assumed when the weight change of the sample was less than 0.001 wt % in 5 min or by a maximum equilibration time of 120 min. The RH was then progressively increased to 70% in increments of 10%. The weight gain at the end of the sorption cycle (70% RH) was calculated on the basis of the dry weight.

4.2.8 Purity Confirmation. Powder X-ray diffraction (PXRD) and atomic absorption spectrometry (AAS) were used to confirm the purity of the ICC. The PXRD pattern (from the bulk sample) was compared to the calculated pattern from the single-crystal structure. Lithium quantification by AAS in equimolar solutions of LICGLU and lithium salicylate (LIS) was used to confirm the purity of bulk preparations of LICGLU.

4.2.9 Stability Studies. Qualitative stability studies were conducted for both LIC and LICGLU at 25 °C and 50% RH by collecting optical digital images of the materials at regular time intervals.

4.2.10 Pharmacokinetics Studies. PK studies were conducted as reported previously [55]. Male Sprague-Dawley rats weighing 200−250 g were purchased from Harlan. The animals were housed at the Moffitt Cancer Centre vivarium (Tampa, FL) with a 12 h light/dark cycle. The rats were allowed to acclimate for a period of 1 week before any experiments were carried out. All experiments were conducted in accordance with USF IACUC-approved protocols. The rats were allowed free access to food and water throughout the experiment. They were dosed via oral gavage with 4 m equiv/kg elemental lithium as LICGLU or LIC dissolved in deionized water. Animals in each treatment group were euthanized at 2, 24, 48, and 72 h (n = 3 per time point), and blood was collected by cardiac puncture and carefully perfused with a pressure-controlled pump to maintain microvasculature integrity before removal of brain tissue. Blood was centrifuged at 1600 g at room temperature for 10 min, and the plasma was separated. A 500 µL aliquot was diluted 10-fold in a 5% TCA and 10% IPA solution, vortexed, and allowed to sit for 10 min in order to precipitate proteins. These aliquots were centrifuged at 3000g for 30 min, and the supernatant was transferred to clean tubes prior to measurement of the lithium content using AAS (Shimadzu AA-6200). Brains were rinsed with PBS and weighed, and then an equal volume of concentrated HNO_3 was added. The brains were heated in this nitric acid solution for 1 h, allowed to cool to room temperature, and then centrifuged at 3000g for 1 h. The supernatant was removed and diluted 10-fold in 10% IPA prior to measurement of the lithium content using AAS. Peak height measurements were carried out by reference to values obtained for standards with known concentrations. Lithium measurements were plotted using GraphPad PRISM software (GraphPad Software, Inc.) as mean ± SEM (see Figure 8). Two-tailed t tests were used to assess the statistical significance at each time point for the PK curves. The criterion for rejection of the null hypothesis was $P < 0.05$. Phoenix WinNonlin v6.3 (Pharsight Corporation, Mountain View, CA) was used to conduct a non-compartmental analysis of the PK data. The reported parameters include C_{MAX}, T_{MAX}, area under the curve (AUC), and relative bioavailability (F_{REL}).

4.3 Results and Discussion

Crystal Structure of LIBGLU. LIBGLU is a 1:2 ICC of lithium bromide and α-D-glucose that crystallizes in space group $P3_1$. The asymmetric unit contains three lithium cations, three chloride anions and six glucose molecules. Each independent lithium cation is coordinated by at least three glucose molecules through OH moieties with Li−O bond distances of 2.097(7), 2.233(8), 2.187(7), 2.082(8), and 2.126(7) Å for Li_1; 2.147(8), 2.103(7), 2.209(8), 2.477(8), 2.249(8), and 2.098(7) Å for Li_2; and 2.085(8), 2.163(8), 2.261(8), 2.032(7), and 2.052(7) Å for Li_3. The three independent lithium cations exhibit coordination numbers of 5, 6, and 5, respectively. Each lithium cation crosslinks glucose molecules to form polymeric chains, and the helical chain observed along the crystallographic c axis is revealed by Figure 4.1. Crystallographic data are presented in Table 4.1.

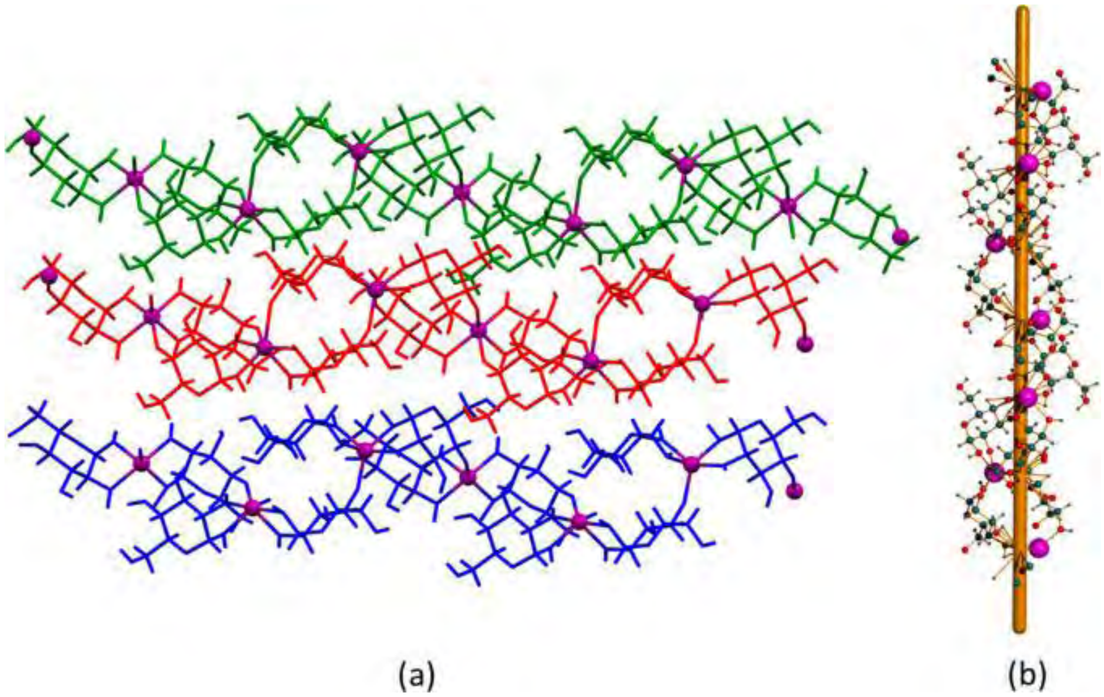

Figure 4.1. (a) Crystal packing in LIBGLU. Bromide anions have been removed for clarity. (b) Helical chain observed in LIBGLU along the crystallographic c axis.

Table 4.1. Crystallographic Data and Structure Refinement Parameters for LIBGLU

Formula	C_{36} H_{72} Br_3 Li_3 O_{36}
MW	1341.49
Crystal system	Trigonal
Space group	*P31*
a (Å)	16.2665(2)
b (Å)	16.2665(2)
c (Å)	17.0945(5)
α (deg)	90
β (deg)	90
γ (deg)	120
V /Å^3	3917.19(13)

D_c/mg m^{-3}	1.706
Z	9
2θ range	3.14 to 66.41 deg
Nref./Npara.	19322 / 7379
T /K	293(2)
R_1 [I>2sigma(I)]	0.0341
wR_2	0.0782
GOF	1.044
Abs coef.	Semi-empirical from equivalents

These chains are in turn cross-linked by O−H···O and O−H···Br hydrogen bonds [with O···Br distances ranging from 3.250(4) to 3.357(3) Å], resulting in a three-dimensional hydrogen-bonding network. Bromide anions Br_1 and Br_3 are engaged in tetrahedral charge-assisted hydrogen bonding with hydroxyl groups of α-D-glucose, whereas Br_2 is involved in three hydrogen bonds with hydroxyl groups. The Br anion environments are illustrated Figure 4.2.

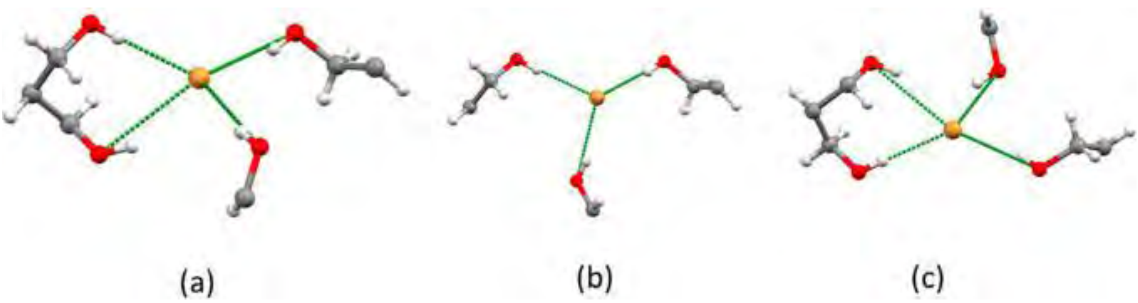

Figure 4.2. Coordination sphere of bromide anions (a) Br1 (2) Br2, and (c) Br3. For clarity, only hydrogen-bonded hydroxyl groups of glucose molecules are shown.

The Li−O bond distances observed in LIBGLU are longer than those observed in Li−O carboxylates [1.899(2)−2.122(2) Å with a mean of 1.971(3) Å] in which the lithium cation is four-coordinate. A Cambridge Structural Database (CSD) survey was conducted to find related structures of glucose, and it revealed that LIBGLU is isostructural with the ICC formed from sodium chloride and α-D-glucose (refcode XOZVOY) [56]. The calculated PXRD patterns of LIBGLU, XOZVOY, and two closely related hydrates (VEGLOI, 0.78 hydrate[57] and VEGLOI01, monohydrate[19]) are presented in Figure 4.3. LIBGLU and XOZVOY are isostructural, whereas the hydrate forms exhibit differences with respect to the higher angle PXRD peaks. The cell parameters of these compounds are given in Table 4.2.

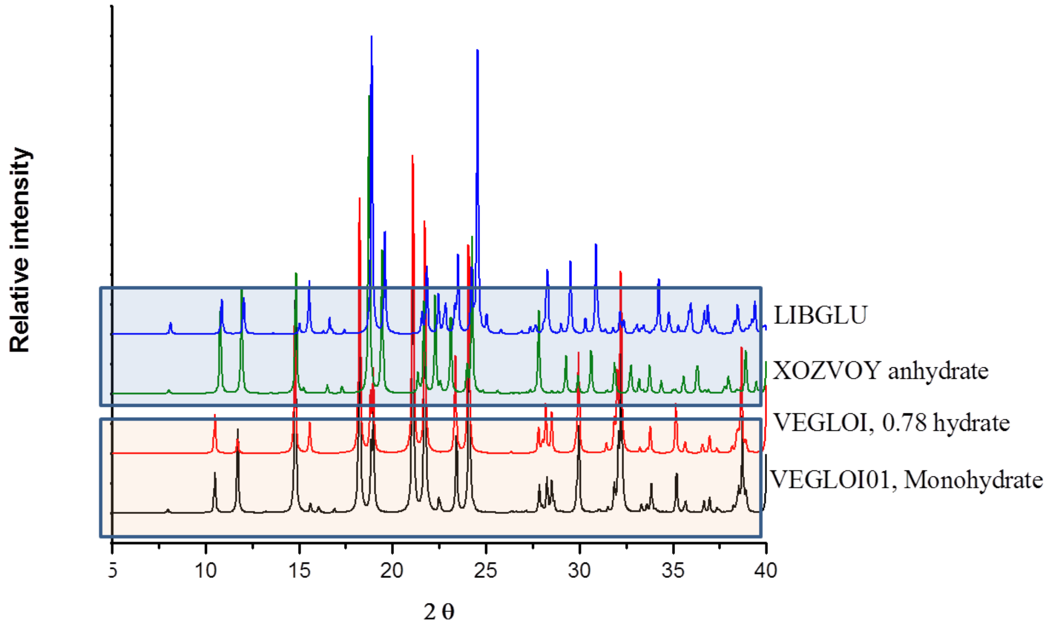

Figure 4.3. Comparison of calculated PXRD patterns: Sodium chloride ICCs are presented in black (monohydrate), red (0.79 hydrate) and green (anhydrate); LIBGLU is presented in blue (anhydrate).

Table 4.2. Unit cell parameters of sodium chloride-glucose and LIBGLU ionic cocrystals

REFCODE	Compounds and stoichiometry	Unit cell parameters	Space group
XOZVOY	Sodium chloride: α-D-glucose	a =16.4 Å b= 16.4 Å c= 17.4	*P*3$_1$

	(1:2)	Å α= 90° β=90° c=120°	
VEGLOI	Sodium chloride: α-D-glucose:water (1:2:0.78)	a =9.7 Å b= 9.7 Å c= 17.0 Å α= 90° β=90° c=120°	*$P3_1 2 1$*
VEGLOI01	Sodium chloride: α-D-glucose:water (1:2:1)	a =16.8 Å b= 16.8 Å c= 17.0 Å α= 90° β=90° c=120°	*$P3_1$*
LIBGLU	Lithium bromide: α-D-glucose (1:2)	a =16.3 Å b= 16.3 Å c= 17.1 Å α= 90° β=90° c=120°	*$P3_1$*

Isostructurality in inorganic compounds was addressed by Faria et al.[58] and in organic molecules by Kitaigorodskii.[59] ICCs containing sugars have shown isostructurality as exemplified by sodium cation−glucose ICCs in which the anions are Cl^{-}, Br^{-} and I^{-}. Another set of ICCs are the dihydrates of sucrose with sodium chloride (ZZZPSY) and sodium bromide (DINYOO10) [60]. However, except for XOZVOY and DINYOO10, crystal structure coordinates are not archived in the CSD. A recent study by Wood et al. [61] reported that isostructurality between sodium and potassium salts is common even though the unit cell parameters tend to be slightly different. Isostructurality was also observed in ICCs of seletracetam and brivaracetam with lithium bromide [46]. In our case, the slight differences in cell parameters and PXRD patterns in the anhydrous forms (LIBGLU and XOZVOY) might be attributed to the relative sizes of the different counterions (Cl^{-} and Br^{-}) and the different coordination geometries of the lithium cations (5, 6, 5) and sodium cations (all exhibit distorted octahedral geometries). The crystal packing with respect to the stereochemistry of α-D-glucose is further explained below. The chemical structure of α-D-glucose and the labelling of the α and β hydrogens are shown in Scheme 4.1.

Scheme 4.1. Chemical structure of α-D-glucose

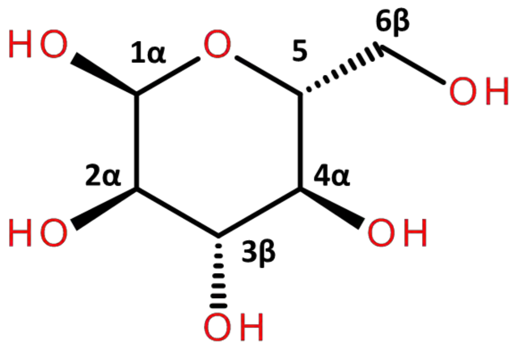

In XOZVOY, each sodium cation is coordinated by two syn-hydroxyl groups (1α, 2α) from each of two glucose molecules, and the distorted octahedral geometry is achieved by coordination of two more hydroxyl groups (4α). The 3β- and 6β-hydroxyl groups are involved in hydrogen boding with chloride anions. In LIBGLU, Li_2 exhibits the same coordination environment as the sodium cations of XOZVOY, whereas Li_1 and Li_3 are coordinated by two syn-hydroxyl groups (1α, 2α) from each of two glucose molecules and one hydroxyl group (4α) from another glucose molecule to achieve fivefold coordination. Three hydroxyl groups (3β, 4α, 6β) from the other glucose molecule are involved in hydrogen bonding with bromide anions. The monohydrate (VEGLOI01) and 0.78 hydrate (VEGLOI)[40] of sodium chloride with α-D-glucose have also been reported. The monohydrate crystallizes in space group $P3_1$, whereas the 0.78 hydrate crystallizes in space group $P3_12_1$. In VEGLOI, each sodium cation is octahedrally coordinated by four glucose molecules, with two syn-hydroxyl groups (1α, 2α) from each of two glucose molecules and a 4α hydroxyl group from each of the other two glucose molecules. The monohydrate VEGLOI01 contains three sodium cations, three chloride anions, three water molecules, and six glucose molecules in the asymmetric unit. The coordination environment of the sodium cations is similar to that in the anhydrate form XOZVOY. Chloride anions and water molecules both exhibit tetrahedral geometry with respect to hydrogen bonding. The chloride anions engage in charge-assisted hydrogen bonding with water and 3β, 4α, and 6β hydroxyl groups. Water molecules act as hydrogen-bond acceptors (4α and 6β hydroxyl groups) and donors (chloride, 3β hydroxyl groups). The two-donor, two-acceptor mode represents the second most common environment (37.36%) observed for water molecules in crystal structures archived in the CSD.[45] α-Hydroxyl groups from glucose are coordinated to metal cations in all of the structures, whereas β-hydroxyl groups are involved in hydrogen bonding either with chloride anions or water molecules in the case of the hydrate. In short, the coformer stereochemistry (α and β hydroxyl groups) seems to be a governing factor in this isostructural series of ICCs.

The experimental PXRD patterns of LICGLU and LIBGLU indicate that they are isostructural (Figure 4.4). The anhydrous nature of LICGLU was confirmed by TGA. DSC and TGA data are provided in the Supporting Information. Lithium quantification by AAS further supported the composition of LICGLU. AAS and FT-IR data are also presented in the Appendix.

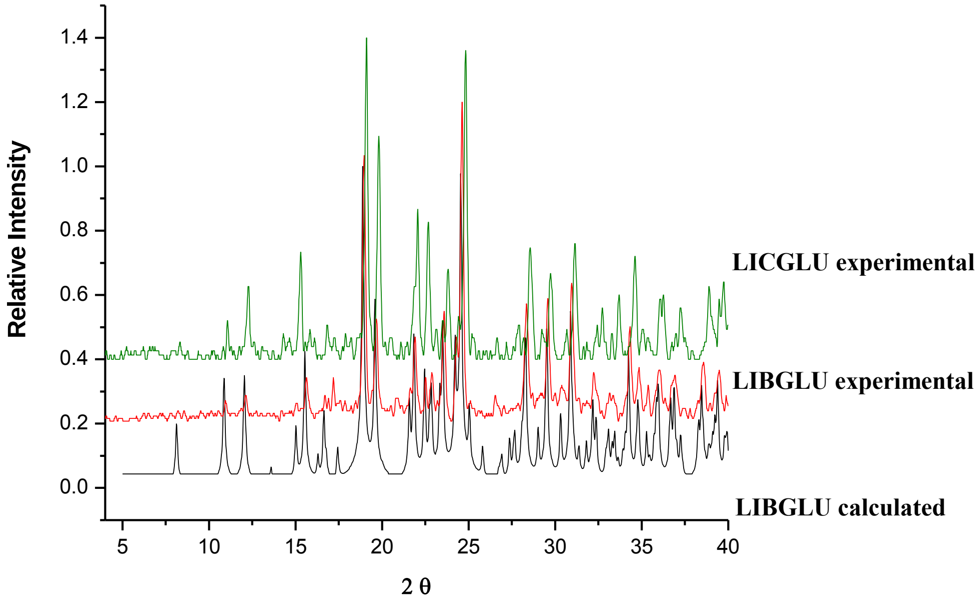

Figure 4.4. Experimental PXRD patterns of LICGLU and LIBGLU and calculated PXRD of LIBGLU.

4.3.1 Stability of LICGLU. a. *Microscopic Observation* at 25 °C and 50% RH. LIC has been reported to be extremely hygroscopic, with deliquescence occurring at 11.30% RH.[20] After the synthesis of LICGLU, we noticed that LICGLU did not deliquesce as rapidly, so we conducted a qualitative stability study by microscopic observation of powder samples at 25 °C and 50% RH. Time-lapsed digital images were obtained using a Zeiss Stereo Discovery V8 microscope with an Achromat S 1.0× FWD 63 mm objective and are given in Figure 4.5.Whereas LIC became liquid (deliquescent) after 18 min, LICGLU appeared unaffected over the same period of time.

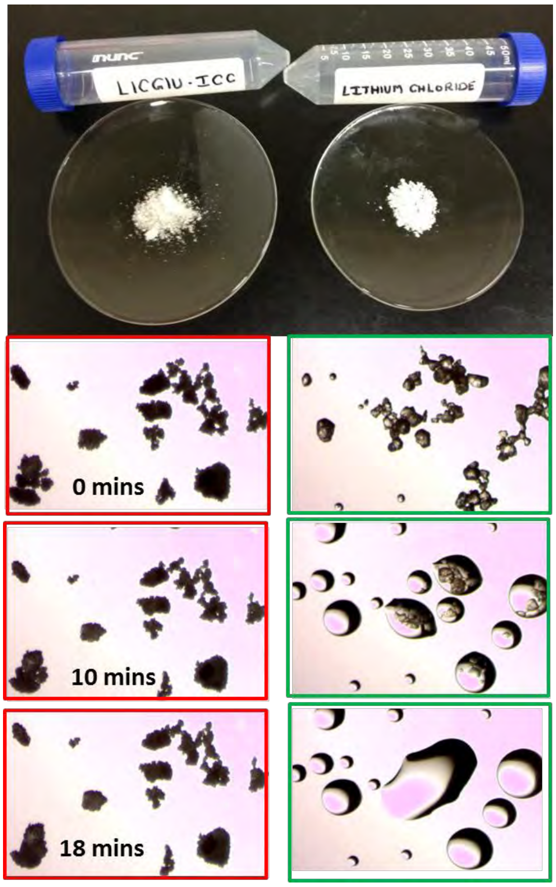

Figure 4.5. Qualitative observation of the physical stability of LICGLU versus LIC. Digital images of LIC and LICGLU were taken at 25°C and 50% RH after 0, 10, and 18 minutes.

4.3.2 Dynamic Vapor Sorption Analysis (DVS). The deliquescence point of LIC was taken from a literature report.[19] A powdered sample of LICGLU was exposed to controlled humidity. In contrast to LIC, LICGLU gained less than 1% weight at 11.3% RH. However, at 30% RH LICGLU exhibited a weight gain of 4.0%, whereas at 40% RH the gain was found to be 6.0%. Above 40% RH, LICGLU was observed to gain weight rapidly. These data suggest that whereas LICGLU is much more stable than LIC at low RH, it is not stable at higher RH. The DVS profile of LICGLU is presented in Figure 4.6.

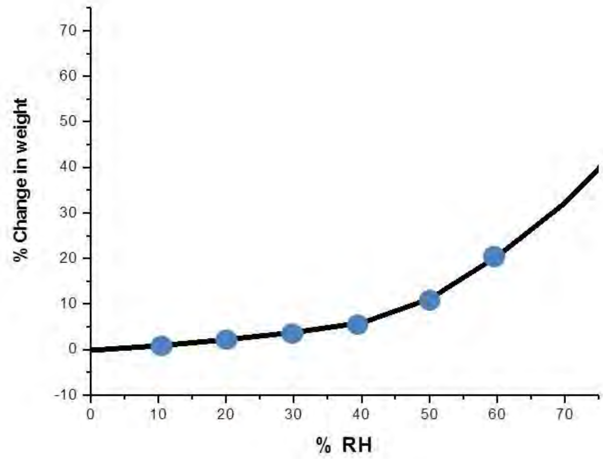

Figure 4.6. Moisture sorption profile of the LICGLU ionic cocrystal

4.3.3 Pharmacokinetic Studies. The recently issued FDA Guidance on the subject of pharmaceutical cocrystals requires that there be "assurance that complete dissociation of the API from its excipient occurs prior to reaching the site of action for pharmacological activity".[46] In this study, we did not observe any pharmacokinetic modulation of LICGLU compared to LIC, as indicated by the results shown in Figure 4.7 and the pharmacokinetic parameters presented in Table 4.3.

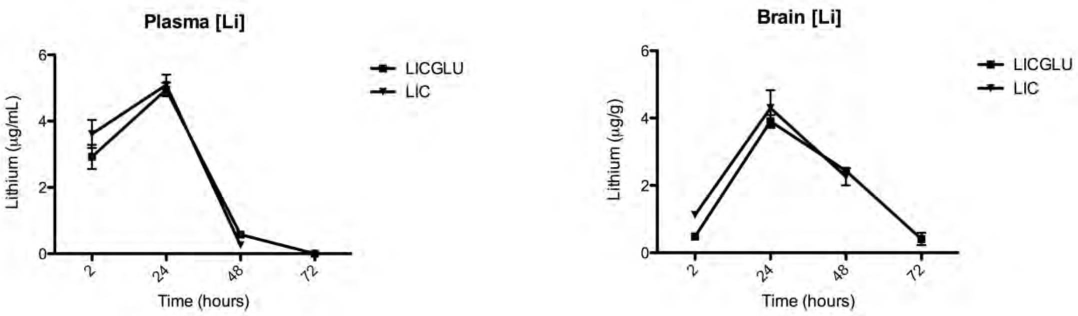

Figure 4.7. Plasma and brain pharmacokinetics of LICGLU versus LIC. Male rats (n=3 per formulation per time point) were dosed with 4 mEq/kg of lithium via oral gavage as LICGLU or LIC. Plasma and brain lithium levels were determined at 2, 24, 48, and 72 hours by atomic absorption spectrometry. Plasma lithium concentration is plotted versus time as mean±SEM.

Table 4.3. Pharmacokinetic Parameters For LICGLU versus LIC

	LICGLU		LIC	
	Blood	Brain	Blood	Brain
T_{MAX} (hour)	24	24	24	24
C_{MAX} (ug/mL or ug/g)	5.0	3.9	5.1	4.3
$AUC_{(0-48)}$ (hour.μg/mL or /g)	155.9	124.7	163.6	139.4
F_{REL}	.95	.89	1	1

These data suggest that LICGLU dissociates upon dissolution and that its existence as an ICC does not impact the PK parameters of lithium. Our in vivo PK protocol involved dissolving LICGLU and LIC in deionized water immediately prior to dosing the animals via oral gavage. If this were indeed the case, this would also mean that simultaneous dosing of glucose would not be expected to affect the LIC PK parameters. LIC and LICGLU were both found to exhibit PK parameters similar to those of lithium carbonate, as reported in our study of a different ICC, LISPRO, in rats. Lithium carbonate was observed to produce a larger C_{max} than LIC in our experiments, but this could be an artefact of different dosing prompted by the low solubility of lithium carbonate in water. Specifically, we used a 1% methylcellulose suspension for dosing via oral gavage. Different gavage vehicles are known produce PK changes for orally administered APIs.[62] The formulation can also drastically impact the oral PK of cocrystals, and a recent study revealed that dosing of unformulated cocrystals might result in a perceived failure to produce accurate PK modulation.[9c]

4.4 Conclusions

Cocrystals of lithium chloride and lithium bromide with α-D glucose (LICGLU and LIBGLU, respectively) were studied. LICGLU and LIBGLU were found to be isostructural with previously reported ICCs of NaCl and glucose even though the coordination environments of Li^+ in LIBGLU differ from those of Na^+. Notably, LICGLU was found to exhibit improved physical stability toward humidity compared with its parent salt, LIC. Specifically, whereas LIC is deliquescent at 11.3% RH, LICGLU is stable at 11.3% RH and exhibits only 4% weight gain at 30% RH. However, LICGLU absorbs significant amounts of water at higher RH values. The blood and brain pharmacokinetics of LICGLU compare closely to those of LIC, which indicates that LICGLU dissociates prior to reaching its site of action. This means that LICGLU could be treated as a drug product intermediate according to FDA guidelines. Future studies in our laboratories will focus upon systematically screening a broader library of coformers for lithium ICCs in order to identify a lead compound with suitable physicochemical properties and clinical performance. This study therefore confirms that ICCs can improve the physical stability of the solid form of a drug substance with respect to humidity without impacting its pharmacokinetic performance.

4.5 References

(1) Pikal, M.; Lukes, A.; Lang, J. E.; Gaines, K., Quantitative crystallinity determinations for β-lactam antibiotics by solution calorimetry: Correlations with stability. *J. Pharm. Sci.,* **1978**, *67*(6), 767-773.

(2) Yoshioka, M. H., B. C.; Zografi, G., Crystallization of indomethacin from the amorphous state below and above its glass transition temperature. *J. Pharm. Sci.,* **1994**, *83*(12).

(3) Callahan, J. C.; Cleary, G. W.; Elefant, M.; Kaplan, G.; Kensler, T.; Nash, R. A., Equilibrium moisture content of pharmaceutical excipients. *Drug Dev. Ind. Pharm.,* **1982**, *8*(3), 355-369.

(4) Newman, A. W.; Reutzel-Edens, S. M.; Zografi, G., Characterization of the "hygroscopic" properties of active pharmaceutical ingredients. *J. Pharm. Sci.,* **2008**, *97*(3), 1047-1059.

(5) Khankari, R. K.; Grant, D. J., Pharmaceutical hydrates. *Thermochimica Acta.,* **1995**, *248*, 61-79.

(6) Rohrs, B. R.; Thamann, T. J.; Gao, P.; Stelzer, D. J.; Bergren, M. S.; Chao, R. S., Tablet dissolution affected by a moisture mediated solid-state interaction between drug and disintegrant. *Pharm. Res.,* **1999**, *16*(12), 1850-1856.

(7) Listiohadi, Y.; Hourigan, J.; Sleigh, R.; Steele, R., Properties of lactose and its caking behaviour. *Aust. J. Dairy Technol.,* **2005**, *60*(1), 33.

(8) Hiatt, A. N.; Ferruzzi, M. G.; Taylor, L. S.; Mauer, L. J., Impact of deliquescence on the chemical stability of vitamins B1, B6, and C in powder blends. *J. Agric. Food Chem.,* **2008**, *56*(15), 6471-6479.

(9) Salameh, A. K.; Mauer, L. J.; Taylor, L. S., Deliquescence lowering in food ingredient mixtures. *J. Food Sci.,* **2006**, *71*(1), E10-E16.

(10) Kontny, M. J.; Zografi, G., Moisture sorption kinetics for water-soluble substances IV: Studies with mixtures of solids. *J. Pharm. Sci.,* **1985**, *74*(2), 124-127.

(11) Salameh, A. K.; Taylor, L. S., Deliquescence in binary mixtures. *Pharm. Res.,* **2005**, *22*(2), 318-324.

(12) Vishweshwar, P.; McMahon, J. A.; Bis, J. A.; Zaworotko, M. J., Pharmaceutical co-crystals. *J. Pharm. Sci.,* **2006**, *95*(3), 499-516.

(13) Shan, N.; Zaworotko, M. J., The role of cocrystals in pharmaceutical science. *Drug Discovery Today.,* **2008**, *13*(9–10), 440-446.

(14) Childs, S. L.; Chyall, L. J.; Dunlap, J. T.; Smolenskaya, V. N.; Stahly, B. C.; Stahly, G. P., Crystal engineering approach to forming cocrystals of amine hydrochlorides with organic acids. Molecular complexes of fluoxetine hydrochloride with benzoic, succinic and fumaric acids. *J. Am. Chem. Soc.,* **2004**, *126*(41), 13335-13342.

(15) Smith, A. J.; Kavuru, P.; Wojtas, L.; Zaworotko, M. J.; Shytle, R. D., Cocrystals of quercetin with improved solubility and oral bioavailability. *Mol. Pharm.,* **2011**, *8*(5), 1867-1876.

(16) McNamara, D.; Childs, S.; Giordano, J.; Iarriccio, A.; Cassidy, J.; Shet, M.; Mannion, R.; O'Donnell, E.; Park, A., Use of a glutaric acid cocrystal to improve oral bioavailability of a low solubility API. *Pharm. Res.,* **2006**, *23*(8), 1888-1897.

(17) Hickey, M. B.; Peterson, M. L.; Scoppettuolo, L. A.; Morrisette, S. L.; Vetter, A.; Guzmán, H.; Remenar, J. F.; Zhang, Z.; Tawa, M. D.; Haley, S.; Zaworotko, M. J.; Almarsson, Ö., Performance comparison of a co-crystal of carbamazepine with marketed product. *Eur. J. Pharm. Biopharm.,* **2007**, *67*(1), 112-119.

(18) Childs, S. L.; Kandi, P.; Lingireddy, S. R., Formulation of a danazol cocrystal with controlled supersaturation plays an essential role in improving bioavailability. *Mol. Pharm.,* **2013**, *10*(8), 3112-3127.

(19) Shan, N.; Perry, M. L.; Weyna, D. R.; Zaworotko, M. J., Impact of pharmaceutical cocrystals: the effects on drug pharmacokinetics. *Expert Opin. Drug Metab. Toxicol.,* **2014**, *10*(9), 1255-1271.

(20) Trask, A. V.; Motherwell, W. D. S.; Jones, W., Pharmaceutical cocrystallization: Engineering a remedy for caffeine hydration. *Cryst. Growth Des.,* **2005**, *5*(3), 1013-1021.

(21) Trask, A. V.; Motherwell, W. D. S.; Jones, W., Physical stability enhancement of theophylline via cocrystallization. *Int. J. Pharm.,* **2006**, *320*(1–2), 114-123.

(22) Grepioni, F.; Wouters, J.; Braga, D.; Nanna, S.; Fours, B.; Coquerel, G.; Longfils, G.; Rome, S.; Aerts, L.; Quéré, L., Ionic co-crystals of racetams: solid-state properties enhancement of neutral active pharmaceutical ingredients via addition of Mg^{2+} and Ca^{2+} chlorides. *CrystEngComm.,* **2014**, *16*(26), 5887-5896.

(23) Almarsson, Ö.; Zaworotko, M. J., Crystal engineering of the composition of pharmaceutical phases. Do pharmaceutical co-crystals represent a new path to improved medicines? *Chem. Commun.,* **2004**, (17), 1889-1896.

(24) Desiraju, G. R.; Parshall, G. W., Crystal engineering: the design of organic solids. *Materials science monographs,* **1989**, *54*.

(25) Moulton, B.; Zaworotko, M. J., From molecules to crystal engineering: supramolecular isomerism and polymorphism in network solids. *Chem. Rev.,* **2001**, *101*(6), 1629-1658.

(26) Trask, A. V., An Overview of pharmaceutical cocrystals as intellectual property†. *Mol. Pharm.,* **2007**, *4*(3), 301-309.

(27) Kobell, F. V., *J. Prakt. Chem.,* **1843**, *28*.

(28) Gill, C. H., XVI.−On some saline compounds of cane-sugar. *J. Chem. Soc.,* **1871**, *24*, 269-275.

(29) Beevers, C.; Cochran, W., X-ray examination of sucrose. *Nature.,* **1946**, *157*, 872.

(30) Wood, R.; James, V.; Mills, J., 2, 5, 0-methylene-D-mannitol sodium chloride C17O6O14 NaCl. *Cryst. Struct. Comm.,* **1976**, *5*, 207.

(31) Ferguson, G.; Kaitner, B.; Connett, B.; Rendle, D., Structure of the α-D-glucose–sodium chloride–water complex (2/1/1). *Acta Crystallogr. Sect. B-Struct. Sci.,* **1991**, *47*(4), 479-484.

(32) Braga, D.; Grepioni, F.; Maini, L.; Prosperi, S.; Gobetto, R.; Chierotti, M. R., From unexpected reactions to a new family of ionic co-crystals: the case of barbituric acid with alkali bromides and caesium iodide. *Chem. Commun.,* **2010**, *46*(41), 7715-7717.

(33) Garrod, A. B., *The nature and treatment of gout and rheumatic gout*. ed.; Walton and Maberly: **1859**.

(34) Cade, J. F., Lithium salts in the treatment of psychotic excitement. *Bulletin World health organization,* **2000**, *78*(4), 518-520.

(35) Schou, M., Lithium in the treatment of manic psychosis. *Folia Clin. Int.(Barc.),* **1955**, *5*(3), 99.

(36) Schou, M., Lithium in psychiatric therapy and prophylaxis. *J. Psychiatr. Res.,* **1968**, *6*(1), 67-95.

(37) Hartigan, G., The use of lithium salts in affective disorders. *Br. J. Psychiatry.,* **1963**, *109*(463), 810-814.

(38) Leeds, P. R.; Yu, F.; Wang, Z.; Chiu, C.-T.; Zhang, Y.; Leng, Y.; Linares, G. R.; Chuang, D.-M., A new avenue for lithium: intervention in traumatic brain injury. *ACS Chem. Neurosci.,* **2014**, *5*(6), 422-433.

(39) Goodwin, F. K.; Fireman, B.; Simon, G. E.; Hunkeler, E. M.; Lee, J.; Revicki, D., Suicide risk in bipolar disorder during treatment with lithium and divalproex. *JAMA.,* **2003**, *290*(11), 1467-1473.

(40) Thies-Flechtner, K.; Müller-Oerlinghausen, B.; Seibert, W.; Walther, A.; Greil, W., Effect of prophylactic treatment on suicide risk in patients with major

affective disorders. Data from a randomized prospective trial. *Pharmacopsychiatry.,* **1996**, *29*(3), 103-107.

(41) Forlenza, O. V.; De-Paula, V. d. J. R.; Diniz, B., Neuroprotective effects of lithium: implications for the treatment of alzheimer's disease and related neurodegenerative disorders. *ACS Chem. Neurosci.,* **2014**, *5*(6), 443-450.

(42) Ong, T. T.; Kavuru, P.; Nguyen, T.; Cantwell, R.; Wojtas, Ł.; Zaworotko, M. J., 2:1 Cocrystals of homochiral and achiral amino acid zwitterions with Li^{+} Salts: Water-stable zeolitic and diamondoid metal–organic materials. *J. Am. Chem. Soc.,* **2011**, *133*(24), 9224-9227.

(43) Braga, D.; Grepioni, F.; Maini, L.; Capucci, D.; Nanna, S.; Wouters, J.; Aerts, L.; Quéré, L., Combining piracetam and lithium salts: ionic co-crystals and co-drugs? *Chem. Commun.,* **2012**, *48*(66), 8219-8221.

(44) Smith, A. J.; Kim, S.-H.; Duggirala, N. K.; Jin, J.; Wojtas, L.; Ehrhart, J.; Giunta, B.; Tan, J.; Zaworotko, M. J.; Shytle, R. D., Improving lithium therapeutics by crystal engineering of novel ionic cocrystals. *Mol. Pharm.,* **2013**, *10*(12), 4728-4738.

(45) Gibbard Jr, H. F.; Scatchard, G., Liquid-vapor equilibrium of aqueous lithium chloride, from 25 to 100. deg. and from 1.0 to 18.5 molal, and related properties. *J. Chem. Eng. Data.,* **1973**, *18*(3), 293-298.

(46) Wouters, J.; Grepioni, F.; Braga, D.; Kaminski, R. M.; Rome, S.; Aerts, L.; Quéré, L., Novel pharmaceutical compositions through co-crystallization of racetams and Li^{+} salts. *CrystEngComm.,* **2013**, *15*(44), 8898-8902.

(47) TrenitÄ, D. K. N.; Edelbroek, P., Antiepileptic drug treatment in the nineties in the Netherlands. *Pharm. World Sci.,* **1997**, *19*(2), 60-69.

(48) Frances, C.; Hoizey, G.; Lamiable, D.; Millart, H.; Trenque, T., Bromism from daily over intake of bromide salt: Case report. *J. Toxicol. Clin. Toxicol.,* **2003**, *41*(2), 181-183.

(49) Lugassy, D. M.; Nelson, L. S., Case files of the medical toxicology fellowship at the New York city poison control: bromism: forgotten, but not gone. *J. Med. Toxicol.,* **2009**, *5*(3), 151-157.

(50) Bruker, A. V., 0 Data collection and processing software. *Bruker AXS Inc., Madison, Wisconsin, USA,* **2008**.

(51) SAINT, P., Data reduction software, version 7.34 a. *Bruker AXS Inc., Madison, WI,* **2005**.

(52) Sheldrick, G. i., SADABS, program for empirical absorption correction of area detector data. *University of Göttingen, Germany,* **1996**.

(53) Dolomanov, O. V.; Bourhis, L. J.; Gildea, R. J.; Howard, J. A.; Puschmann, H., OLEX2: a complete structure solution, refinement and analysis program. *J. Appl. Crystallogr.,* **2009**, *42*(2), 339-341.

(54) Farrugia, L., WinGX suite for small-molecule single-crystal crystallography. *J. Appl. Crystallogr.,* **1999**, *32*(4), 837-838.

(55) Smith, A. J.; Kim, S.-H.; Tan, J.; Sneed, K. B.; Sanberg, P. R.; Borlongan, C. V.; Shytle, R. D., Plasma and brain pharmacokinetics of previously unexplored lithium salts. *RSC advances.,* **2014**, *4*(24), 12362-12365.

(56) Wong, K. C.; Hamid, A.; Baharuddin, S.; Quah, C. K.; Fun, H.-K., catena-Poly[[sodium-di-[µ]-[ß]-d-glucose] chloride]. *Acta Crystallogr. Sect. E:,* **2009**, *65*(11), m1308-m1309.

(57) Cho, Y.; Honzatko, R. B., Coordination complex of Na^+ and-D-glucose. *Acta Crystallogr., Sect. C: Cryst. Struct. Commun.,* **1990**, *46*(4), 587-590.

(58) Lima-de-Faria, J.; Hellner, E.; Liebau, F.; Makovicky, E.; Parthé, E., Nomenclature of inorganic structure types. Report of the International Union of Crystallography commission on crystallographic nomenclature subcommittee on the nomenclature of inorganic structure types. *Acta Crystallogr., Sect. A: Found. Crystallogr.,* **1990**, *46*(1), 1-11.

(59) Kitaigorodskii, A., Organic Chemical Crystallography; Consultants Bureau: New York, 1961, **1955**, 222-231.

(60) Accorsi, C. A.; Bellucci, F.; Bertolasi, V.; Ferretti, V.; Gilli, G., Re-determination of the crystal structure of NaBr· Sucrose· $2H_2O$. *Carbohydr. Res.,* **1989**, *191*(1), 105-116.

(61) Wood, P. A.; Oliveira, M. A.; Zink, A.; Hickey, M. B., Isostructurality in pharmaceutical salts: How often and how similar? *CrystEngComm.,* **2012**, *14*(7), 2413-2421.

(62) Smith, A. J.; Kavuru, P.; Arora, K. K.; Kesani, S.; Tan, J.; Zaworotko, M. J.; Shytle, R. D., Crystal engineering of green tea epigallocatechin-3-gallate (EGCg) cocrystals and pharmacokinetic modulation in rats. *Mol. Pharm.,* **2013**, *10*(8), 2948-2961.

Chapter 5: Conclusion and Future Directions

5.1 Conclusions

The development of new solid form of an active pharmaceutical ingredient (API) is an important aspect to the modern pharmaceutical science for the improvement of physicochemical properties in relevance to clinical performance.[1] Solid-form screening in drug development has traditionally limited to crystalline forms such as polymorphs, hydrates, solvates and salts. Nonetheless these crystalline forms offer limited opportunities in terms of design, diversity and properties. In this context, cocrystals offer advantages in terms of design that means by manipulating inter molecular interactions (i.e. crystal engineering) it is possible to modulate the properties.[2, 3]

Cocrystals have been known from long time but understudied in context to drug molecules. However, four publications during 2003-2006 triggered rapid evaluation of cocrystals both in academia and industry.[4-7] By visualising the cocrystal drug product development in eight stages (i.e. coformer selection/design; discovery; characterization; properties; pharmacokinetics; formulations; process/scale-up and regulatory approval), there are substantial advances at each stage during the last decade. The advantages offered by cocrystals with respect to physicochemical properties and clinical performance, cocrystals became an integral part of the pre-formulation stage in drug development.[8]

As detailed, cocrystals can be classified into two broad categories: molecular cocrystals (MCCs) that contain only neutral components (coformers); ionic cocrystals (ICCs), which are comprised of at least one ionic coformer that is a salt. Screening for novel ICCs have the following advantages 1) library of ionic coformers: large number of salts available as potential ionic coformers from GRAS and EAFUS. 2) diverse; two components can be varied without changing the chemical structure of the drug molecule 3) design; ICCs are sustained by strong interactions such as charge assisted hydrogen bond interactions[9] and coordination bonds[10] which are amenable to design. Thus, screening for ICCs offer a new pre-formulation approach that could improve the physicochemical properties of drug molecules including salts.

Crystal engineering strategies have been delineated during the past decade for the design of multi-component molecular crystals (molecular cocrystals, MCCs). However, the same depth of understanding has not yet been established for cocrystals that are comprised of at least one ionic compound (ionic cocrystals, ICCs). We addressed this long known but understudied class of cocrystals through the use of organic cation chloride salts as cocrystal formers with carboxylic acids and phenols. We evaluated the propensity to form chloride···carboxylic acid versus chloride···phenol hydrogen bonds (supramolecular heterosynthons) through a combination of Cambridge Structural Database (CSD) data mining and the structural characterization of 12 novel ICCs, including 4 hydrates containing carboxylic acids, phenol groups, and chloride anions. Analysis revealed that the charge-assisted hydrogen bonds between phenol moieties and chloride anions persist even in the presence of carboxylic acid moieties, which form carboxylic acid dimers in 11/21 crystal structures. These observations are also supported by lattice energy calculations and hydrogen bond strengths derived from density functional theory calculations. That phenol groups are better suited than carboxylic acid moieties to form ICCs with chloride salts has important implications for the design of drug substances with improved properties since chloride salts are so prevalent as drug substances.

Current lithium drugs are plagued with a narrow therapeutic window and tend to be hygroscopic. However, they remain the gold standard for treating manic episodes in bipolar disorder. We reported a crystal engineering study aimed at the preparation and characterization of ionic cocrystals (ICCs) of lithium chloride (LIC) and lithium bromide (LIB) with glucose (GLU). The structure of LIBGLU was studied by single-crystal X-ray diffraction and found to be isostructural with related sodium chloride−glucose ICCs. The physical stability of LICGLU was compared to that of LIC at 50% RH and 25°C and through dynamic vapor sorption analysis. The blood and brain pharmacokinetics of LICGLU were compared to those of LIC in rat models and revealed little change in performance. This study reveals that ICCs can modestly improve the solid-form stability of lithium salts without impacting in vivo performance, a step toward enabling the development of the next generation of lithium therapeutics.

5.2 Future Directions

Our systematic studies and preliminary studies of lithium ICCs indicated the change in organic anion and coformer has been modulating the physical stability as well as bioavailability of lithium salts. We became further interested to investigate the possibility of number of ICCs for the lithium salts that could lead to better performance of drug products compared to that of existing marketed lithium salts. The important stages to develop lithium drug product would be

1) Synthesis and characterization of 40-50 novel ICCs: As there are number of anions and coformers available, by systematically varying the two components it is possible obtain number of crystalline forms.
2) Stability testing: Some of the lithium salts are tend to be hygroscopic, stability studies would be conducted to the prepared ICCs at different relative humidity and temperature conditions.
3) Bioavailability studies for 20 ICCs: The stable compositions (ICCs) will be further subjected to bioavailability studies.

4) Scale-up: As our current method to prepare most of the ICCs is involved evaporation of water or cooling crystallization. This approach has some limitations to prepare lithium ICCs in bulk. Therefore alternative methods should be explored. One of the approaches could be slurry mediated transformation in alcohols. For each ICC, ternary phase diagrams would be constructed to understand stable solid phase region of ICC.
5) In depth pharmacokinetic studies: So far we have studied the lithium concentrations both in plasma and brain of rat models. As lithium is known to distribute to other organs our future studies would be more focussed to measure lithium concentrations in all other organs such as liver, kidney and spinal card.

The design of ICCs, i.e. the charge assisted interactions such as sulfate-sulfonic acid, nitrate-carboxylic acid and sulfate-carboxylic acid are not well studied. The understanding of above supramolecular heterosynthons will allow designing ICCs with modulated properties of drug molecules. For example COOH···$^{-}$OOC heterosynthon has been explored and systematic studies have been reported. ICCs of this type involving compounds and drug molecules are shown in the Figure 5.1. A quick CSD analysis of this synthon in presence of all the other functional groups revealed that COOH···$^{-}$OOC (2.40–2.85 Å, mean of 2.54 (1) Å) is robust and is observed in ca. 85 % of the time (restrictions, 3D coordinates determined, Not disorder, no errors and only organics). Höpfl research group investigated the hydrogen bond interaction of energies COOH···$^{-}$OOC by ab initio methods and revealed that the synthon is significantly stronger (≈ − 31 Kcal/mol) than that of carboxylic acid dimers (≈ −19 Kcal/mol).[11] Subsequently examined the formation of different motifs for COOH···$^{-}$OOC hetero synthon by using ICCs as model compounds.[9] Recently Lou et al. explored COOH···$^{-}$OOC synthon for salicylate salt with chemically distinct carboxylic acids and successfully cocrystallized ICCs.[12] Therefore the $COOH\cdots{}^{-}OOC$ supramolecular hetero synthon is a subject of crystal engineering due to its ability to form strong hydrogen bonds and can be robust enough for the design of novel ICCs.

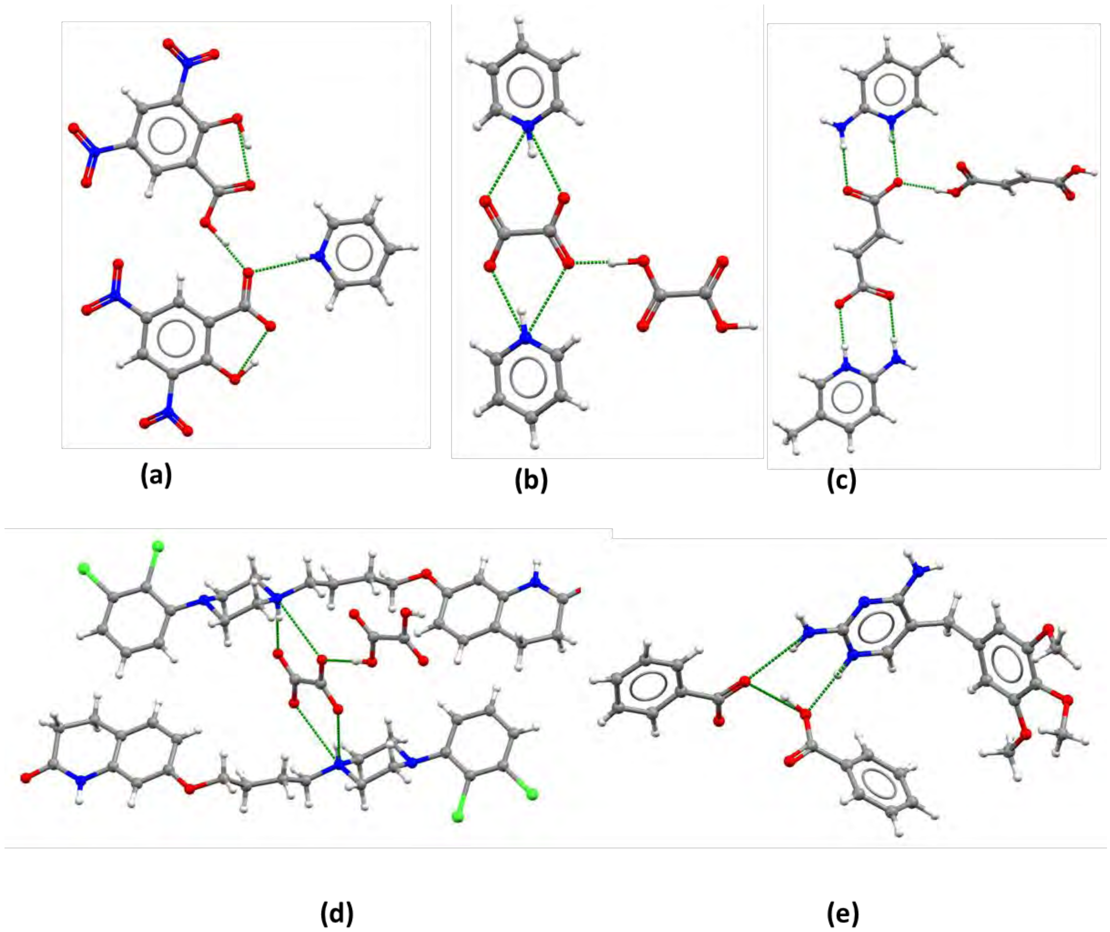

Figure 5.1. ICCs involving organic cation carboxylates and carboxylic acids; (a) pyridinium 3,5-dinitrosalicylate 3,5-dinitrosalicylic acid (b) bis(pyridinium) oxalate oxalic acid (c) bis(2-Amino-5-methylpyridinium) fumarate fumaric acid (d) bis (aripiprazole) oxalate oxalic acid (e) Trimethoprim monobenzoate benzoic acid.

I close my thesis, that there should be more systematic studies should be conducted to understand the robustness and hierarchy of supramolecular synthons via ionic coformers as model compounds. With increased concerns of physicochemical properties of drug molecules, new pre-formulation approaches are constantly needed. That is with recent emerging subclass of ionic cocrystals, now it is possible to create number of crystalline forms for a drug molecule to achieve the desired property to develop into final medicinal products.

5.3 References

(1) Huang, L.-F.; Tong, W.-Q., Impact of solid state properties on developability assessment of drug candidates. *Adv. Drug Deliv. Rev.,* **2004**, *56*(3), 321-334.

(2) Shan, N.; Zaworotko, M. J., The role of cocrystals in pharmaceutical science. *Drug Discovery Today,* **2008**, *13*(9–10), 440-446.

(3) Vishweshwar, P.; McMahon, J. A.; Bis, J. A.; Zaworotko, M. J., Pharmaceutical co-crystals. *J. Pharm. Sci.,* **2006**, *95*(3), 499-516.

(4) Walsh, R. D. B.; Bradner, M. W.; Fleischman, S.; Morales, L. A.; Moulton, B.; Rodriguez-Hornedo, N.; Zaworotko, M. J., Crystal engineering of the composition of pharmaceutical phases. *Chem. Commun.,* **2003**, (2), 186-187.

(5) Fleischman, S. G.; Kuduva, S. S.; McMahon, J. A.; Moulton, B.; Bailey Walsh, R. D.; Rodríguez-Hornedo, N.; Zaworotko, M. J., Crystal Engineering of the composition of pharmaceutical Phases: Multiple-component crystalline solids involving carbamazepine. *Cryst. Growth Des.,* **2003**, *3*(6), 909-919.

(6) Remenar, J. F.; Morissette, S. L.; Peterson, M. L.; Moulton, B.; MacPhee, J. M.; Guzmán, H. R.; Almarsson, Ö., Crystal Engineering of novel cocrystals of a triazole drug with 1,4-dicarboxylic acids. *J. Am. Chem. Soc.,* **2003**, *125*(28), 8456-8457.

(7) Childs, S. L.; Chyall, L. J.; Dunlap, J. T.; Smolenskaya, V. N.; Stahly, B. C.; Stahly, G. P., Crystal engineering approach to forming cocrystals of amine hydrochlorides with organic acids. Molecular complexes of fluoxetine hydrochloride with benzoic, succinic and fumaric Acids. *J. Am. Chem. Soc.,* **2004**, *126*(41), 13335-13342.

(8) Shan, N.; Perry, M. L.; Weyna, D. R.; Zaworotko, M. J., Impact of pharmaceutical cocrystals: the effects on drug pharmacokinetics. *Expert Opin. Drug Metab. Toxicol.,* **2014**, *10*(9), 1255-1271.

(9) Rodríguez-Cuamatzi, P.; Arillo-Flores, O.; Bernal-Uruchurtu, M.; Höpfl, H., Experimental and theoretical analysis of the hydrogen-bonding motifs formed between the carboxyl and the carboxylate group: towards a systematic classification of their supramolecular motifs. *Supramol. Chem.,* **2007**, *19*(8), 559-578.

(10) Ong, T. T.; Kavuru, P.; Nguyen, T.; Cantwell, R.; Wojtas, Ł.; Zaworotko, M. J., 2:1 Cocrystals of homochiral and achiral amino acid zwitterions with Li^+ salts: Water-stable zeolitic and diamondoid metal–organic materials. *J. Am. Chem. Soc.,* **2011**, *133*(24), 9224-9227.

(11) Rodríguez-Cuamatzi, P.; Arillo-Flores, O. I.; Bernal-Uruchurtu, M. I.; Höpfl, H., Theoretical and experimental evaluation of homo- and heterodimeric hydrogen-bonded motifs containing boronic acids, carboxylic acids, and carboxylate anions: Application for the generation of highly stable hydrogen-bonded supramolecular systems. *Cryst. Growth Des.,* **2005**, *5*(1), 167-175.

(12) Lou, B.; Perumalla, S. R.; Sun, C. C., Significant expansion of the solid state landscape of salicylic acid based on charge-assisted hydrogen bonding interactions. *Cryst. Growth Des.,* **2015**, *15*(1), 24-28.

Appendix-1

1.1 Characterization of pyridine hydrochloride. 4-hydroxybenzoic acid, PHC4HBA

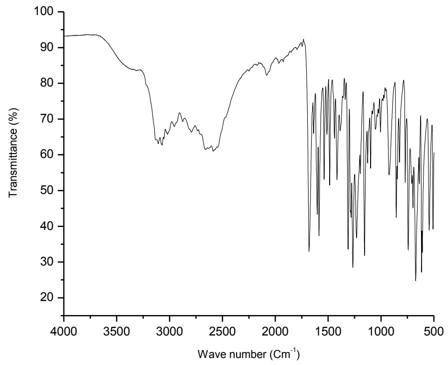

IR

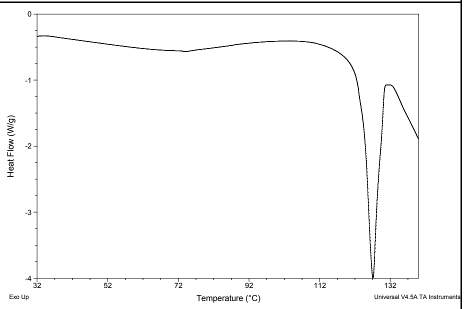

DSC

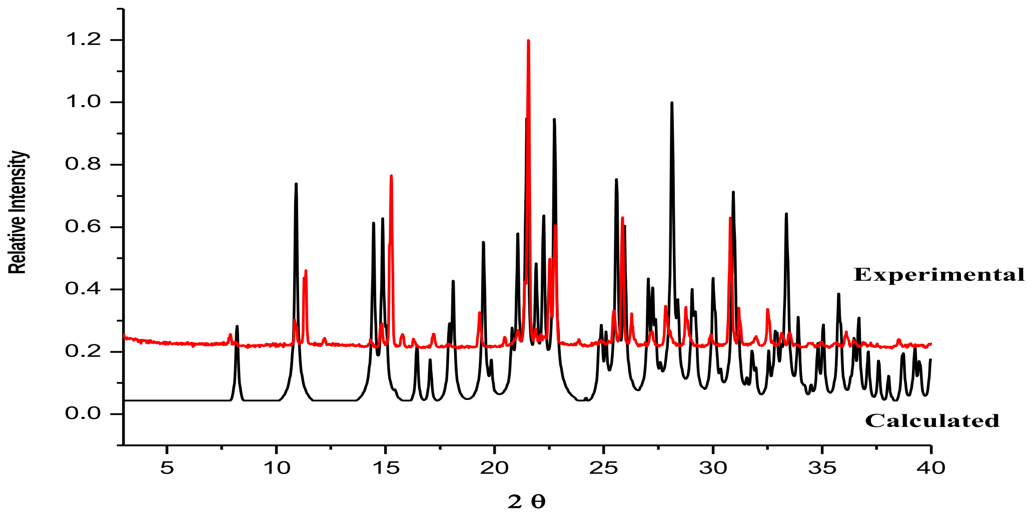

XRD comparison

1.2 Characterization of pyridine hydrochloride. 6-hydroxynapthoic acid, PHC6HNA

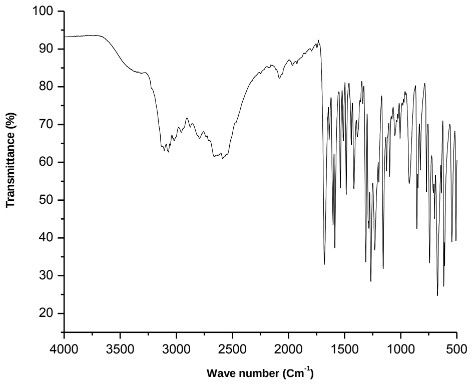

IR

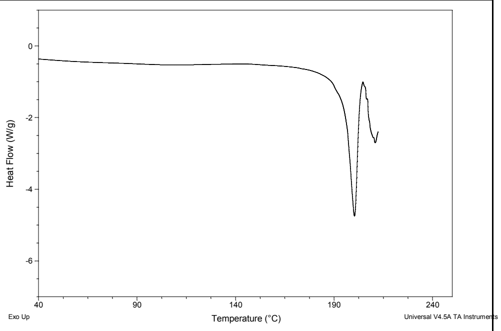

DSC

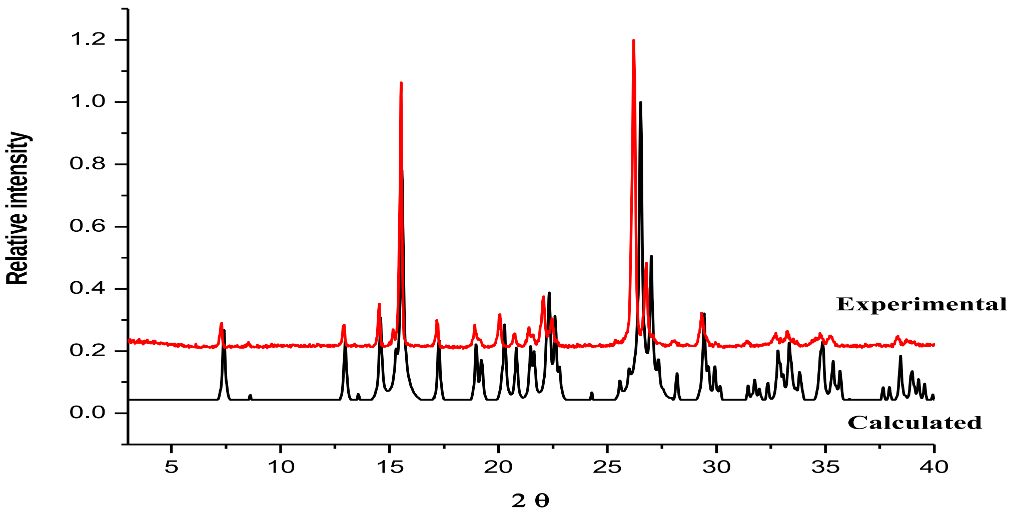

XRD comparison

1.3 Characterization of pyridine hydrochloride. 2, 4-dihydroxybenzoic acid, PHCDBA

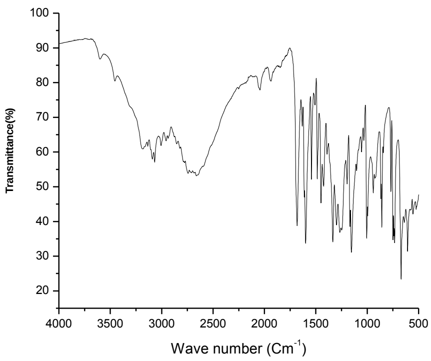

IR

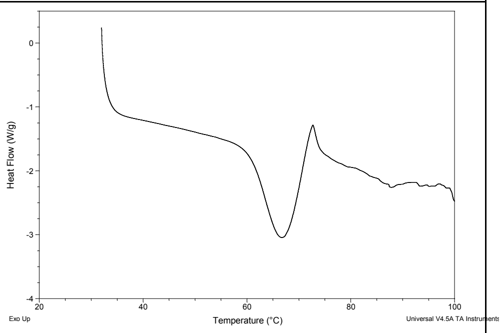

DSC

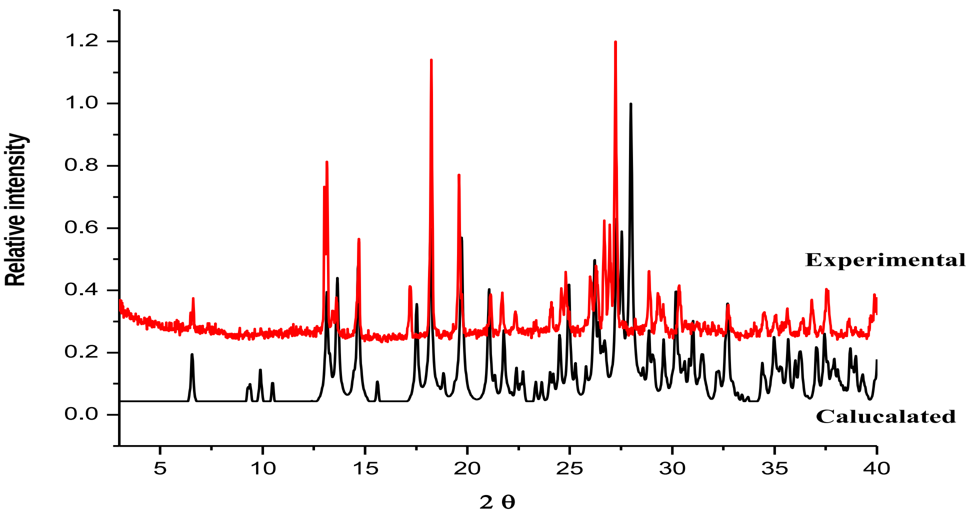

XRD comparison

1.4 Characterization of pyridine hydrochloride. gallic acid, PHCGAL	
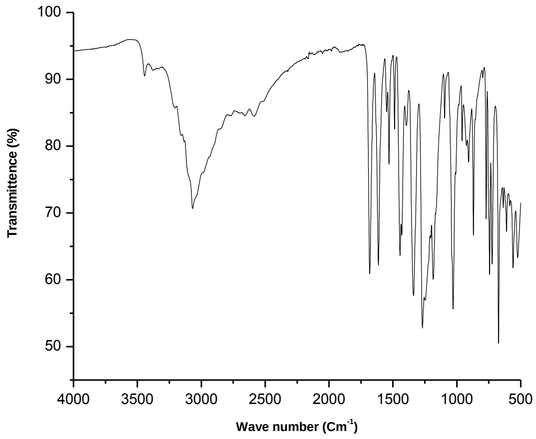	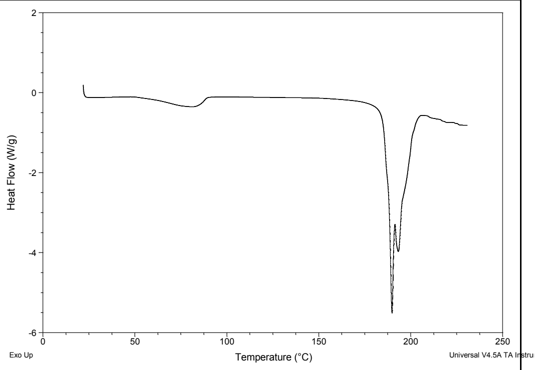
IR	**DSC**
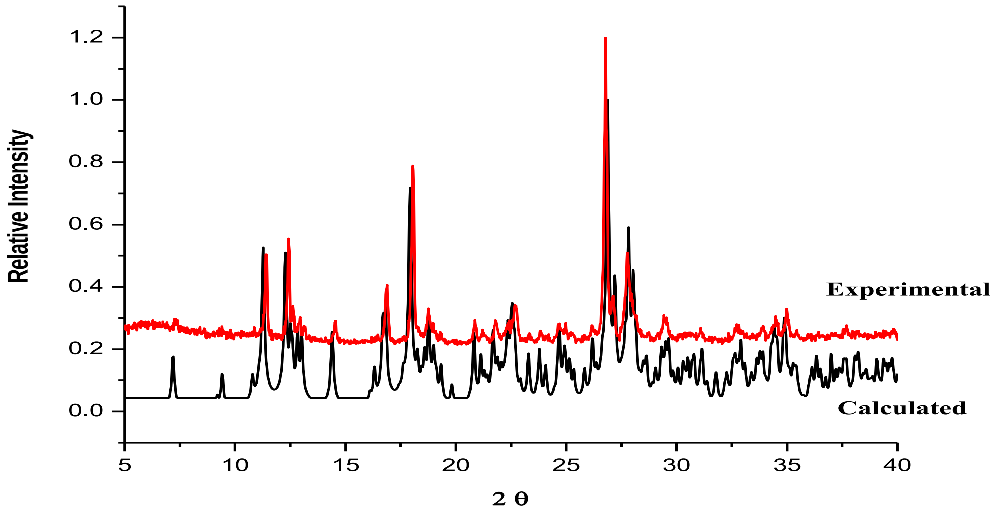	
XRD comparison	

1.5 Characterization of tetraethylammonium chloride. 3-hydroxybenzoic acid, TEA3HBA

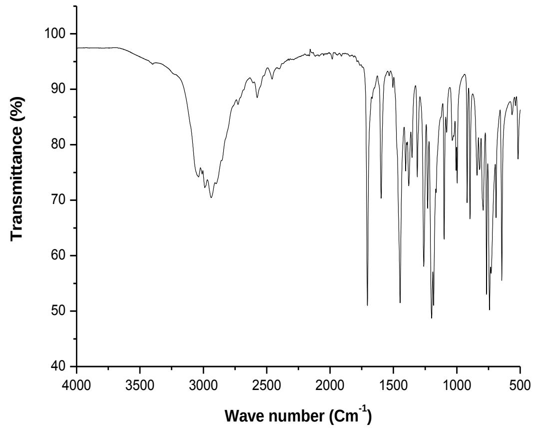

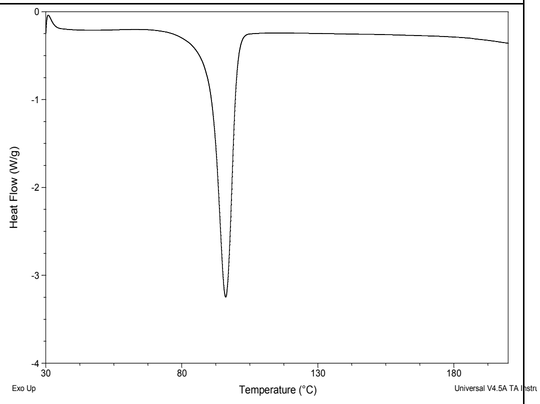

IR	DSC

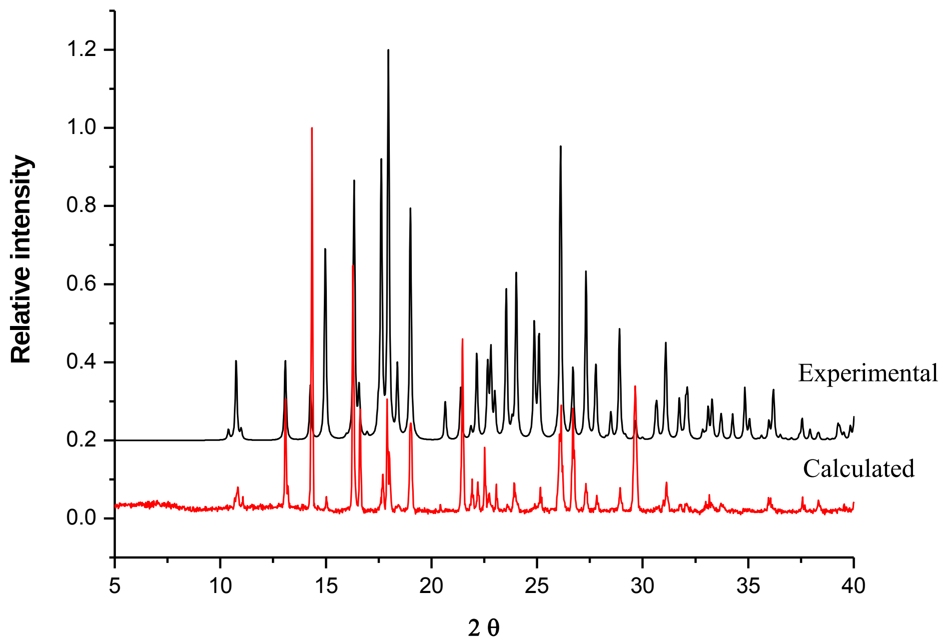

XRD Comparison

1.6 Characterization of tetraethylammonium chloride. coumaric acid, TEACOU

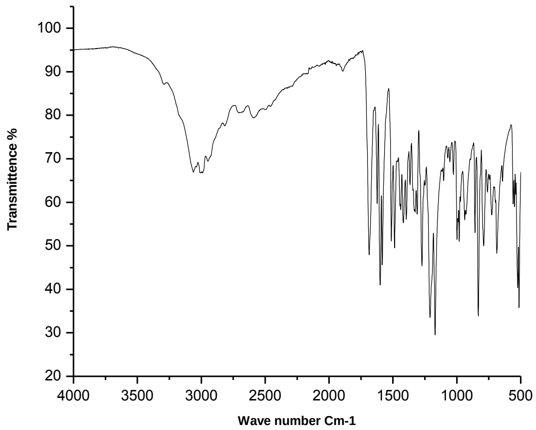

IR

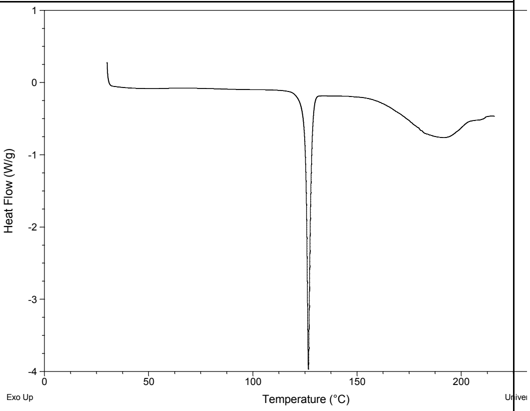

DSC

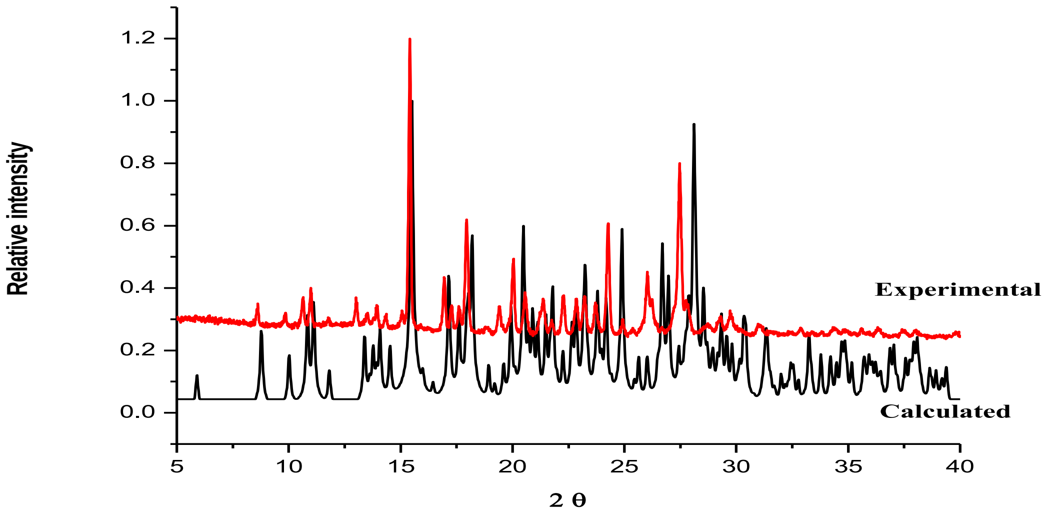

XRD comparison

1.7 Characterization of tetraethylammonium chloride. hydroxyisophthalic acid, TEAHPA

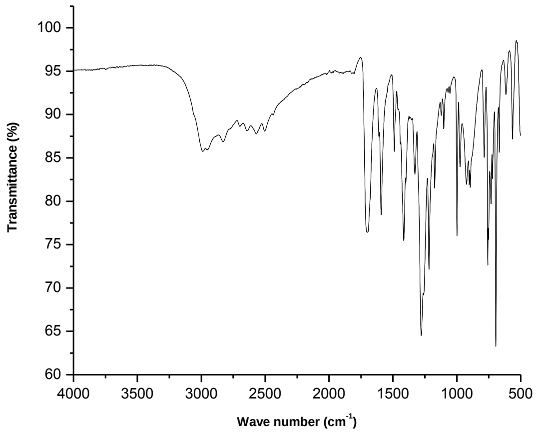

IR

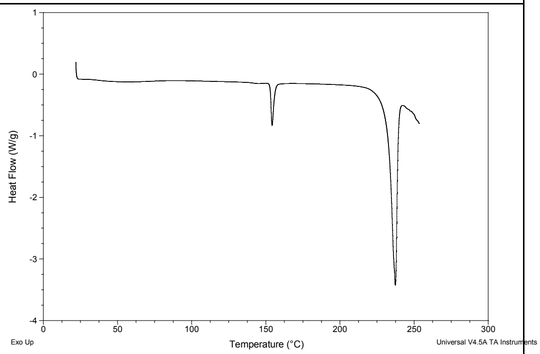

DSC

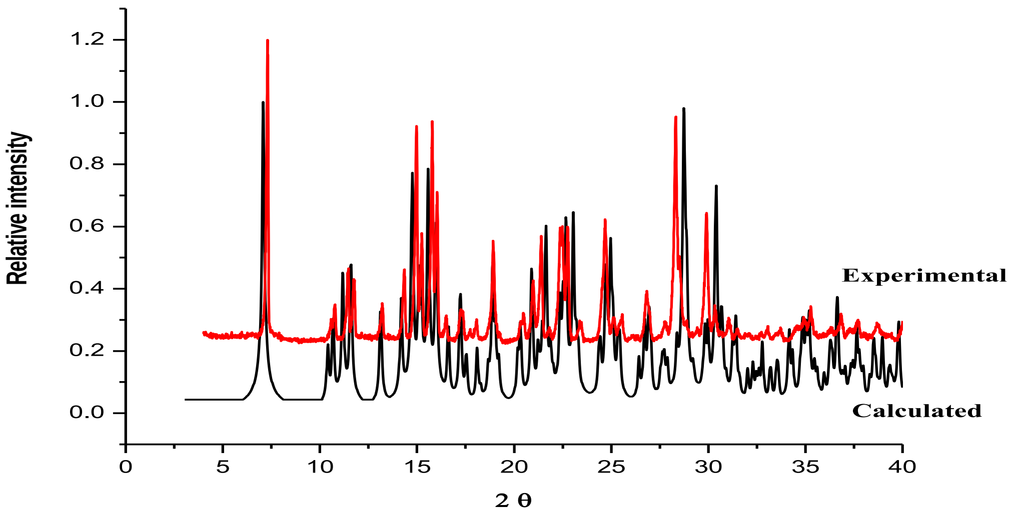

XRD comparison

1.8 Characterization of tetraethylammonium chloride. protocatechuic acid, TEAPCA

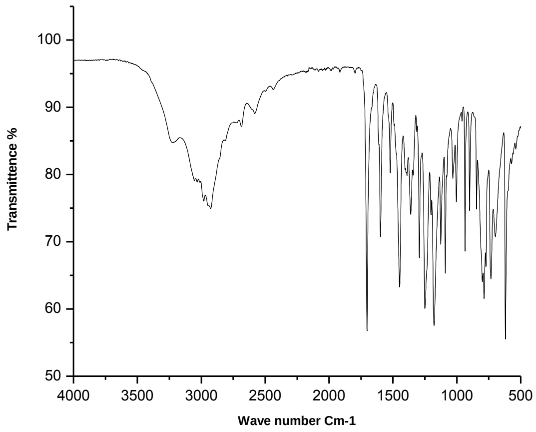

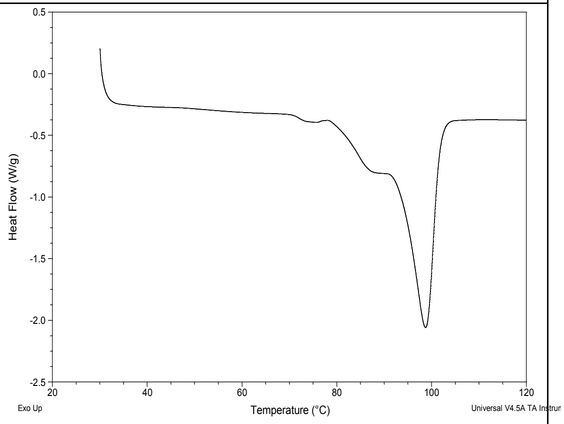

IR	DSC

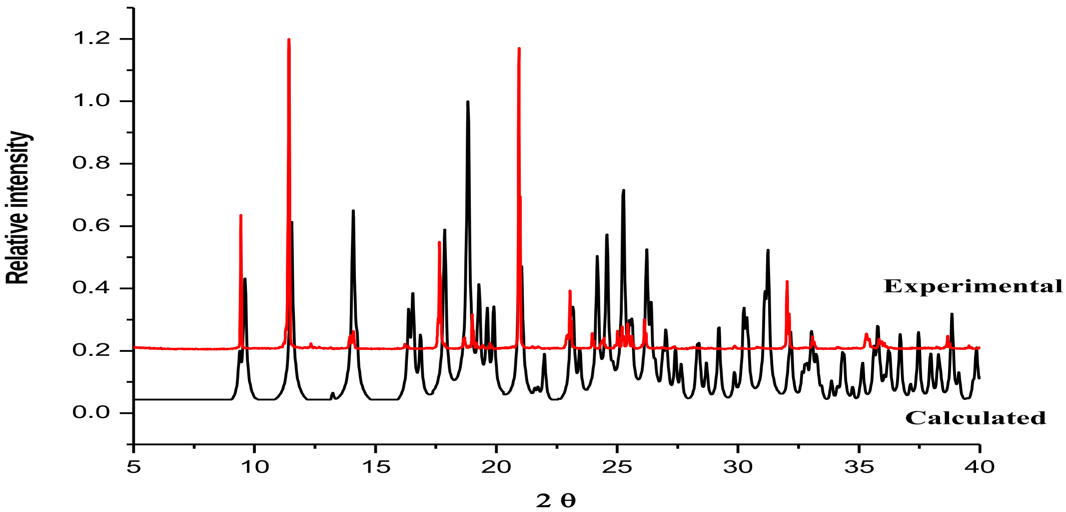

XRD comparison

1.9 Characterization of tetramethylammonium chloride. 4-hydroxybenzoic acid, TMA4HBA

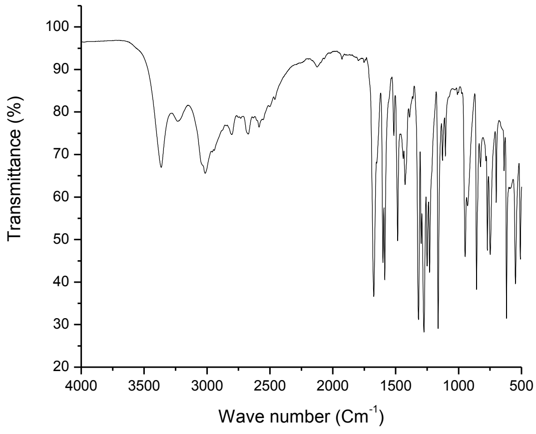

IR

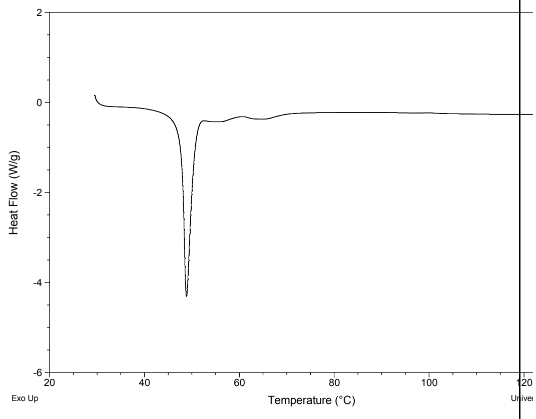

DSC

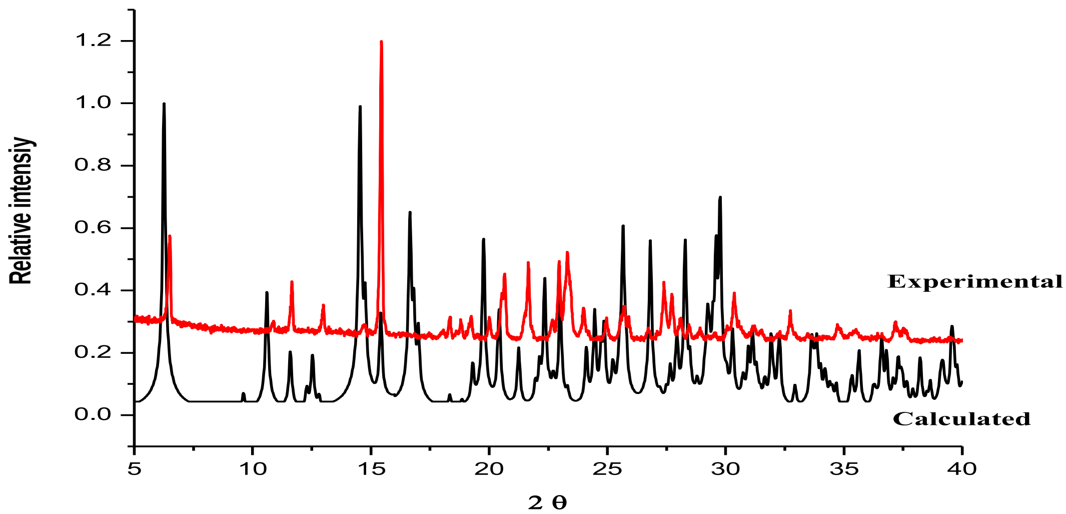

XRD comparison

1.10 Characterization of tetramethylammonium chloride. dihydroxybenzoicacid, TMADBA	
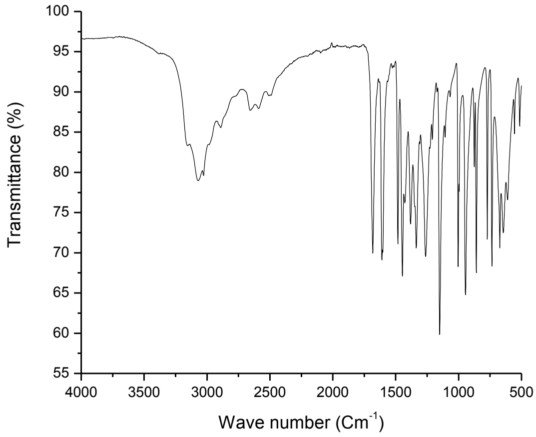	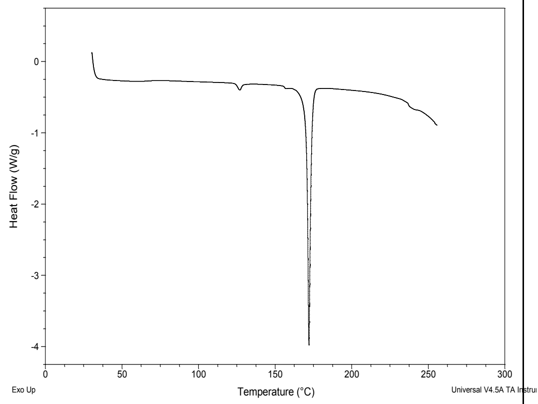
IR	**DSC**
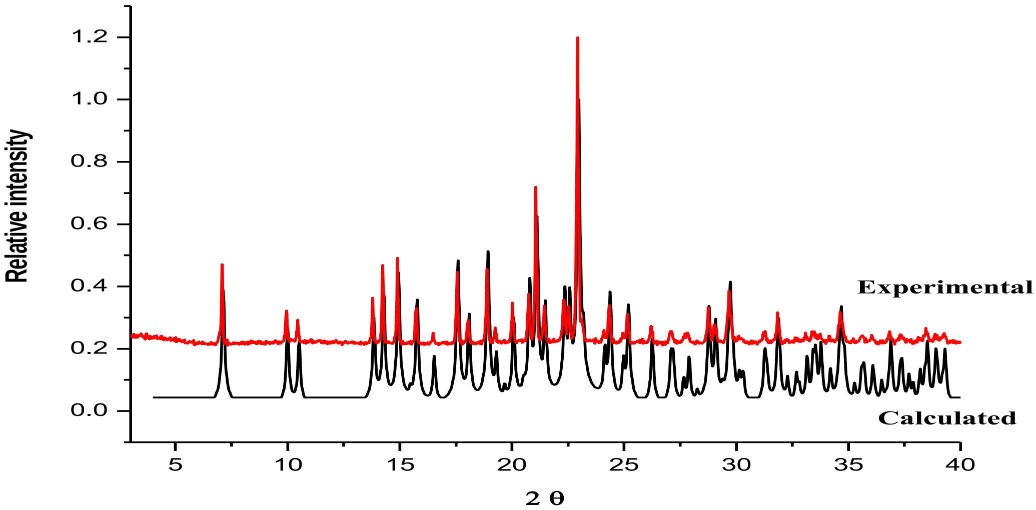	
XRD comparison	

1.11 Characterization of tetramethylammonium chloride. gallic acid, TMAGAL

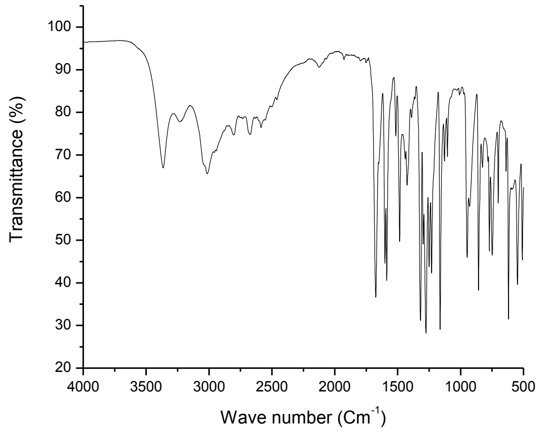

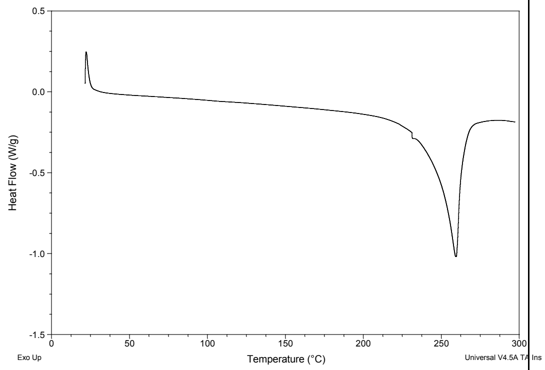

IR	DSC

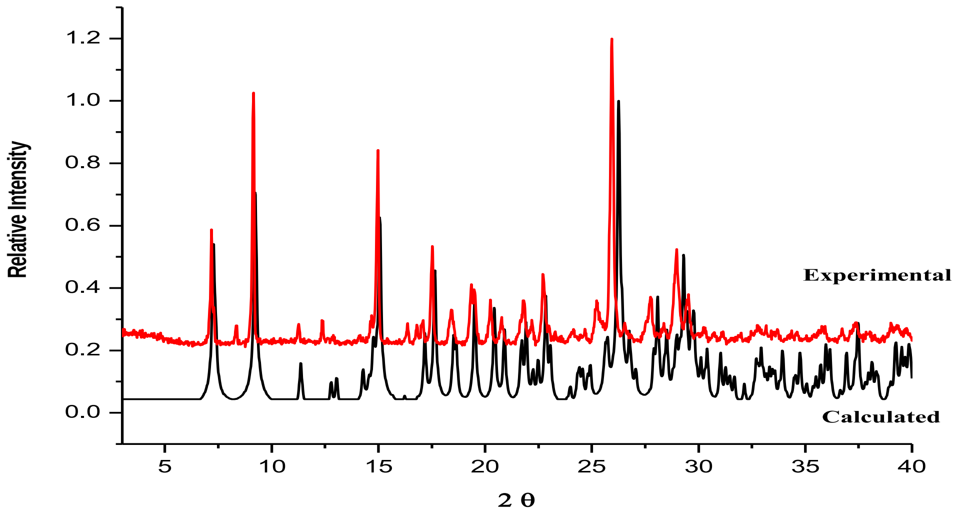

XRD comparison

1.12 Characterization of tetraethylammonium chloride. protocatechuic acid, TMAPCA

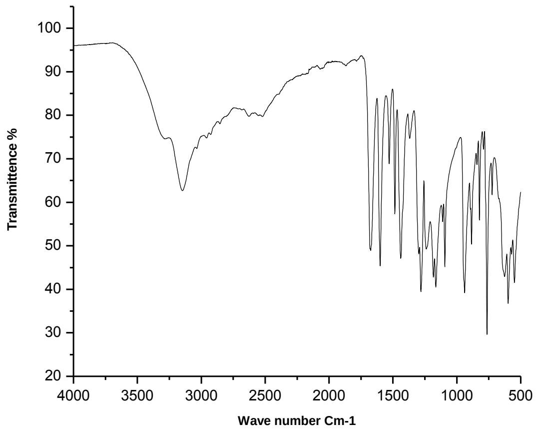

IR

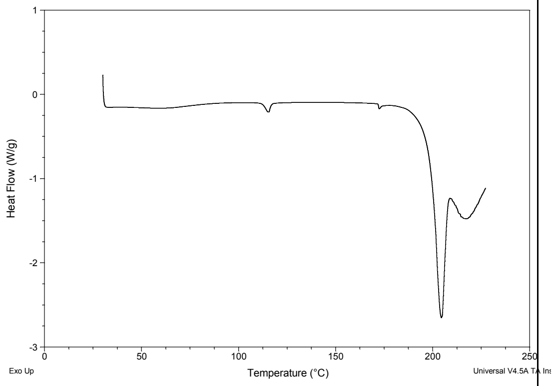

DSC

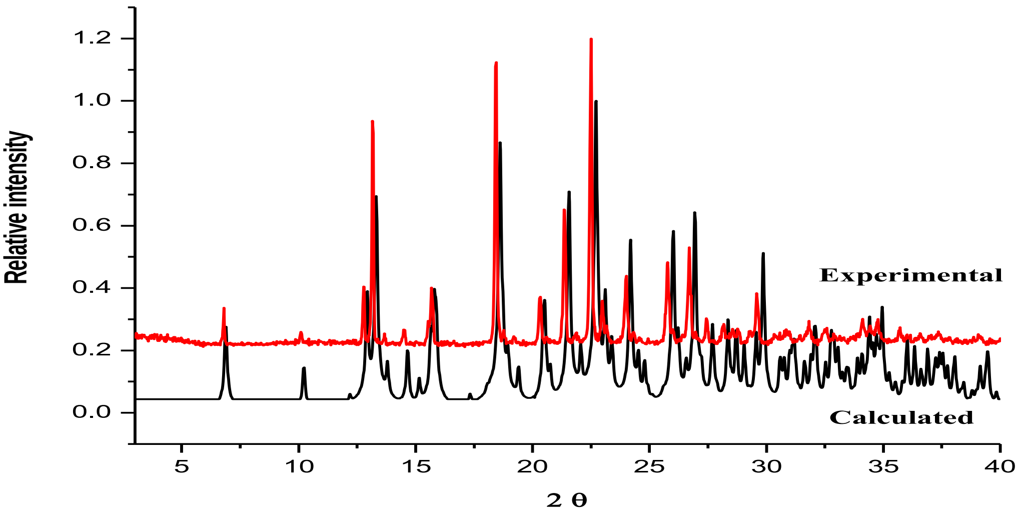

XRD comparison

Table 1. Selected Hydrogen Bond Parameters

	H-Bond	*d* (H••• A) /Å	*D* (D···A)/Å	*θ* /º
PHC4HBA	O-H···O	1.67	2.6384 (15)	174.9
	O-H···O	1.73	2.6384 (15)	173.2
	O-H···Cl⁻	2.25	3.0797(13)	174.0
	N-H···Cl⁻	2.23	3.0814(14)	164.0
PHC6HNA	O-H···O	1.76	2.6015 (15)	161.8
	O-H···O	1.59	2.6015(15)	174.9
	O-H···Cl⁻	2.33	3.0723(16)	170.0
	N-H···Cl⁻	2.16	3.037(2)	180.0
PHCDBA	O-H···O	1.53	2.5895(19)	170.8
	O-H···O	1.69	2.632(2)	166.0
	O-H···O	1.71	2.5895(19)	164.0
	O-H···O	1.82	2.632(2)	167.0
	C-H···O	2.20	3.064(3)	150.1
	O-H···O	2.20	3.021(2)	151.0
	O-H···O	2.19	3.0194(15)	166.0
	N-H···Cl⁻	2.15	3.0609(18)	172.0
	O-H···Cl⁻	2.25	3.0712(16)	167.0
	O-H···O	1.92	2.758(2)	168.0
	O-H···Cl⁻	2.20	3.0922(19)	177.0
PHCGAL	O-H···O	1.71	2.5932(19)	174.9
	O-H···O	1.64	2.6237(19)	169.2
	O-H···O	1.80	2.5932(19)	160.7
	O-H···O	1.56	2.6070(19)	165.6
	O-H···O	1.80	2.6070(19)	169.0

	O-H···Cl⁻	2.28	3.0449(15)	174.0
	O-H···Cl⁻	2.29	3.126(2)	166.0
	O-H···Cl⁻	2.27	3.110(2)	172.0
	O-H···Cl⁻	2.21	3.0319(14)	173.0
	O-H···O	1.71	2.6237(19)	173.0
	O-H···Cl⁻	2.24	3.0088(18)	166.0
	O-H···Cl⁻	2.25	3.0088(14)	153.0
	O-H···Cl⁻	2.24	3.0024(17)	161.0
	O-H···O	2.13	2.8172(18)	144.0
	O-H···O	1.82	2.653(2)	179.0
	O-H···O	2.05	2.820(2)	144.0
	N-H···O	2.09	2.863(2)	134.0
	N-H···O	1.92	2.757(2)	147.0
	O-H···Cl⁻	2.15	2.9532(15)	168.0
TEA3HBA	O-H···Cl⁻	2.08	2.9852(11)	174.0
	O-H···Cl⁻	2.15	3.0447(13)	179.0
	C-H···O	2.53	3.3593(18)	145.8
	C-H···O	2.48	3.3864(18)	158.7
	C-H···O	2.55	3.3568(19)	138.8
TEACOU	C-H···O	2.31	3.2736(18)	164.9
	O-H···O	1.73	2.6584(15)	174.0
	O-H···O	1.65	2.6155(15)	173.0
	O-H···Cl⁻	2.14	3.0395(13)	170.0
	O-H···Cl⁻	2.25	3.1209(13)	175.0
TEAHPA	O-H···Cl⁻	2.08	3.0177(14)	168.8
	O-H···O	1.82	2.6414(18)	171.0
	O-H···O	1.73	2.6073(17)	176.0
	O-H···Cl⁻	2.15	3.0263(15)	162.0
	O-H···O	1.71	2.6328(18)	176.0

	O-H···O	1.66	2.6020(18)	174.0
TEAPCA	C-H···O	2.60	3.296(2)	131.0
	C-H···O	2.22	3.177(2)	163.7
	O-H···Cl⁻	2.22	3.0554(12)	171.0
	O-H···Cl⁻	2.19	3.0188(12)	172.0
	O-H···O	1.99	2.7898(17)	176.0
TMA4HBA	O-H···O	1.62	2.6145(14)	174.3
	O-H···O	1.61	2.6120(14)	171.8
	O-H···O	1.64	2.6145(14)	168.5
	C-H···O	2.54	3.2796(18)	135.1
	O-H···O	1.62	2.6120(14)	174.0
	C-H···O	2.55	3.2125(19)	124.9
	O-H···Cl⁻	2.38	3.2245(14)	170.0
	O-H···Cl⁻	2.36	3.2223(13)	171.0
	O-H···O	1.89	2.6929(18)	177.0
	O-H···Cl⁻	2.22	3.0201(12)	173.0
TMADBA	O-H···Cl⁻	2.19	3.001(2)	165.0
	O-H···Cl⁻	2.25	3.050(2)	155.0
	O-H···O	1.70	2.626(2)	171.2
	O-H···O	1.66	2.626(2)	174.8
TMAGAL	O-H···O	1.82	2.6281(17)	170.2
	O-H···O	1.73	2.5808(17)	166.9
	O-H···O	1.71	2.5808(17)	174.3
	O-H···O	1.78	2.6281(17)	175.0
	C-H···O	2.54	3.280(5)	132.0
	O-H···Cl⁻	2.27	3.1017(14)	172.0
	O-H···O	2.11	2.913(2)	157.0
	O-H···O	1.95	2.7417(18)	173.0
	O-H···O	1.86	2.6805(18)	163.0

	O-H···Cl^-	2.19	3.0265(14)	171.0
	O-H···O	2.05	2.7297(16)	139.0
	O-H···O	2.10	2.8042(17)	144.0
TMAPCA	O-H···Cl^-	2.26	3.0822(14)	175.0
	O-H···Cl^-	2.25	3.0288(14)	177.0
	O-H···Cl^-	2.43	3.1366(17)	145.0
	O-H···Cl^-	2.44	3.1506(16)	151.0
	O-H···O	1.81	2.636(2)	178.0
	O-H···O	1.68	2.6011(19)	175.0

Appendix-2

2.1 Characterization of lithium chloride and α-D glucose ionic cocrystal (LICGLU)

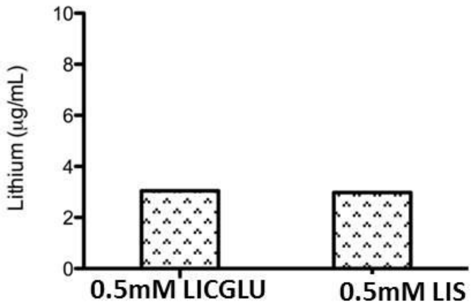

AAS

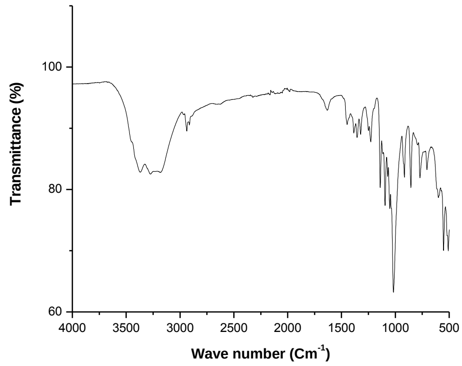

IR

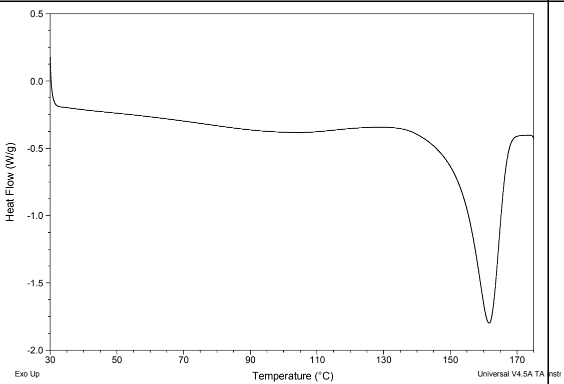

DSC

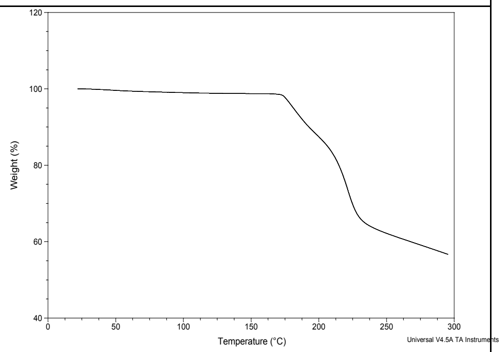

TGA